BULLETIN

OF THE AMERICAN PHYSICAL SOCIETY

PROGRAM OF THE 58th ANNUAL GASEOUS ELECTRONICS CONFERENCE

October 16–20, 2005
San Jose, California

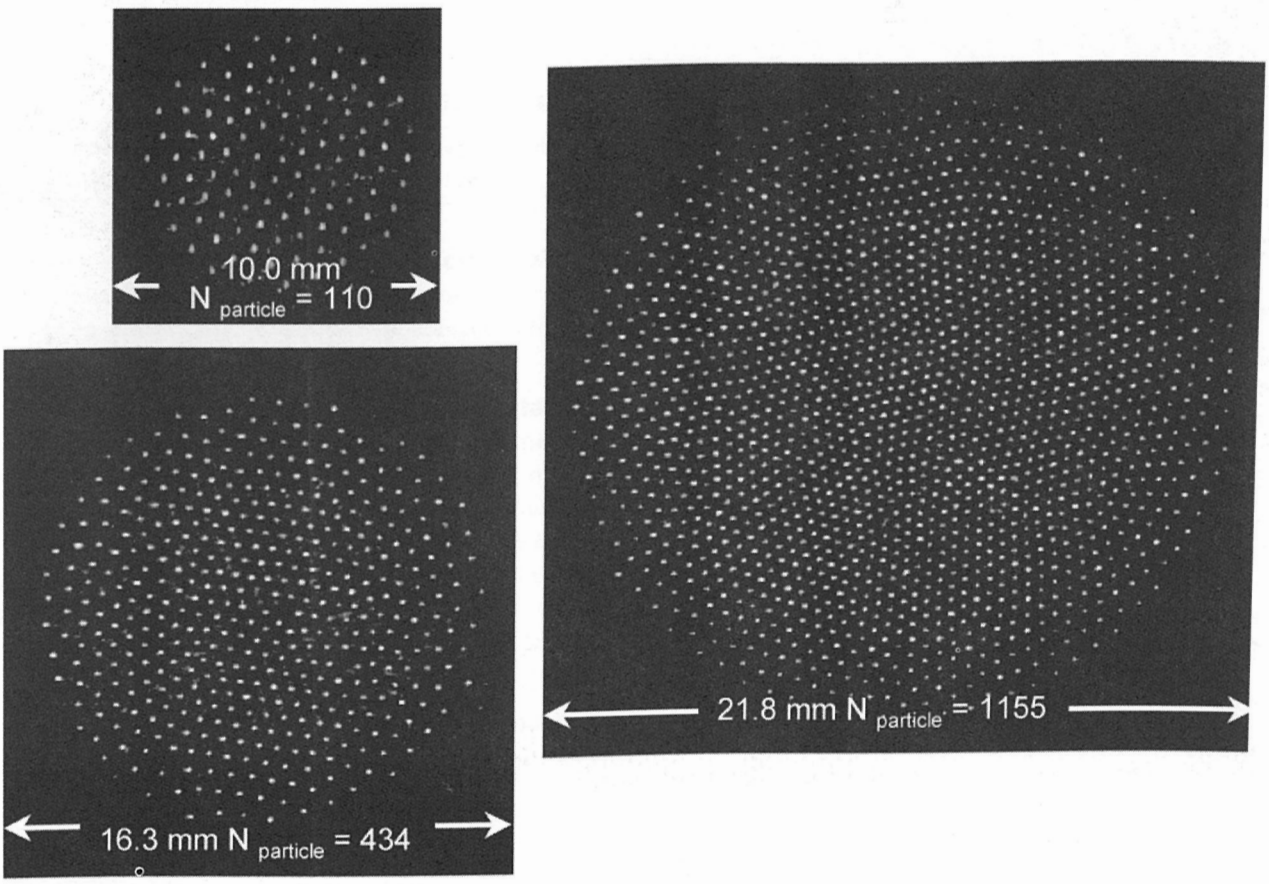

World Year of PHYSICS 2005
www.physics2005.org

October 2005
Volume 50, No. 7

APS

BULLETIN
OF THE AMERICAN PHYSICAL SOCIETY

Coden BAPSA6 ISSN: 0003-0503
Series II, Vol. 50, No. 7 **October 2005**

APS COUNCIL 2005

President
Marvin L. Cohen,* *University of California, Berkeley*

President-Elect
John J. Hopfield,* *Princeton University*

Vice President
Leo Kadanoff,* *University of Chicago*

Executive Officer
Judy R. Franz,* *University of Alabama, Huntsville (on leave)*

Treasurer
Thomas McIlrath,* *University of Maryland (emeritus)*

Editor-in-Chief
Martin Blume,* *Brookhaven National Laboratory*

Past-President
Helen R. Quinn,* *Stanford University (SLAC)*

General Councillors
Janet Conrad, Frances Houle,* Evelyn Hu, Gerald Mahan,* Ann Orel, Arthur Ramirez, Richart Slusher, Laura Smoliar*

Division, Forum and Section Councillors
Edward "Rocky" Kolb (*Astrophysics*), Kate Kirby* (*Atomic, Molecular & Optical Physics*), Robert Eisenberg (*Biological*), Charles S. Parmenter (*Chemical*), Moses H. Chan (*Condensed Matter Physics*), Richard M. Martin (*Computational*), Harry Swinney* (*Fluid Dynamics*), Peter Zimmerman (*Forum on Education*), Gloria Lubkin (*Forum on History of Physics*), Patricia Mooney (*Forum on Industrial and Applied Physics*), James Vary* (*Forum on International Physics*), Philip "Bo" Hammer (*Forum on Physics and Society*), J. H. Eberly (*Laser Science*), Leonard Feldman (*Materials*), Bunny C. Clark* (*Nuclear*), John Jaros (*Particles & Fields*), Stephen Holmes (*Physics of Beams*), James Drake* (*Plasma*), Timothy Lodge (*Polymer Physics*), Gianfranco Vidali (*New York Section*), Paul Wolf (*Ohio Section*)

Members of the APS Executive Board

Meetings Abstracts Coordinator:
Laura Walsh

APS MEETINGS DEPARTMENT
One Physics Ellipse
College Park, MD 20740-3844
Telephone: (301) 209-3286
FAX: (301) 209-0866
Donna Baudrau, *Director of Meetings & Conventions*
Terri Gaier, *Senior Meeting Planner*
Don Wise, *Registrar*
Christine Parvez, *Meetings Program Coordinator*

International Councillor
Sukekatsu Ushioda

Chair, Nominating Committee
Philip Bucksbaum

Chair, Panel on Public Affairs
Frank Von Hippel

ADVISORS

Representatives from other Societies
Richard Peterson, *AAPT*; Marc Brodsky, *AIP*

International Advisors
Maria Esther Ortiz, *Mexican Physical Society*;
Walter Davidson, *Canadian Association of Physicists*

Staff Representatives
Alan Chodos, *Associate Executive Officer*; Amy Flatten, *Director of International Affairs*; Ted Hodapp, *Director of Education and Outreach*; Robert L. Park, *Director, Public Information*; Michael Lubell, *Director, Public Affairs*; Stanley Brown, *Editorial Director*; Charles Muller, *Director, Journal Operations*; Michael Stephens, *Controller and Assistant Treasurer*

Administrator for Governing Committees
Ken Cole

The *Bulletin of the American Physical Society* is published 10X in 2005—March, April, May, July (2X), September, October (2X), November, and December—by the American Physical Society through the American Institute of Physics. It contains information about meetings of the Society, including abstracts of papers to be presented, as well as transactions of past meetings. Reprints of papers can be obtained only by writing directly to the authors.

MARK KUSHNER

BULLETIN
OF THE AMERICAN PHYSICAL SOCIETY

Vol. 50, No. 7, October 2005

GEC Meeting 2005

TABLE OF CONTENTS

General Information 3
Special Sessions and Events 3
Sessions 3
Presentation Formats 3
GEC Student Award for Excellence 4
Registration 4
Banquet and Reception 4
E-mail and Other Business Services 4
Audio-Visual Equipment 4
Dining Options 4
Guest Program 4
Call for Nominations for GEC General and Executive Committees 5
GEC Executive Committee 5
Conference Secretary 5
Please Note 6
Epitome 7
Main Text 8
Monday, October 17 9

Tuesday, October 18 33

Wednesday, October 19 42

Thursday, October 20 63

Author Index 67

Floor Plans ..... **At End of Issue**

58th Annual Gaseous Electronics Conference

October 16–20, 2005

San Jose, California

GENERAL INFORMATION

Welcome to San Jose for the Fifty-Eighth Annual Gaseous Electronics Conference (GEC) of the American Physical Society. The GEC 2005 will address a broad range of topics at the forefront of Gaseous Electronics. The program includes a Foundation talk, The GEC Student Award for Excellence Talks, 26 invited talks, and over 250 contributed papers presented in oral and poster sessions. The conference will be located at the Double Tree Hotel, San Jose, CA.

SPECIAL SESSIONS AND EVENTS

The GEC Executive Committee is pleased to announce that the Foundation Talk for 2005 will be presented by Dr. M. A. Lieberman. His talk is entitled *''Plasma'' and ''Sheaths''—The Discharge Science of Irving Langmuir*, and will be presented on Tuesday morning at 10 a.m. The Foundation series of talks, alternating each year with the Will Allis Prize talk, is to remind us of the fundamental background of Gaseous Electronics, and to stimulate new ideas by presenting a critical review of one aspect of this field.

SESSIONS

Session AS	Opening Reception
Session BM1	Plasma Propulsion and Combustion I
Session BM2	Magnetically-enhanced Plasmas
Session CM1	Dissociation, Recombination, and Attachment
Session CM2	Nanoparticles and Nanotubes
Session DM1	High Pressure Plasma I
Session DM2	Plasma Chemistry and Plasma-Surface Interactions
Session EM1	Electronegative Plasmas
Session EM2	Plasma Diagnostics I
Session FM	Poster Session I
Session GT1	Ionization of Atoms and Molecules
Session GT2	Plasma Propulsion and Combustion II
Session HT	GEC Foundation Talk
Session LT1	Electron-Molecule Collisions
Session LT2	High Pressure Plasmas II
Session MT1	Material Processing
Session MT2	Glows I
Session NT	Reception and Banquet
Session PW1	Lighting and Lasers
Session PW2	Plasma Sheaths
Session QW1	Electron and Positron Collisions
Session QW2	Inductively Coupled Plasmas
Session RW1	Capacitively Coupled Plasmas
Session RW2	Biological Applications of Plasmas
Session SW	Poster Session II
Session UH1	Etching Mechanisms
Session UH2	Glows II
Session VH1	Plasma Diagnostics II

PRESENTATION FORMATS

Papers that have been accepted for presentation are listed in the technical program. Invited papers are allotted 25 minutes, with 5 additional minutes for questions and discussion. Oral contributed presentations are allotted 12 minutes, with 3 additional minutes for questions. Poster sessions will be provided with 48 in. by 96 in. posterboards. Presenters may mount their posters anytime earlier in the day upon which their presentation is scheduled. Poster materials must be removed at the close of the poster session.

GEC STUDENT AWARD FOR EXCELLENCE

In order to recognize the outstanding contribution students make to the GEC and to encourage further student participation, the GEC will continue to award a

prize for the best paper presentation by a student. A subcommittee of the GEC Executive Committee will choose the award winner. Students competing for the $500 award, in the order of their appearance in the program, are:

Lorenzo Mangolini, University of Minnesota, ''Synthesis of Photoluminescent Nanoparticles in a Continuous Flow Non-thermal Plasma Reactor'', Monday, October 17, 10:30

Jeanna Royal, University of California at Davis, ''Dissociative Recombination of the Rare Gases'', Monday, October 17, 11:00

Garrett Curley, Ecole Polytechnique, ''Charged Species' Densities and Fluxes in a Dual-Frequency Capacitive Plasma'', Monday, October 17, 16:00

Jose Lopez, Stevens Institute of Technology, ''Time-Resolved Studies of Pulsed Plasmas'', Tuesday, October 18, 16:15

Tatiana Babkina, Ruhr-University Bochum, Germany, ''Hyper-Thermal Hydrogen Atoms Produced by Surface Neutralisation'', Monday, October 17, 14:45

Dan Haxton, University of California – Berkeley & Lawrence Berkeley Lab, ''Dissociative Electron Attachment to H_2O and H_2S'', Monday, October 17, 11:15

Junfang Gao, University of Missouri-Rolla, ''An Elementary Method for Averaging over Molecular Orientations in the Calculation of Electron-Impact Ionization of Molecules'', Tuesday, October 18, 9:00

REGISTRATION

The registration desk will be located in the Doubletree Hotel. Registration will be available Sunday evening and later in the week. The on-site conference registration fee is $310 for regular registrations and $190 for students and retirees.

BANQUET AND RECEPTION

An opening reception will be held on the evening of Sunday, October 16, 2005, at the Doubletree Hotel, starting at 18:00, in the Pine/Cedar Rooms.

The conference banquet will be held in the Pine/Cedar Rooms of the Doubletree Hotel on Tuesday evening, October 18, starting with a reception in the lobby at 6 p.m. Banquet tickets are $40 and are available upon registration. Conference participants are encouraged to attend the reception and the banquet.

E-MAIL AND OTHER BUSINESS SERVICES

Wireless internet access will be available to conference participants in the lobby of the Doubletree Hotel. Other business services (fax, photocopy services, etc.) will be available from the hotel business center.

AUDIO-VISUAL EQUIPMENT

Each conference room will be equipped with an overhead projector and an LCD projector. If additional equipment is required, please contact the conference secretary.

DINING OPTIONS

A list with dining options in the vicinity of the Doubletree Hotel is included in the registration packet provided to each conference participant.

GUEST PROGRAM

San Jose offers a wide variety of attractions for guests. The Doubletree Hotel is close to many tourist sites, such as: Japanese Friendship Garden; Japantown; San Jose State University Art Galleries; San Jose Museum Quilts and Textiles; Works San Jose Gallery; San Jose Museum of Art; Technical Museum of Innovation; Children's Discovery Museum; Japanese American Resource Center; and the Military Medal Museum. San Jose, the Gateway to the Bay Area, is the third largest city in California and the 10th largest city in the nation. The city's accessible location, comfortable climate and affordable amenities make it an ideal destination for hosting meetings and conventions or the leisure visit. San Jose is conveniently situated 45 minutes south of San Francisco and 1.5 hours north of Monterey. Rich in history and cultural diversity, and recognized as a city of innovation and entrepreneurial success, it's no wonder more than six million people visit San Jose each year.

Recently named the third Most Fun City in America

by Cranium Inc., San Jose offers world-class cultural arts, nightlife and professional sports (including the NHL's San Jose Sharks), theme parks, wineries, shopping, and nationally recognized hotels and restaurants.

CALL FOR NOMINATIONS FOR GEC GENERAL AND EXECUTIVE COMMITTEES

The GEC Executive Committee (ExComm) is the governing body of the GEC. It is the responsibility of the ExComm to oversee all aspects of the conference. This includes selection of meeting sites, budgetary decisions, selection of special topics and invited speakers, accepting and rejecting abstracts, and arranging of the program. The General Committee and the ExComm meet during the GEC, and the ExComm meets again during the summer to plan the program of the next GEC. There are numerous communications between members of the ExComm (usually via e-mail) during the year to ensure the successful completion of their duties. We have been fortunate over the years to have a dedicated group of volunteers who have been willing to take on these very necessary roles.

The by-laws of the Gaseous Electronics Conference describe the process whereby members of the ExComm are elected. At the GEC Business Meeting (to be held on Tuesday, October 18, at 11:15 in the Pine/Cedar Ballrooms of the Doubletree Hotel), nominations are accepted for members of the GEC General Committee (GenComm).

The GenComm consists of the ExComm and 6 at-large members elected at the Business Meeting. The eligible voting membership of the GEC (defined as those attending the Business Meeting) elects 6 at-large members. The GenComm then meets to fulfill its only duty: to elect new members of the ExComm.

The ExComm membership consists of the Chair, Treasurer, Past-Secretary, Secretary, Secretary-elect, past or incoming Chair, and 4 at-large members. The Chair is a 4-year term (1 year incoming, 2 years Chair, and 1 year past-Chair), the Secretary is a 3-year term (1 year incoming, 1 year Secretary, 1 year past-Secretary), and all other ExComm members serve 2 years. The Secretary is the person who manages the local arrangements for the meeting and is usually ''recruited'' and appointed to the ExComm.

The ExComm welcomes nominations, including self-nomination, for both the GenComm and the ExComm. Becoming a GenComm and/or ExComm member provides a unique opportunity both to see how the GEC is run and to influence its future direction by helping to define the programs and choosing future sites.

Please submit your nominations to the GEC Chair or any member of the ExComm. The ExComm also welcomes inquiries on hosting future GECs.

GEC 2005 EXECUTIVE COMMITTEE

Greg Hebner, Chair Sandia National Laboratory

Lepsha Vušković, Past Chair Old Dominion University

Jong Shon, Secretary JuSung Engineering Corporation

Bill Graham, Past Secretary Queen's University Belfast

William Rich, Secretary-Elect Ohio State University

Don Madison, Treasurer University of Missouri-Rolla

Uwe Czarnetzki Ruhr Universitat Bochum

Michael Brunger Flinders University

Murtadha Khakoo California State University Fullerton

Tom Rescigno Lawrence Berkeley Laboratory

Yukio Sakai Hokudai University

CONFERENCE SECRETARY

Jong Shon, Secretary

Shon Ju Sung Engineering Corporation

49, Neungpyung-Ri, Opo-Eup

Gwangju-Si, Gyuggi-Do

Korea 464-892

Phone: +82-31-760-7104

Email: jw_shon@jseng.com

PLEASE NOTE

The APS has made every effort to provide accurate and complete information in this *Bulletin.* However, changes or corrections may occasionally be necessary and may be made without notice after the date of publication. To ensure that you receive the most up-to-date information, please check the meeting Corrigenda distributed with this *Bulletin.*

Epitome of the 58th Annual Gaseous Electronics Conference of the American Physical Society

18:00 SUNDAY EVENING 16 OCTOBER 2005

AS **Opening Reception**
Pine/Cedar, Doubletree Hotel

8:00 MONDAY MORNING 17 OCTOBER 2005

BM1 **Plasma Propulsion and Combustion I**
Ono, Williams
Pine, Doubletree Hotel

BM2 **Magnetically-enhanced Plasmas**
Kushner
Cedar, Doubletree Hotel

10:00 MONDAY MORNING 17 OCTOBER 2005

CM1 **Dissociation, Recombination, and Attachment**
Orel, Mitchell
Pine, Doubletree Hotel

CM2 **Nanoparticles and Nanotubes**
Kortshagen
Cedar, Doubletree Hotel

13:30 MONDAY AFTERNOON 17 OCTOBER 2005

DM1 **High Pressure Plasma I**
Akashi
Pine, Doubletree Hotel

DM2 **Plasma Chemistry and Plasma-Surface Interactions**
van de Sanden
Cedar, Doubletree Hotel

16:00 MONDAY AFTERNOON 17 OCTOBER 2005

EM1 **Electronegative Plasmas**
Chabert
Pine, Doubletree Hotel

EM2 **Plasma Diagnostics I**
Chen
Cedar, Doubletree Hotel

19:15 MONDAY EVENING 17 OCTOBER 2005

FM **Poster Session I**
Fir/Oak, Doubletree Hotel

8:00 TUESDAY MORNING 18 OCTOBER 2005

GT1 **Ionization of Atoms and Molecules**
Childers, Colgan
Pine, Doubletree Hotel

GT2 **Plasma Propulsion and Combustion II**
Starikovskaia, Macheret
Cedar, Doubletree Hotel

10:00 TUESDAY MORNING 18 OCTOBER 2005

HT **GEC Foundation Talk**
Lieberman
Pine/Cedar, Doubletree Hotel

11:15 TUESDAY MORNING 18 OCTOBER 2005

JT **Business Meeting**
Doubletree Hotel

12:00 TUESDAY NOON
18 OCTOBER 2005

KT — **General Committee Meeting**
Boardroom, Doubletree Hotel

13:30 TUESDAY AFTERNOON
18 OCTOBER 2005

LT1 — **Electron-Molecule Collisions**
Allan, Tanaka, Zajfman
Pine, Doubletree Hotel

LT2 — **High Pressure Plasmas II**
Eden
Cedar, Doubletree Hotel

16:00 TUESDAY AFTERNOON
18 OCTOBER 2005

MT1 — **Material Processing**
Pine, Doubletree Hotel

MT2 — **Glows I**
Cedar, Doubletree Hotel

18:00 TUESDAY EVENING
18 OCTOBER 2005

NT — **Reception and Banquet**
Pine/Cedar, Doubletree Hotel

8:00 WEDNESDAY MORNING
19 OCTOBER 2005

PW1 — **Lighting and Lasers**
Jonkers
Pine, Doubletree Hotel

PW2 — **Plasma Sheaths**
Barnat
Cedar, Doubletree Hotel

10:00 WEDNESDAY MORNING
19 OCTOBER 2005

QW1 — **Electron and Positron Collisions**
Bartschat, Dimopoulou
Pine, Doubletree Hotel

QW2 — **Inductively Coupled Plasmas**
Cedar, Doubletree Hotel

13:30 WEDNESDAY AFTERNOON
19 OCTOBER 2005

RW1 — **Capacitively Coupled Plasmas**
Lee, Hoffman
Pine, Doubletree Hotel

RW2 — **Biological Applications of Plasmas**
Fridman, Grill
Cedar, Doubletree Hotel

16:00 WEDNESDAY AFTERNOON
19 OCTOBER 2005

SW — **Poster Session II**
Fir/Oak, Doubletree Hotel

8:00 THURSDAY MORNING
20 OCTOBER 2005

UH1 — **Etching Mechanisms**
Pine, Doubletree Hotel

UH2 — **Glows II**
Cedar, Doubletree Hotel

10:00 THURSDAY MORNING
20 OCTOBER 2005

VH1 — **Plasma Diagnostics II**
Pine, Doubletree Hotel

MAIN TEXT

SESSION AS: OPENING RECEPTION
Sunday evening, 16 October 2005
Pine/Cedar, Doubletree Hotel at 18:00
Greg Hebner, Sandia National Laboratories, presiding

18:00
AS 1 Opening Reception

SESSION BM1: PLASMA PROPULSION AND COMBUSTION I
Monday morning, 17 October 2005; Pine, Doubletree Hotel at 8:00
L. Vuskovic, Old Dominion University, presiding

Invited Papers

8:00
BM1 1 Micro plasma thruster for small spacecraft.
KOUICHI ONO, *Department of Aeronautics and Astronautics, Kyoto University*

A microplasma thruster of electrothermal type has been proposed using azimuthally symmetric microwave-excited plasmas, which consists of a microplasma source and a micronozzle. The microplasma source is made of a dielectric chamber 2 mm in inner diameter and 10 mm long covered with a metal grounded, producing high temperature plasmas at around atmospheric pressures. The micronozzle has a throat 0.2 mm in diameter, converting high thermal energy of plasmas into directional kinetic energy of supersonic plasma flows. First, we have developed a numerical model for microwave-excited microplasmas in Ar and plasma flows in the micronozzle. The model consists of three modules: a volume-averaged global model and an electromagnetic model for microplasma sources, and a two-temperature fluid model for micronozzle flows. Numerical results indicated that the microwave power absorbed in plasmas increases with increasing microwave frequency f and relative permittivity ε_d of dielectrics, and that a certain combination of frequency and permittivity significantly increases the power absorption. The micronozzle flow was found to be heavily affected by viscous dissipation in thick boundary layers, indicating that shortening the nozzle length with increasing half-cone angles suppresses the effects of viscous loss and thus enhances the thrust performances. A thrust of 2.5-3.5 mN and a specific impulse of 130-180 s were obtained for a given microwave power range ($P_t < 10$ W), which is applicable to a station-keeping maneuver for microspacecraft less than 10 kg. Moreover, we have developed a microwave-excited microplasma source, based on the model analysis, with mullite ($\varepsilon_d \approx 6$) and zirconia ($\varepsilon_d \approx 12$-25) being employed for dielectrics. Experiments were performed at f=2 and 4 GHz,$P_t < 10$ W, Ar flow rate of 50 sccm, and microplasma chamber pressure of 10 kPa. Optical emission spectroscopy and Langmuir probe measurement were employed for diagnostics of microplasmas, indicating that the ArI emission intensity and plasma density n_e increase with increasing f and ε_d, and that the n_e is in the range $10^{12} - 10^{13}$ cm^{-3}. Moreover, the rotational temperature T_{rot} of N_2 added was in the range 1100-1500 K, and the specific impulse estimated was about 70s.

8:30
BM1 2 Diode Laser Diagnostics for Combustion Environments.
SKIP WILLIAMS, *AFRL, Propulsion Directorate*

The current state-of-the-art in hypersonic air-breathing propulsion system development relies heavily on a combination of ground tests and numerical simulations. Generally, wall measurements (e.g., pressure, temperature, and heat flux) dominate the instrumentation suite available in most ground test facilities. If in-stream information (usually pitot pressure) is available, it is usually sparse and is generally available only at the inflow and outflow planes of the test article. While valuable for various analyses, these types of information provide little or no detailed descriptions of the mean and turbulent velocity fields, the turbulence-chemistry interactions, or the local state properties within the device. Advanced laser-based techniques can provide this information but impose significant challenges on test article design which are not practical for flight systems. The aim is to develop simpler diode laser based techniques which are practical in terms of weight, power, and optical access requirements. The presentation will outline some of the key issues relating to the development and application of these techniques to plasma and combustion environments.

Contributed Papers

9:00
BM1 3 Development of Micro Hall Thruster TSUYOHITO ITO, NICOLAS GASCON, MARK CAPPELLI, *Stanford University* There is a growing need for advanced propulsion options for small spacecraft. Hall plasma thrusters have intrinsic properties that are attractive for potential Micropropulsion applications – high thrust densities; minimal space charge effects; the discharge is stable over a wide range of input parameters; and the thrust and specific impulse is throttled by varying the discharge voltage. In this study, we are developing a micro-Hall plasma thruster with an operating power of less than 50W. The channel has a 4 mm outer diameter and a Sm-Co magnet is employed for generating the nearly 1T magnetic field strength required for the scaling of these thrusters to low power. I-V curves with the discharge operating on Xe propellant have been measured and the characteristic breathing-mode oscillations have been observed, as expected, at higher frequency in comparison to higher power thrusters. The first prototype studied is actively cooled, and no detrimental damage to thruster components was observed in the operating conditions explored. Ongoing studies include the measurements of near-field ion energy distribution using a retarding potential analyzer.

9:15
BM1 4 Fuel Oxidation and Ignition in Premixed Hydrocarbon-Air Flows by Nonequilibrium Plasmas IGOR ADAMOVICH, AINAN BAO, GUOFENG LOU, MUNETAKE NISHIHARA, J.WILLIAM RICH, WALTER LEMPERT, *Ohio State University* We present nonequilibrium RF plasma assisted combustion experiments in ethylene-air and methane-air flows using FTIR absorption and visible emission spectroscopy. Results

show highest oxidation efficiency (~ 100% of ethylene and ~ 70% of methane) under conditions which do not produce a flame (T=250-300° C). Under these conditions, oxidation occurs by plasma chemical reactions which differ from those leading to ordinary thermal combustion. These results, combined with previous measurements demonstrating very low temperature ignition, suggests the following nonequilibrium plasma ignition mechanism: (i) plasma generation of active radical species, (ii) plasma fuel oxidation with participation of these radicals, (iii) heating by net exothermal fuel oxidation, and (iv) ordinary thermal ignition and combustion. Emission spectroscopy shows that O, H, and OH emission intensities are highest in lean fuel-air mixtures, when a significant fraction of fuel is oxidized by plasma chemical reactions without producing ignition.

SESSION BM2: MAGNETICALLY-ENHANCED PLASMAS

Monday morning, 17 October 2005
Cedar, Doubletree Hotel at 8:00
A. Kono, Nagoya University, presiding

Contributed Papers

8:00
BM2 1 Experimental and Theoretical Investigation of Dual Frequency Magnetically Enhanced Reactive Ion Etch Plasmas ALEX PATERSON, THEODOROS PANAGOPOULOS, VALENTIN TODOROW, SHARMA PAMARTHY, DECLAN SCANLAN, THORSTEN LILL, JOHN HOLLAND, *Applied Materials* Dual Frequency Magnetically Enhanced Reactive Ion Etch tools (DF-MERIE) are the technology of choice for the etching of deep silicon trenches, which are required for the capacitor structures of DRAM cells. This presentation will focus on the characterization of a DF-MERIE, both experimental and theoretical, where the low and high frequencies are applied to the same wafer platen. Investigations suggest that the magnetic field produces many novel attributes to this type of etch that can not be obtained otherwise. Wafer voltage and DC bias measurements show that as the B-field increases above a certain value, dependent on frequency, the wafer voltage and DC bias decrease rapidly, becoming less negative. Inspection of the RF waveform shows that the cathodic part of the RF cycle reduces dramatically but the anodic part of the cycle increases. This suggests that sheath reversal is taking place to compensate for the electron inertia produced by the B-field, as proposed by [1]. [1] M. Kushner, J. Appl. Phys. 94/3 (2003), 1436

8:15
BM2 2 A self-consistent modeling of an RF magnetron plasma with metallic and dielectric target for sputtering TAKASHI YAGISAWA, *Keio University* SHUNJI KUROIWA, *Shibaura Mechatronics Corp.* TOSHIAKI MAKABE, *Keio University* Radio frequency (RF) magnetron plasma has been developed as a promising candidate for various kinds of material processing. Magnetron-RIE is traditionally operated as an etching tool of dielectric (high-k) materials in industry. In addition, dielectric thin film prepared by RF magnetron plasma is widely used as a reflective layer for optical disks, such as CD DVD, Blue-ray disk and super-RENS disk. Deposition uniformity on a substrate is to a great extent influenced by the target erosion profile. There exist two major differences in erosion profile between a metallic target and a dielectric one. One is the presence of double minima in the erosion profile. The other is the discrepancy in the radial position between the maximum of the ion flux and the erosion depth. These are caused by a distinctive sheath profile in front of a dielectric target based on the surface charging. In this paper, we will focus on the 2D-t structure of an RF magnetron plasma with dielectric target at 5 mTorr in Ar. Emphasis will be given on the causation between the profile of the sheath potential and the ion velocity distribution incident on the target surface.

8:30
BM2 3 LIF Measurement of Time-Dependent Spatial Density Distribution of Cu Atoms Ejected from a YBaCuO Target in Magnetron Sputtering Plasmas JUNSI GAO, NAYAN NAFARIZAL, KOICHI SASAKI, HIROTAKA TOYODA, MASUMI INOUE, AKIRA FUJIMAKI, SATOSHI IWATA, HIDEO SUGAI, *Department of Electrical Engineering and Computer Science, Nagoya University, Furo-cho, Chikusa-ku, Nagoya 464-8603, Japan* Magnetron sputtering deposition techniques have a great potential in high quality high T_c superconductor film. We used a two- dimensional laser-induced fluorescence method to measure the time-dependent spatial density distribution of Cu atoms ejected from a YBaCuO target in RF-magnetron sputtering plasma. It has been first found that the sputtered Cu density was changed with both time and discharge conditions. This was different from the case of Cu metal target, where the Cu density depends only on discharge conditions. Therefore, the time-dependent spatial distribution of Cu density was investigated systematically in various discharge conditions. At low gas pressure, the density was increased at the beginning of discharge, then decreased, and finally reached a stationary value within a few minutes. The differences between initial value and stationary value were about two times. However, at high gas pressure, the stationary density was decreased to one-fifth of the initial value, and the transition time became 16 min. These observations are crucial for optimizing the deposition conditions of high T_c superconductor film.

8:45
BM2 4 Time-Resolved Imaging of a Pulsed DC Magnetron Plasma During the Sputter Deposition of TiO_2 Films ABE BELKIND, KURT BECKER, JOSE LOPEZ, *Stevens Institute of Technology* SHANMUGAMURTHY SHANMUGAMURTHY, WEIDONG ZHU TEAM,*GUY BUYLE TEAM† Time resolved images from a pulsed DC titanium target magnetron plasma were taken with a Roper Scientific ICCD camera. The camera was exposed to the discharge for 0.05-0.2 μs with 0.05-0.2 μs separation between each exposure. At the beginning of the on-time when the power is turned on, the discharge initially starts preferentially in the cross corners of the race track. During the rest of the on-time, the emission from the straight sections of the trace track of the magnetron is always slightly stronger than the emission from the two rounded corners of the itrace track. This pattern extends into the start of the off-time when the power is turned off. The optical

emissions persist for several microseconds into the off-time. Spectral filters were used in order to record the temporal behavior of the emissions from various species (Ar, O). The observed ''corner effect'' at the beginning of the on time was modeled using a Monte Carlo method by retracing the high energy electrons. Work supported by the U.S. National Science Foundation and the U.S. Army.

*Center for Bioelectrics, Old Dominion University.
†Ghent University, Ghent, Belgium.

Invited Paper

9:00
BM2 5 Magnetically Enhanced Multiple Frequency Capacitively Coupled Plasmas: Dynamics and Strategies.*
MARK J. KUSHNER, *Iowa State University*

The desire to independently control the magnitude and energy of ion fluxes to wafers during plasma materials processing has motivated development of a variety of plasma tools, from inductively coupled with a separate bias to the increasingly popular dual frequency capacitively coupled plasmas (CCPs). The success of these strategies has in part been due to, for example, CCPs being able to produce more favorable radical fluxes to achieve selectivity compared to ICPs. At the same time, there is a resurgence in the use of magnetically enhanced CCPs which also have an ability to control the shape of ion energy and angular distributions by radically changing the structure of the sheath. For example, a static magnetic field of sufficient magnitude applied parallel to the sheath results in ions being more mobile than electrons; and a reversal of the electric field in the sheath.[1] The combination of dual (or multiple) frequency CCPs and magnetic enhancement provides additional parameters with which to control reactive fluxes to the substrate. Using results from a 2-dimensional plasma equipment model, the dynamics of magnetically enhanced, multiple frequency CCPs will be discussed. Strategies to use their unique properties will be proposed. [1] M. J. Kushner, J. Appl. Phys. J. Appl. Phys. **94**, 1436 (2003)

*Supported by National Science Foundation, Semiconductor Research Corp. and Applied Materials Inc. The author thanks Mr. Yang Yang for his contributions.

SESSION CM1: DISSOCIATION, RECOMBINATION, AND ATTACHMENT
Monday morning, 17 October 2005; Pine, Doubletree Hotel at 10:00
Stephen Buckman, Australian National University, presiding

Invited Papers

10:00
CM1 1 Theoretical Studies of Electron-Molecule Collision Processes .*
ANN E. OREL, *University of California, Davis, Department of Applied Science*

Electron collisions with molecules and molecular ions that lead to excitation and dissociation play a key role in a number of environments, since they produce the radicals and molecular fragments that initiate and drive the relevant chemistries. Examples range from the technologically important plasmas used in plasma enhanced chemical vapor deposition, to planetary atmospheres and interstellar clouds, to DNA damage driven by secondary electron cascades produced by radiation. In general, due to the large mass difference between the electron and target, the cross section is dominated by resonant processes, where the electron can temporarily attach to the molecule and change the forces felt between its atoms for a period of time comparable to a vibrational period. This can lead to resonant vibrational excitation and dissociative attachment, for neutral targets, or dissociative recombination in the case of ions. In this talk, I will outline the basic theory that underlies these processes, and our approach to study them. I will illustrate these methods with application to dissociative attachment in ClCN and BrCN, vibrational excitation and dissociative attachment in NO and CF, and dissociative recombination in the HCN^+ and HNC^+ systems. This work was supported by DOE-OBES Division of Chemical Sciences and NSF PHY-02-44911.

*This work was carried out in collaboration with C. W. McCurdy, V. Ngassam, T. N. Rescigno, J. Royal and C. Trevison.

10:30 de Rennes I

CM1 2 Recent Studies of Cross Sections, Rates and Branching Ratios for the Recombination of Ions in Industrial Plasmas.

BRIAN MITCHELL, *Université de Rennes I*

Branching ratios for the dissociative recombination of hydrocarbon ions with the general formula $C_2H_3^+$, $C_3H_m^+$ (m=1-8) and $C_4H_m^+$ (m=1-9) have been measured using the ASTRID storage ring in Aarhus [1-3]. The detector used did not have sufficient energy resolution to distinguish hydrogen atoms either free or attached to carbon atoms so the relative distributions of carbon atoms among the dissociation products were measured. For most of the ions that were in linear isomeric form, the fragmentation patterns were predictable from the structure of the parent ion. For cyclic isomers however, this was not so clear and indications are that ring opening occurs prior to dissociation. Results obtained for $C_2H_3^+$ and $C_3H_7^+$ are in excellent agreement with studies performed by the CRYRING group in Stockholm [4,5]. Rare gas hydride ions are important in several industrial applications and recent cross section measurements have shown that while NeH^+ [6] does recombine at low energies, ArH^+ [7] does not. Both these ions display recombination resonances and dissociative excitation onsets at higher electron energies. The fluorocarbon ions, CF^+, CF_2^+ and CF_3^+ that are found in semiconductor etching plasmas have been examined in a collaborative effort with the CRYRING group and results for cross sections and branching ratios will be presented [8-10]. Work supported by the European Union, AFOSR, EOARD, the Danish and Swedish Research Councils and the French Centre National pour la Recherche Scientifique (CNRS) (1) J.B.A. Mitchell, et al. Int. J. Mass Spec. 227, 273, 2003 (2) G. Angelova et al (2004) Int. J. Mass Spec. 232, 195, 2004 (3) G. Angelova, et al Int. J. Mass Spec. 235,7, 2004. (4) S.S. Khalori, et al Astron & Astrophys. 391, 1159, 2002 (5) A. Ehlerding, et al J. Phys. Chem. A 107, 2179, 2003 (6) J.B.A. Mitchell et al. J. Phys. B 38, 693, 2005 (7) J.B.A. Mitchell et al. J. Phys. B 38, L175, 2005 (8) G. Angelova et al. J. Phys. B 37, 1, 2004 (9) O. Novotny et al. J. Phys. B 38, 1471, 2005 (10) A.Ehlerding et al. (In preparation)

Contributed Papers

11:00

CM1 3 Dissociative Recombination of the Rare Gases J. ROYAL, V. NGASSAM, A.E. OREL, *Department of Applied Science, University of California at Davis* We report cross sections for the dissociative recombination of the He_2^+ ,Ne_2^+ and Ar_2^+ molecular ions following collisions with low energy electrons. Dissociative recombination of the rare gases are important processes in the ionosphere as well as laboratory plasmas and gaseous discharges. This research will explore the similarities and differences between the three processes as well as the trend in the DR cross section as the atomic mass increases. The energy positions and autoionization widths of these doubly excited dissociative states are obtained from electron scattering calculations using the Complex Kohn Variational method. The dissociation dynamics is studied using either multichannel quantum defect theory (MQDT), discrete variable representation (DVR) with exterior complex scaling (ECS), or time-dependent wave packet methods. The calculated cross sections will be compared to available experiment. Work supported by the NSF PHY-02-44911 and The Center for Biophotonics, an NSF Science and Technology Center PHY 0120999, and NATO science program PST.GLG.9794033.

11:15

CM1 4 Dissociative Electron Attachment to H_2O and H_2S DANIEL HAXTON, *University of California - Berkeley and Lawrence Berkeley Lab* THOMAS RESCIGNO, *Lawrence Berkeley Lab* C. WILLIAM MCCURDY, *University of California - Berkeley and Lawrence Berkeley Lab and University of California - Davis* Dissociative electron attachment (DA) to H_2O is of direct importance for both biological and techological systems. The calculations on H_2O and H_2S presented comprise the first itab initio treatment of DA to a polyatomic molecule employing the full dimensionality of nuclear motion. Cross sections obtained for DA via the $^2B_1$ state of H_2O agree well with experiment, reproducing the high degree of vibrational excitation of the OH fragment. Several interesting features of the A' manifold of resonances for H_2O have been discovered, including a conical intersection between the $^2A_1$ and $^2B_2$ Feshbach resonances and a branch-point degeneracy between the $^2B_2$ shape and Feshbach resonances. This latter feature has no analogue in bound-state theory. We show results of recent calculations on the Renner-Teller coupled $^2A_1$ and $^2B_1$ surfaces, and on electronically coupled diabatic $^2A_1$ and $^2B_2$ surfaces. The angular dependence of the H^- + OH channel for the $^2B_1$ state of H_2O and that of the analagous channel and state of H_2S have been calculated by incorporating the mixing of different partial waves into the entrance amplitude, and for H_2S, the variation of this mixing with geometry.

11:30

CM1 5 Dissociative recombination of HCO^+* STEFANO TONZANI, *University of Colorado Boulder* AASA LARSON, *KTH, Stockholm, Sweden* VIATCHESLAV KOKOOULINE, *University of Central Florida, Orlando* IVAN MIKHAYLOV, *University of Central Florida* ROBIN SANTRA, *ITAMP, Harvard* CHRIS H. GREENE, *University of Colorado Boulder* The dissociative recombination (DR) mechanism of the important interstellar ion HCO+ at low electron energies is studied theoretically. Our work suggests that DR is driven through capture into Rydberg states, and that no direct mechanism operates at collision energies below a few eV. Our approach includes accurate quantum chemical calculations, the three-dimensional vibrational dynamics and a treatment of the joint electron-nuclear dynamics is treated using quantum defect theory and a frame transformation approach. Results are presented for the calculated autoionization widths of Rydberg states and the dissociative recombination cross sections, and compared with available experiments.

*This work is supported by NFS.

11:45
CM1 6 Numerically Solvable Model of Low-Energy Resonant Electron-Molecule Collisions without Born-Oppenheimer Approximation K. HOUFEK, *LBNL* C.W. McCURDY, *UC Davis* T.N. RESCIGNO, *LBNL* We suggest a simple model with one nuclear and one electronic degree of freedom that can be solved exactly (without the Born-Oppenheimer approximation) employing the exterior complex scaling method and the finite-element method with discrete variable representation. Using this model it is possible to study basic electron-molecule collisions: the vibrational excitation of a molecule by electron impact and the dissociative electron attachment to a molecule. The full Hamiltonian of our model is $H = -1/2\mu\, d^2/dR^2 - 1/2\, d^2/dr^2 + V_0(R) - \lambda(R)e^{-\alpha r^2} + l(l+1)/2r^2$ where $V_0(R)$ is a Morse potential for the vibrational motion of the neutral molecule, the forth term describes the interaction between the molecule and the electron and the centrifugal term with $l \neq 0$ is added to provide a resonant behavior in our system. The suggested model enables us to compare various approximations used in low-energy resonant electron-molecule collisions (for example the boomerang model or the non-local resonance model) with the exact solution and to investigate when these approximations are valid.

SESSION CM2: NANOPARTICLES AND NANOTUBES
Monday morning, 17 October 2005; Cedar, Doubletree Hotel at 10:00
Larry Overzet, University of Texas at Dallas, presiding

Invited Paper

10:00
CM2 1 Nonthermal Plasmas: Silicon Nanocrystals made easy.*
UWE KORTSHAGEN, *University of Minnesota*

In this presentation, low pressure plasmas are discussed as a superior source for the controlled synthesis of semiconductor nanocrystals. Among the prime advantages of low pressure plasmas are their ability form highly monodisperse, single-crystal nanoparticles which are prevented from agglomeration due to the electrical charge that particles acquire in the plasma. Two examples of this approach are presented: In the first example, a constricted mode capacitive discharge is used to produce single-crystal, virtually defect-free, cube shaped silicon nanoparticles. Particles are between 20-50 nm in diameter with a highly monodisperse particle size distribution. These particles have enabled our recent success in manufacturing single-nanoparticle-based Schottky barrier vertical transistors. Electrical characterization of these devices provides insight into the electronic properties of the silicon nanoparticles. In the second example, a high-yield plasma process is used to form luminescent semiconductor quantum dots in a flow-through reactor. Our work has focused on several Group IV elements due to their compatibility with silicon technology and their low toxicity. Results of the synthesis and application of various materials systems will be presented.

*This work is supported by NSF under NIRT grant DMI-0304211 and under partial support by MRSEC grant DMR-0212302 and by InnovaLight, Inc.

Contributed Papers

10:30
CM2 2 Synthesis of photoluminescent nanoparticles in a continuous flow non-thermal plasma reactor* LORENZO MANGOLINI, ELIJAH THIMSEN, UWE KORTSHAGEN, *Department of Mechanical Engineering, University of Minnesota* Silicon nanoparticles small enough to show quantum confinement effects exhibit intense room temperature luminescence and might find applications in novel light emitting devices, in microelectronics, and as biological tagging agents. A new approach for the synthesis of luminescent silicon nanocrystals is presented. Silicon nanoparticles with an average size below 5 nm are produced in a continuous flow non-thermal plasma reactor. The reactor consists of a simple 3/8'' quartz tube through which an Argon/Silane mixture is flown. RF power is fed into the system through two ring electrodes. The produced particles are crystalline and show bright red-orange photoluminescence. The influence of the experimental parameters and plasma properties on the produced material is discussed. The system is capable of producing several tens of milligrams per hour of luminescent powder. The process has also been modified to synthesize amorphous hydrogenated carbon nanoparticles, which show efficient luminescence in the blue-green range. These particles are synthesized in an Argon/Methane discharge. The photoluminescence and quantum yield efficiency have been characterized with respect of the experimental conditions.

*This work was supported in part by NSF through MRSEC grant DMR-0212302 and by InnovaLight, Inc.

10:45
CM2 3 Synthesis of nanoparticles in microplasma reactor TOMOHIRO NOZAKI, *Tokyo Institute of Technology* DAISUKE ASAHI, KEN OKAZAKI, KENJI SASAKI, Synthesis of silicon-based nanoparticle has been studied in capacitively coupled VHF (144 MHz) microplasma reactor. A mixture of He/H_2/TEOS(Tetraethoxysilane) was processes in a 470 μm capillary tube. The process starts with the creation of supersaturated radical condition, followed by homogeneous nucleation, cluster formation and/or particle growth, and annealing including aggregation of particles. The proposed microplasma reactor has several advantages over these processes: (1) Microplasma under high frequency operation easily provides supersaturated environment regardless of thermodynamic equilibrium ($Ne\sim 4\times 10^{15}cc^{-1}$ at $T_{rot} \sim 1800K$), (2) Micrometer scale reactor equalizes radical density and temperature, realizing uniform nucleation, (3) Charged

particles prevent aggregation, (4) Particle synthesis due to consecutive reaction is easily optimized with short-residence time reactor ($\sim \mu$s). Optimum gas mixture such as He/1000sccm, H_2/1sccm, and TEOS/(less than 100 ppm) deposited 50 nm particles on a substrate. Detailed analysis of those particles is now being conducted. This work has been supported by the Grants-in-Aid for Scientific Research on the Priority Area of Microplasmas from the Japanese Ministry of Education, Culture, Sports, Science and Technology.

11:00

CM2 4 Spatial-grid-independent 1D hybrid kinetic-hydrodynamic plasma simulations for nanoparticle deposition PAVLO RUTKEVYCH, *Plasma Sources and Applications Center, NIE, Nanyang Technological University, Singapore* The present code is created in order to describe nanoparticle movement in a combined bulk-presheath-sheath region and confirm our earlier proposed simple models of nanoparticle deposition. The required quantities are densities and average velocities of each species at each spatial cell; the plasma particles are described according to their velocity distribution function, and they are moving with respect to their velocities. The time evolution is performed until the stabilization process is finished. The model is found to be sensitive to the time step (the optimum time step has been investigated for each species separately), however it is much less sensitive to the spatial grid, allowing strongly irregular coordinate cells. The model includes external electric field, collision with neutrals, ionization and various boundary conditions at the wall. Currently the model describes electrons, one kind of positive ions and nanoparticles, though it can be easily extended to a larger number of species, common for chemically-active discharges.

11:15

CM2 5 Deposition of Aligned Carbon Nanofibers in Highly Collisional Sheath TOMOHIRO NOZAKI, KUMA OHNISHI, KEN OKAZAKI, *Tokyo Institute of Technology* JOACHIM HEBERLEIN, UWE KORTSHAGEN, *University of Minnesota* TOKYO INSTITUTE OF TECHNOLOGY TEAM, UNIVERSITY OF MINNESOTA TEAM, Deposition of vertically oriented carbon nanofibers (CNFs) has been studied in atmospheric pressure radio frequency discharge (APRFD) where dielectric barrier is not inserted between metallic electrodes. If frequency is sufficiently high so that ions are trapped in the gap, the operating voltage is remarkably decreased. Then transition of glow discharge into arc discharge is suppressed without dielectric barrier. More importantly, trapped ions produce cathodic sheath in the boundary of bulk plasma and electrode where large potential drop exists. The primary interest of present work is to study how such highly collisional cathodic sheath works on the alignment of CNFs. The absence of dielectric barrier enables us to superpose external DC potential to the substrate, which might provide sufficient field strength in the boundary for the orientation of CNFs, while the damage of CNFs due to ion bombardment should be negligible in atmospheric pressure. Emission distribution of He (706 nm), Hα (656 nm), and CH (432 nm) clearly showed that negative DC bias enhances the formation of cathodic sheath near the substrate. Both deposition rate and alignment of CNFs are remarkably improved by the application of negative DC bias.

11:30

CM2 6 Atmospheric Pressure Plasma Jet Process for Carbon Nanotube growth ANAND CHANDRASHEKAR, JEONG SOO LEE, GIL SIK LEE, LAWRENCE OVERZET, *University of Texas at Dallas* In this study, an atmospheric jet RF helium plasma (13.56 MHz) is used to synthesize Carbon nanotubes on large area silicon substrates, using acetylene precursor gas. Downstream, a copper hot plate is heated to temperatures of 600C and above, after the substrate is set on it. Iron (catalyst) is either evaporated on the substrate and annealed, or added to the process by evaporating ferrocene in a Vapor Delivery System (VDS). The plasma and thermal energy dissociate the precursor molecules, and carbon nanotubes deposit on the substrate. SEM micrographs of film cross-section predict that taller nanotubes can be obtained at higher plate temperatures and plasma powers. Film growth saturates with time if only pre-evaporated iron catalyst is used, but this phenomenon is overcome by introducing ferrocene. It was determined using Raman spectroscopy that higher plasma power and temperature lend purer nanotube films, due to efficient graphitization.

SESSION DM1: HIGH PRESSURE PLASMA I

Monday afternoon, 17 October 2005
Pine, Doubletree Hotel at 13:30
Antoine Rousseau, LPTP, Ecole Polytechnique, presiding

Contributed Papers

13:30

DM1 1 Temporal behaviour of helium metastables and molecular nitrogen ions in a He APGD GAGIK NERSISYAN, JEAN-PIERRE VAN HELDEN,*WILLIAM GRAHAM, *Physics and Astronomy, Queen's University Belfast, Northern Ireland* Laser-aided methods are used to characterize the temporal behaviour two of the important species, helium metastables (He_m) and N_2^+ ions, in the development of an atmospheric pressure glow discharge (APGD) in helium generated in a planar configuration of a dielectric barrier discharge with quartz dielectrics. The discharge modes are monitored by electrical and optical measurements and fast imaging. Under certain conditions, mainly when the impurity level is low, there is a residual discharge between the APGD pulses. The termination of this residual discharge and generation of a more typical pulse APGD happens when the impurity level is relatively high. The temporal behaviour of He_m obtained by both optogalvanic and the laser induced fluorescence (LIF) signals is well correlated with the discharge current. The temporal variation of the N_2^+ ion density is also measured using LIF. When the mode of APGD with a residual discharge is generated the density between the discharge pulses is higher than during the pulses. In the typical APGD mode the N_2^+ ion density has a maximum which is delayed a few μs from the current peak followed by a decrease of the density to below the detection limit.

*Permanent address: Eindhoven University of Technology, The Netherlands.

13:45

DM1 2 Dynamics of a Homogeneous Dielectric Barrier Discharge in Xenon Excited by Short Voltage Pulses ROBERT CARMAN, RICHARD MILDREN, *Physics Dept, Macquarie University, Australia* IAN FALCONER, *School of Physics, University of Sydney* In a Xenon dielectric barrier discharge (DBD) lamp, the use of short pulse voltage waveforms ($<$ 100ns FWHM) can dramatically increase the electrical-VUV (172nm) conversion efficiency and VUV output, compared with conventional AC excitation. The discharge visually appears to fill the region between the electrodes more or less uniformly, rather than appearing as discrete microdischarges as seen for sinusoidal (AC) voltages. A previous modeling study of a short-pulse Xe DBD predicted that electrical breakdown of the discharge gap would be characterised by the appearance of a fast-moving ionization wave or a streamer propagating from the anode toward the cathode, strongly correlated with the spatio-temporal evolution of the visible and infrared emission from the discharge, but weakly correlated with the more intense VUV emission [1]. To investigate the dynamics of electrical breakdown under various operating conditions, streak images of the infrared emission from a cylindrical DBD lamp have been recorded using a Hamamatsu 4187 streak camera, where the spatial information is provided as a function of position across the discharge gap. [1] R.J. Carman and R.P. Mildren, J. Phys. D: Appl. Phys., 36, 19-33, 2003.

14:00

DM1 3 Experimental study of an aerodynamics plasma actuator using emission spectroscopy* TSITSI MADZAWA-NUSSINOV, YONGHO KIM, JAEYOUNG PARK, LOUIS ROSOCHA, VINCENT FERRERI, GABRIEL BECERRA, *Los Alamos National Laboratory* In this paper, we report on studies of the aerodynamic plasma actuator, a special asymmetric surface discharge configuration of the dielectric barrier discharge. The configuration of the plasma actuator (one electrode exposed and a second embedded in a dielectric) employing ac power, has been proposed for flow control in aerodynamics applications[1]. The actuator operates over a wide range of frequencies with no resonant behavior, and produces stable plasma at atmospheric pressure. The mechanisms for momentum transfer to the gas molecules are still a subject of debate. Recently, studies and simulations done at Kinema Research[2] suggest that due to the non-equilibrium nature of the actuator, ions contribute more to the momentum transfer than electrons. By measuring detailed emission spectra for various discharge gases such as nitrogen and air, we compare our experimental results on electron energy distribution function with simulations done at Kinema Research. We also measure flow patterns and velocities as a function of input power and gas species, and correlate these to the changes in the calculated distribution functions.

*This work funded by USAF in collaboration with USAF Academy.

Invited Paper

14:15

DM1 4 Modeling of nitrogen atmospheric pressure discharges.

HARUAKI AKASHI, *Dept. of Appl. Phys., National Defense Academy, Japan*

Recently, dielectric barrier discharges at atmospheric pressure have been widely applied to ozone production, surface treatment, gas cleaning and so on. Two forms of discharges can be seen at this condition; filamentary discharges and homogeneous discharges. The former discharge form has been applied to ozone productions for years. Recently, latter form of discharge has been investigated for applying to efficient surface treatment processes. At atmospheric pressure, it is known that filamentary discharges are normally formed, however, their discharge characteristics are not clearly understood. Moreover, homogeneous barrier discharge characteristics are not known neither. The homogeneous barrier discharges are obtained in helium, nitrogen and other gases. And there are two types of discharges, Townsend discharge and glow discharge. For efficient surface treatment processes, atmospheric pressure glow discharge (APGD) in nitrogen is necessary. To investigate APGD in nitrogen, two dimensional fluid model has been developed. The discharge characteristics of high pressure barrier discharges in simple gas system have been simulated. As a result, homogeneous barrier discharges have been obtained and discharge developments are simulated clearly. Applying electric field uniformly between the gap and the slight photoionization are key points to obtain homogeneous barrier discharges. For further study, more complicated gas system will be considered in the model.

Contributed Papers

14:45

DM1 5 High Pressure NEQ Plasma Formation by Non-Self-Sustained Repetitively Pulsed Discharges WALTER LEMPERT, ADAM HICKS, MUNETAKE NISHIHARA, SETH NORBERG, J. WILLIAM RICH, IGOR ADAMOVICH, *Ohio State University* We describe generation of large volume ($\sim$ 1-2 cm dimension) stable, high pressure non-equilibrium plasmas, utilizing non-self sustained repetitive high voltage pulsing. Ionization is created by means of $\sim$ 10 KV – 10 nsec duration pulses, repeated at 100 kHz repetition rate. In between the high voltage pulses, the plasma is sustained by application of a relatively low DC or RF field, in which the reduced electric field, E/n, is selected to optimize energy loading into desired molecular degrees of freedom. Detailed measurements of i-V characteristics, plasma lifetime, and heavy species temperature will be presented, along with recent results documenting creation of large ($\sim$ 5% or more) fractional excitation of O_2 into the metastable ''single delta'' electronic state, which is the upper lasing level for the oxygen – iodine laser. Demonstration of turbulent supersonic boundary layer control using Lorentz forces will also be presented.

15:00
DM1 6 Air-Plasma Test Cell, Electron-Beam Source, and Measurements of Electron Density and Ozone Concentration ROBERT VIDMAR, *University of Nevada, Reno* KENNETH STALDER, *Stalder Technologies and Research* MEGAN SEELEY, *University of Nevada, Reno* An experimental facility at the University of Nevada, Reno, has recently been completed and initial testing is underway. A description of the facility for generation of air plasma from sea level to 300,000 ft, the electron-gun source, and two diagnostics will be discussed. The test cell has a volume of 400 liter, provisioning for electrodes to provide a sustaining electric field, and additional ports for future diagnostics. The ionization source consists of a pulsed 100 kV 10-20 mA electron beam and a thin-foil transmission window. The source provides plasma generation for approximately 1 ms and the diagnostics have sufficient bandwidth to resolve microsecond time dependencies. Electron concentration is measured using RF absorption and phase shift at X-band. Ozone concentration is measured by means of absorption at 254 nm in a White's cell. Results on initial measurements and plans for additional diagnostics to quantify other species will be discussed. This material is based on research sponsored by the Air Force Research Laboratory, under agreement numbers FA9550-041-1-0015 and FA9550-04-1-0444.

15:15
DM1 7 A comparison of lifted jet diffusion flame stabilization using corona, dielectric barrier, and repetitively- pulsed plasma discharges WOOKYUNG KIM, HYUNGROK DO, GODFREY MUNGAL, MARK CAPPELLI, *Stanford University* Three different types of discharges are applied to a lifted jet diffusion flame in coflow, and their abilities regarding flame stabilization enhancement are compared. First, a single-electrode corona discharge is obtained between a crown shaped platinum electrode and the flame base. It is observed that the flame is maintained at 20% higher coflow speed. Also, it is shown that the discharge direction is self-adjusting with varying electrode position. Second, an asymmetric dielectric barrier discharge is implemented and results in increased flame stabilization; here a flame stably resides at up to 50% higher coflow speed. In addition, the nonthermal aspect of the DBD is verified by a spectral line analysis and simulation of the nitrogen 2^{nd} positive system. Finally, an ultra short pulse generator (pulse width of ~ 10ns), is used in an opposed platinum electrode configuration. This approach further enhances the stability limit by nearly ten-fold. As discussed in the presentation, the degree of nonequilibrium of this pulsed discharge is found to be higher than the DBD.

SESSION DM2: PLASMA CHEMISTRY AND PLASMA-SURFACE INTERACTIONS
Monday afternoon, 17 October 2005; Cedar, Doubletree Hotel at 13:30
Zoran Petrovic, Institute of Physics, Belgrade, presiding

Invited Paper

13:30
DM2 1 Plasma-surface interaction: in situ and real time studies during plasma processing of materials. RICHARD VAN DE SANDEN, *Dept. Applied Physics, Eindhoven University of Technology*

In this talk I will review our approach to study in situ and in real time the surface kinetic processes occurring during plasma deposition and etching. We have chosen for a photon-in-photon-out approach and have developed novel ultra sensitive techniques to unravel the radical- and ion-surface interactions. I will discuss specifically the techniques of evanescent wave cavity ring down spectroscopy, second harmonic generation and spectroscopic ellipsometry which in combination with gas phase diagnostics such as cavity ring down spectroscopy and threshold ionization mass spectrometry provide an unique possibility to understand the surface kinetic processes. These studies enable the manipulation of the plasma properties to obtain specific material applications. Examples include the understanding of the plasma oxidation of ultra-thin aluminum films for magnetic tunnel junctions, the deposition of dense barrier layers for plastic electronics applications and the high rate deposition of surface and bulk passivating films for multi-crystalline solar cells.

Contributed Papers

14:00
DM2 2 FTIR characterization of the gas phase chemistry in pulsed 1,3-butadiene discharges in a Gaseous Electronics Conference (GEC) Cell ASHISH JINDAL, LAWRENCE OVERZET, MATTHEW GOECKNER, *The University of Texas at Dallas* FTIR Spectroscopy is used to characterize the gas phase chemistry of various pulsed regimes in a 1,3-butadiene ($H_2C{=}CHCH{=}CH_2$) discharge in an inductively coupled GEC reactor. Characterization is done as a function of the plasma on to off time at both constant and varying duty cycles. The power delivered during the on time is adjusted such that the time averaged power for all runs is maintained at a constant 10 W (13.56 MHz). The dissociation mechanisms for the observed chemical densities are investigated. For example, it appears that only the π bond of the C=C bond is cleaved for the shorter on times. At longer on times the remaining σ bond is also broken and a sizable fraction of the gas becomes free CH_2. This bond destruction has a profound impact on film growth and thus a link between the gas and surface phase processes will also be examined.

14:15
DM2 3 Influence of chamber scaling on different level polymerizing processing gases SANKET SANT, ERIC JOSEPH, BAOSUO ZHOU, LAWRENCE OVERZET, MATTHEW GOECKNER, *University of Texas at Dallas* We have previously examined influence of chamber scaling (both diameter and source to chuck gap) on fluorocarbon film deposition/etch for CF_4 plasmas[1,2]. In this paper, we extend those studies to more polymerizing fluorocarbon chemistry, C_4F_8. In CF_4 discharges, film growth on unbiased substrates go from deposition to etch as the

source to chuck gap increases. In C_4F_8 discharges film growth occurs for all gaps and chamber diameters examined. It is found that ions play an important role in deposition with CF_4 but not with C_4F_8. This difference may be attributed to the structures of the parent gases. Dissociation of a C-C bond in C_4F_8 may result in an 'unwrapping' of the cyclic structure. When this radical fills an open bond site on a surface, a new site is created. On the other hand, CF_3 will cap bond sites in CF_4 plasmas. Thus ion impact is required for site formation in CF_4 plasmas but not in C_4F_8 plasmas. [1] EA Joseph, et al., J. Vac. Sci. Technol. A 22 (3), May/Jun 2004 [2]BS Zhou, et al., J. Vac. Sci. Technol. (submitted).

14:30

DM2 4 O-atom Recombination on Anodized Aluminum in an Oxygen Plasma, Studied by a New "Spinning Wall" Technique. VINCENT M. DONNELLY, PETER KURUNCZI, JOYDEEP GUHA, *University of Houston* We have developed a new method for studying plasma-surface interactions. A cylinder coated with the material of interest (here, anodized Al) is embedded in the plasma chamber wall. Skimmers and differential pumping allow the plasma chamber to be operated at standard pressures (e.g. 10 mTorr) while the chamber on the opposite side of the cylinder is at high or ultrahigh vacuum, allowing the surface to be studied by line-of-sight mass spectrometer or Auger electron spectroscopy. When the sample is rotated at up to 200,000 rpm, the surface can be examined in as little as 0.2 ms after exposure to the plasma. By varying the rotation frequency the reaction time can be varied, thus allowing the kinetics of atom-surface interactions to be extracted. O_2 is observed to desorb when the surface is exposed to an oxygen plasma, due to heterogeneous recombination of O. The signal falls off rapidly as a function of decreasing rotation frequency at high frequency, and much more slowly at lower frequencies. This time dependence can be well represented by a multi-site adsorption model with mobile O diffusing from site to vacant site. Supported by ACS/PRF.

14:45

DM2 5 Hyper-Thermal Hydrogen Atoms Produced by Surface Neutralisation* TATIANA BABKINA, TIMO GANS, UWE CZARNETZKI, *Institute for Plasma and Atomic Physics, Ruhr-University Bochum, Germany* Hyper-thermal neutrals have significant potential for technological applications and can also play an important role in the power balance of plasmas. We present experimental investigations of the energy distribution function of the flux of hyper-thermal hydrogen atoms and compare results with data obtained using a computer simulation (TRIM). Hydrogen ions are produced in a magnetically confined inductively coupled RF plasma. They are accelerated from the plasma bulk towards a biased electrode by the plasma boundary sheath potential in front of the surface. Neutralisation and reflection of impinging ions at the surface result in hyper-thermal atoms. These atoms are investigated by optical emission spectroscopy; and a quantitative analysis of the energy distribution function is carried out using a mass resolved energy analyser. The obtained energy spectra can be explained as a superposition of individual spectra of the various ion species (H^+, H_2^+, H_3^+). Negative ions created at the electrode surface produce hyper-thermal neutrals with energies exceeding the sheath potential.

*The work is supported by the DFG (SFB 616).

15:00

DM2 6 Oxygen Plasma Ion Implantation in MgF2 Anti-Reflection Coatings M. TUSZEWSKI, K. SCARBOROUGH, *Los Alamos National Laboratory* Low-energy ($<$ 10 kV) oxygen (O+) plasma ion implantation is performed in the (100-nm-thick) MgF2 anti-reflection coatings of various solar panel coverglasses. O+ implantation could cause MgF2 darkening, and associated degradation of solar array power observed in Global Positioning Satellites (GPS). We irradiate various GPS coverglass samples with O+ doses up to 1015 cm-2, corresponding to a 10 year-exposure in simulated average oxygen environment at GPS orbit (20,000 km altitude). The O+ implants are performed with a low-pressure (0.5 – 3 mTorr) inductive plasma source and a commercial high-voltage pulser. Negative high-voltage pulses (5 – 20 microsecond widths, 1 – 10 kV amplitudes, 0.1 - - 2 kHz repetition rates) are applied to samples mounted on a downstream, water-cooled, electrode. The optical transmission (200 – 800 nm) of the samples is measured before and after each implant. Preliminary results suggest that the O+ implants indeed cause some optical transmission loss in the MgF2 coatings. The oxygen plasma density profiles, the electron temperatures, and the plasma potentials are measured with Langmuir probes. The oxygen species content are measured with optical and mass spectrometry. These measurements are required to estimate as accurately as possible the incident O+ doses.

SESSION EM1: ELECTRONEGATIVE PLASMAS
Monday afternoon, 17 October 2005
Pine, Doubletree Hotel at 16:00
Miles Turner, Dublin City University, presiding

Contributed Papers

16:00

EM1 1 Charged species' densities and fluxes in a dual-frequency capacitive plasma GARRETT CURLEY, JEAN-PAUL BOOTH, CORMAC CORR, JEAN GUILLON, SEBASTIEN DINE, *LPTP, Ecole Polytechnique, 91128 Palaiseau, France* Dual-frequency capacitively-coupled plasmas in fluorocarbon- based gases are widely used for etching holes in SiO_2- based dielectric films in integrated circuit manufacture. We are studying a customized 2 + 27 MHz industrial etch reactor, running in $Ar/C_4F_8/O_2$ gas mixtures at 50 mTorr. We have used an RF planar probe [1] to measure the positive ion flux and a microwave resonator probe [2] to measure the electron density. The ratio of the (central) electron density to the ion flux was observed to vary significantly with the feedstock composition, sometimes reaching values three times higher than that predicted by simple electropositive theories. We believe this indicates the presence of significant densities of F^- negative ions. We are currently attempting to measure the F^- density directly by high-sensitivity optical absorption techniques. [1]Braithwaite et al, PSST, 5 (1996), 677-684 [2]Piejak et al, J. Appl. Phys. 95 (2004), 3785-3791.

16:15

EM1 2 Ion Transport in Ion-Ion Plasmas* M. LAMPE, R.F. FERNSLER, S.P. SLINKER, S.G. WALTON, D. LEONHARDT, *Plasma Physics Div., Naval Research Lab* G. JOYCE, *George Mason University* When strongly electronegative source gases are used, the LAPPS e-beam-generated plasma device at NRL* is capable of producing a steady-state nearly electron-free positive ion / negative ion plasma. It is commonly thought that ion flux to a substrate, in such a plasma, is limited by thermal diffusion of ions in the core plasma. We present a new theoretical treatment which shows that strong ion flux occurs even in the limit of itzero ion temperature, if a DC bias is applied to the substrate. We show how this ion current scales with source strength, bias voltage, ion temperature, and device geometry. The theory will be used to interpret experimental results from the LAPPS experiment.* *See adjacent paper, ''Etching with Electron Beam-Generated Ion-Ion Plasmas,'' by S. G. Walton

*Supported by ONR

16:30

EM1 3 Electron and Ion Processes in Weak Plasmas THOMAS M. MILLER, *Air Force Research Laboratory* JANE M. VAN DOREN, *College of the Holy Cross* A.A. VIGGIANO, *Air Force Research Laboratory* I. New Plasma Effects Observed in a Flowing-Afterglow Plasma. In a study of electron attachment to C_6F_5Cl in a helium bath gas), we found the first case we know of in which a thermally-detaching ion product ($C_6F_5Cl^-$) results in competition with a thermally-stable ion product (Cl^-), at elevated temperatures (500-550 K). We hypothesize that the heavier ions are more confined to the core of the plasma, releasing fresh electrons all the while. A sudden transition is observed in the electron density decay as the $C_6F_5Cl^-$ concentration dies away. II. Electron Attachment to Fluorinated Pyridines. In this experiment we measured rate constants for electron attachment and electron detachment for C_5F_5N and C_5HF_4N. From the attachment/ detachment reaction rate constants, electron affinities were determined to be $EA(C_5F_5N) = 0.70 \pm 0.05$ eV and $EA(C_5HF_4N) = 0.40 \pm 0.08$ eV. The neutrals are planar, but calculations show the negative ions to have the F or H opposite the N atom to be significantly out-of-plane. Experimental and calculated values show an average decrease in EA of 0.25 eV per substitution of H for F. III. Ion-Molecule Reactions at High Temperatures. We will present data on negative ion-molecule reactions with molecules, obtained in a high-temperature flowing afterglow apparatus at temperatures from 300-1440 K.

16:45

EM1 4 Shading effect of electrons and positive ions in charging free plasma etching; In-situ measurement of temporal change of a contact hole charging in a pulsed two frequency CCP TAKESHI OHMORI, TAKUMI AKAIKE, TAKESHI K. GOTO, *Keio University* TAKESHI KITAJIMA, *NDA, Keio University* TOSHIAKI MAKABE, *Keio University* Miniaturization in ULSI progresses toward device elements of nanometer size, and charging damages during plasma etching will be actualized. All kinds of particle injected into a trench or SiO_2 contact hole with a miniaturized structure on a wafer is shaded base on the topographical and electrical profile. While it is common that the electron shading causes a bottom charging, we will exhibit an ion shading effect by using a measurement of the temporal change of the charging potential on the bottom surface in the pulsed 2f-CCP. In our previous work using an optical emission CT and contact hole potential[1], we showed a qualitative behavior of the charge reduction on the bottom during a short time by applying a single positive component (SPC) of the bias pulse in a pulsed 2f-CCP in CF_4/Ar. In the present work, we analyze and discuss the details of a temporal change of a SiO_2 hole charging during one on/off period of the VHF. The charging potential on the bottom increases and decreases by the injection of low energy negative charges and high energy positive ions during the period of the VHF, respectively. In addtion, negative charges accelerated by a double layer structure decrease the charging potential in a phase of SPC. [1] T. Ohmori, T. Akaike. T. K Goto and T. Makabe, 2004 57th GEC (2004).

Invited Paper

17:00

EM1 5 Double Layers in the expanding region of electronegative plasmas.
PASCAL CHABERT, *Ecole Polytechnique*

Double layers (DLs) have been studied over the past decades theoretically, numerically and experimentally (see the review by Raadu in Physics Report 178, 25 1989, and references therein). The biggest part of the literature treats the case of electropositive plasmas, however, DLs were also found in electronegative plasmas (both theoretically and experimentally). Recently, Charles and co-workers (Appl. Phys. Lett. 82, 1356, 2003) have observed a current-free DL in the expanding region of a helicon wave excited plasma at very low pressures (typically less than a millitorr). A strongly diverging static magnetic field seemed to be required in order to reach the conditions for double layer formation. Their system also had an abrupt change in radius at the boundary between the source and the diffusion chambers, which could possibly be a source of DL formation. Following this work, we have observed and studied double layers in a system of similar geometry but without B field and with electronegative gas mixtures. The DL's were not observed in pure argon. They seem to have a spherical shape and be formed at the boundary between the source and the diffusion chambers. They act as an internal boundary between a high electron density, high electron temperature, low electronegativity plasma upstream, and a low electron density, low electron temperature, high electronegativity plasma downstream. They are only stable for a small window of electronegativity. In most of the parameter space explored, they periodically form at the interface between the two chambers and they propagate at low speed (about 150 m/s) in the expanding chamber. We measured their amplitude and their dynamics by space and time-resolved langmuir probe experiments. Some explanations for their formation and propagation will be given.

SESSION EM2: PLASMA DIAGNOSTICS I
Monday afternoon, 17 October 2005; Cedar, Doubletree Hotel at 16:00
U. Czarnetzki, Ruhr University-Bochum, presiding

Invited Paper

16:00
EM2 1 RF Langmuir probes, revisited.
FRANCIS F. CHEN, *UCLA*

Though probes have been used for n_i and T_e measurements in rf plasmas for many years and commercial systems are available for automatic scans of $I - V$ curves, accurate results are by no means guaranteed. Strange $I - V$ curves obtained in the past two years have led us to re-examine the problem of Langmuir probes in low-density plasmas in severe rf environments. There are five main problems. First, the Bernstein-Laframboise theory used for small λ_D/R_p (Debye length/probe radius) have been shown to be inaccurate[1]. We therefore use thin probes and the OML (orbital-motion-limited) theory for large λ_D/R_p, but at low n the electron curve is not exponential. Second, we find that the plasma potential drifts with probe voltage V_p on a msec or longer timescale. This can be explained, but the effect is larger than expected. Third, the drift can be overcome by rapid sweeping of the $I - V$ curve, but too fast a V_p scan would be distorted by the inductance of the choke chain. Fourth, rf compensation is done with a chokes and a large compensation electrode[2] (CE). We find that CE cannot do most of the job; the chokes have to have large impedance at their self-resonant frequencies. But tuning the choke chain is not easy. Finally, cleaning the probe tip is difficult at $n \approx 10^9$ cm^{-3} because not enough current can be drawn to the probe. This is seen in very slow drifts of the ion current, in the order of seconds. A good rf probe requires careful construction of the compensation elements and judicious choice of the scan speed. [1]F.F. Chen, Phys. Plasmas **8**, 3029 (2001). [2]I.D. Sudit and F.F. Chen, Plasma Sources Sci. Technol. **3**, 162 (1994).

Contributed Papers

16:30
EM2 2 Absolute electron density measurement using the cut-off method in magnetized plasmas IKJIN CHOE, CHINWOOK CHUNG, *Division of Electrical Engineering, Hanyang University* Electron density measurement in magnetized plasmas is very difficult because electron saturation currents to Langmuir probes are greatly distorted. Recently, the cut-off probe measuring the plasma frequency in unmagnetized plasmas was developed [J.H. Kim, et. al., Appl. Phys. Lett., 83, 4725(2003)]. We constructed a cut-off probe and applied this method to measure electron densities in weakly magnetized plasma. The ordinary wave is used because its cutoff frequency is equal to the plasma frequency even in the DC magnetic field. The electron density is compared with the ion densities from the ion currents that are not affected by the magnetic fields. It is found that the measured electron density is proportional to the ion density. This cut-off method is expected to be one of reliable methods to measure electron density in magnetized plasmas.

16:45
EM2 3 Electron density measurements in inductively coupled plasmas using phase resolved optical emission spectroscopy* TIMO GANS, DEBORAH O'CONNELL, VICTOR KADETOV, UWE CZARNETZKI, *Institute for Plasma and Atomic Physics, Ruhr-University Bochum, Germany* The optical emission from radio frequency (rf) discharges exhibits temporal variations within the rf-cycle. Neglecting these variations in classical time averaged optical emission spectroscopy (OES), based on balance equations, can result in serious misinterpretation. The effect of neglecting temporal changes is not as pronounced in inductively coupled plasmas (ICPs) as in capacitively coupled plasmas (CCPs). However, even the relatively small modulations in ICPs can be exploited as a novel access for plasma diagnostics. The modulations of the optical emission are caused by temporal changes of the electron energy distribution function (EEDF). These modulations can be described within the two-term approximation of the Boltzmann-equation. This allows us to determine the induced electric field in the discharge. The penetration of the field into the plasma is determined by the Helmholtz-equation. A spatially resolved measurement of the amplitude and phase of the induced electric field, therefore, yields a 2-dimensional spatial map of the electron density.

*The project is funded by the DFG in the frame of SFB 591

17:00
EM2 4 Plasma density determination from surface-wave transmission spectra SEBASTIEN DINE, JEAN-PAUL BOOTH, GARRETT CURLEY, CORMAC CORR, JACQUES JOLLY, JEAN GUILLON, *LPTP, Ecole Polytechnique* We have developed a new plasma density measurement technique based on the transmission spectra of surface waves (SW) propagating along a plasma-sheath boundary. Simple theory indicates that the lowest frequency at which SWs can propagate is equal to $1/\sqrt{2}$ of the plasma frequency, allowing the plasma density to be determined. Our probe (Plasma Transmission Probe or PTP) consists of emitting and receiving antennas joined by a dielectric cylinder, all immersed in the plasma. A sheath forms around this device, creating a cylindrical wave-guide between the antennas along the sheath-plasma interface. The transmission spectrum was measured with a network analyser. Experimental spectra were measured in CCP discharges in argon (40-750 mTorr) and in an ICP, and are compared to the results of an axi-symmetric finite element model. The densities determined by this method were found to be lower by a factor 0.5-0.6 compared to those obtained with Langmuir and

hairpin probes. We attribute this to the density gradient in the pre-sheath around the PTP, which determines the sheath-edge density. The PTP is promising for the measurement of low densities ($< 10^{10}$ cm^{-3}) at relatively high gas pressure (> 0.5 Torr).

17:15

EM2 5 On the floating type Langmuir probe using the harmonic technique in inductively coupled plasmas SUNGHO JANG, MINHYONG LEE, CHINWOOK CHUNG, *Division of Electrical Engineering, Hanyang University* A floating type Langmuir probe using the harmonic technique and its driving circuit are developed and applied to measure the electron temperature and the ion density in inductively coupled plasmas(ICP). The reliability of the harmonic technique is checked by varying the amplitude and the frequency of the applied voltage and the current sensing resistance. Comparisons with a single Langmuir probe show that the electron temperature and the ion density from the floating-type probe are in good agreement with those from single Langmuir probes at various pressures and input rf powers.

SESSION FM: POSTER SESSION I
Monday evening, 17 October 2005
Fir/Oak, Doubletree Hotel at 19:15

FM 1 MATERIAL PROCESSING

FM 2 Low Pressure PECVD of SiO_xN_y Thin Films with Electron-Beam Generated Plasmas* DARRIN LEONHARDT, SCOTT WALTON, *Naval Research Laboratory* The deposition of thin films of SiO_2/SiO_xN_y is an integral part of flexible displays/electronics, medical implant bio-functionalization, as well as a robust barrier layer ideal for space applications. In all of these applications, such insulating layers must be uniform and defect free over large areas. In this work, modulated electron beam-generated plasmas were used to produce SiO_x/SiO_xN_y films from organic precursors (TEOS or HMDSO) with $Ar/O_2/N_2$ gases. The inherent low electron temperature of these plasmas results in low plasma fields and potentials, which in turn provide low energy (< 3 eV) ions to the substrate. Film properties (electrical, optical and chemical) with respect to gas mixtures, substrate temperature and ion energy will be presented. The incorporation of ion energy during deposition was critical in producing films with lower defect densities than typical deposition processes. Using the ion energy as an additional process control 'knob' the film composition ranged from stoichiometric SiO_2 to heavily hydrolyzed films. The incorporation of additional ion energy showed more dramatic effects at higher than anticipated values ($\sim$ 50 eV vs. 15 eV). Ion fluxes and energies to the substrate determined by mass spectrometry measurements will be correlated to the process variables, final film composition and recent studies in other plasma sources.

*Work supported by the Office of Naval Research

FM 3 Niobium surface modification in a microwave discharge MARIJA RASKOVIC, SVETOZAR POPOVIC, LEPOSAVA VUSKOVIC, *Old Dominion University* Surface preparation techniques for Niobium superconducting RF cavities commonly employ chemical or electrochemical polishing. With wet chemical polishing and the final dry air treatment, the formation of a non-superconductive Niobium oxide layer is unavoidable since oxidation starts as soon as the chemical process stops. For that reason a dry surface modification is highly desirable. Plasma etching may provide a unique opportunity to explore oxide-free surfaces by directly testing a cavity surface after processing without exposure to air. We studied the effects of a cavity microwave discharge in Ar and Ar-Cl_2 mixtures on removal of oxide layer of an electrically biased Niobium samples. Results on discharge characterization during the process will be presented at the conference.

FM 4 Anisotropic fluorocarbon plasma etching of Si/SiGe heterostructures* RUHANG DING, AMY WENDT, LEVENTE KLEIN, MARK ERIKSSON, *University of Wisconsin - Madison* Fluorocarbon plasma etching of SiGe heterostructures for fabrication of quantum devices is investigated. The heterostructures consist of layers of silicon and SiGe, and anisotropic etching of the heterostructures using plasmas to isolate device elements is an attractive approach to fabricating devices. A challenge that has limited the use of fluorocarbon etching is the difference in Si and Ge etch rates. Preferential etching of SiGe can lead to undercutting beneath the top silicon layer, causing a reduction in critical device dimensions of unknown magnitude. To improve anisotropy of the etch process, we propose the use of flourocarbon etch gases with higher carbon content, making use of fluorocarbon sidewall passivation to improve the anisotropy of etched feature profiles by preventing lateral etching of SiGe. Initial etch results in a $C_4F_8/Ar/N_2$ gas mixture show a straight sidewall profile through the layers of the heterostructure. Furthermore, control of the energy distribution of bombarding ions has been implement to enhance etch selectivity to PMMA used as an etch mask.

*Supported in part by the NSA and ARDA under ARO contract number W911NF-04-1-0389, NSF under Grant No. DMR-0325634, and by WARF.

FM 5 Industrial Carbon-Doped SiO_2 (CDO) Film Etching in $Ar/O_2/c\text{-}C_4F_8$ High Density Plasmas A. ISLYAIKIN, V. KRASTEV, I. REID, G. HUGHES, A.R. ELLINGBOE, *Dublin City University, Ireland* Etching of Si samples covered by a carbon-doped SiO_2 (CDO) film was performed using high-density $Ar/c\text{-}C_4F_8/O_2$ plasmas produced in an industrial TCP reactor under a wide range of plasma conditions. Mass spectral diagnostics were used for analysis of the chemical composition of the plasma neutral components and dominant etching products. A complete dissociation of $c\text{-}C_4F_8$ was found for all the experimental conditions. Analysis of chemical composition of the surface layer as well as the depth elemental distributions in the bulk of the CDO layers were performed by means of X-ray photoelectron spectroscopy (XPS). Deposition of a thin fluorocarbon surface layer was recorded. Correlation between the plasma characteristics and results of the plasma processing is the object of current investigation.

FM 6 Three-dimensional etching profile simulation using level set methods GON JUN KIM, SUNG JIN KIM, BRANISLAV RADJENOVIC, JAE KOO LEE, *Pohang University of Science and Technology* Surface evolution in plasma etching and deposition is a significant challenge for numerical methods. A level set method is a robust and accurate computational technique for mov-

ing interfaces. We have developed 2D/3D simulators for etching profile evolution using level set methods. A sparse field method, which is an alternative to the usual combination of narrow band and fast marching procedures for computationally effective solutions, is applied for solving the level set equation in the 3D etching profile simulation. In the level set equation, a speed function represents etching rate and depends on physical and chemical reactions. Thus, we find out the speed function, considering reactions of injected ions and redicals. Kinetic information of injected ions is obtained by one-dimensional particle-in-cell Monte Carlo collision (PIC-MCC) simulations. Charge-up potential is calculated during surface evolution. Ion reflections which have influence on etching profiles such as trenching and bowing are included to the 3D etching profile simulation. Etching profiles are investigated in respect to injected particles and physical and chemical reactions. *This work is supported by the national program for Tera-level nanodevices in Korea Ministry of Science and Technology.

FM 7 Ti Surface Oxidization by Microwave Discharge Oxygen Plasma and Plasma Parameters SATORU KAKIZAKA, TAKESHI SAKAMOTO, HARUAKI MATSUURA, HIROSHI AKATSUKA, *Tokyo Institute of Technology* TOKYO INSTITUTE OF TECHNOLOGY TEAM We made an experimental study on Ti surface oxidization by microwave discharge oxygen plasma, which was generated in a cylindrical quartz tube (26 mm id.) with its discharge pressure 0.5 - 10.0 Torr. The microwave frequency was 2.45 GHz and the output power was set at 600 W. The gas flow rate was set at about 0.01 – 1.6 l/min. The titanium sheet ($15 \times 15 \times 0.2$ mm^3) was set at the position 60 mm down from the centerline of the microwave guide. The treatment time was 1 hour. We measured basic parameters of microwave oxygen plasma, such as electron density (N_e), electron temprature (T_e) by a double probe, vibrational and rotational temperatures (T_v, T_r) by OES. It was found that the $N_e \sim 10^{11}$cm^{-3}, $T_e \sim 5$ eV, $T_r \sim 0.14$ eV and $T_v \sim 0.25$ eV, respectively, at a low discharge pressure. Only the rutile pattern was found for the samples by XRD. We are examining the effect of admixture of noble gases with oxygen.

FM 8 Plasma CVD of a-C:F Films Using C_8F_{18} and Characterization of their Properties YOSUKE SAKAI, SHOTA TAZAWA, YOSHIYUKI SUDA, HIROTAKE SUGAWARA, *Hokkaido University* We have composed low-k amorphous fluorocarbon (a-C:F) dielectric films on the surface of spherical Al electrodes using a C_8F_{18} plasma CVD for development of a composite insulation system. The relative dielectric constant k of the a-C:F films was less than 2.5. An a-C:F film of the thickness of 1 μm on the electrode enhanced the insulation tolerance of sphere-to-sphere electrodes systems in Ar, N_2 and He about 700 V around the pd values of their Paschen minima. The C_8F_{18} plasma was analyzed with optical emission spectroscopy and mass spectrometry. It was found that CF_3 was one of the major fragment species derived from C_8F_{18}. The intensity of the CF_3 appearance was 6–10 times as much as that of CF_2, which was considered to be a primary precursor of a-C:F@. In addition, C_2F_4 (= 100), C_2F_5 (= 119), C_3F_5 (= 131), C_3F_7 (= 169) and C_4F_7 (= 181) were detected by the mass spectrometry done in a molecular weight range $\leqslant$ 200. An FT-IR measurement showed that $=CF_2$ bonds more than $\equiv$ CF bonds were involved in the deposited a-C:F films. The F/C ratio measured by an XPS observation was 1.4–1.5, and this ratio seemed independent of the CVD condition in the range of the C_8F_{18} pressure of 0.2–0.4 Torr and the input power of 80–100 W@. The deposition rate was over 300 nm/min. This work was in part supported by a Grant-in-Aid of JSPS@.

FM 9 Noninvasive Measurement of Ion Energy Distributions in a Plasma Etching System SEJIN OH, CHINWOOK CHUNG, *Division of Electrical Engineering, Hanyang University* SUNGHO CHA, GICHUNG KWON, *Jusung Engineering Corporation* A monitoring of ion energy distributions is important during plasma etching processes. A commercial invasive ion energy analyzer is not well-suited to measure ion energy distributions because of various difficulties. A noninvasive monitoring technique in inductively coupled plasmas has been developed by M.A Sobolewski. We applied this technique to a plasma etching system. Plasma characteristic parameters and the rf bias dependent plasma potential were deduced by using the equations of power balance and particle balance to maintain completely noninvasive processes. The effects of source power, rf bias frequency, rf bias power, pressure and gas composition were measured. The experimental results agreed well with the predicted ion energy distributions.

FM 10 Laser Ablation Plasma Deposition and Ion Implantation of Hafnium and Hafnium-Oxide Thin Films* NICHOLAS M. JORDAN, RON GILGENBACH, MICHAEL JONES, LUMIN WANG, SHA ZHU, MICHAEL ATZMON, DONGCHAN JANG, Y.Y. LAU, NUCLEAR ENG. DEPT., UNIVERSITY OF MICHIGAN, ANN ARBOR, MI 48105 COLLABORATION, Experiments are underway to deposit and implant films of hafnium and hafnium-oxide on silicon substrates. A KrF laser (400 mJ @ 248 nm) ablates solid Hf foils or sintered pellets of hafnium-oxide. Silicon substrates can be negatively biased (either pulsed or DC) by voltages up to 10 kV for ion implantation. Ablation plasma plumes are characterized by optical emission spectroscopy, dye laser resonance absorption photography, resonant/non-resonant interferometry, and Langmuir probe diagnostics. Composition and morphology of deposited films are analyzed by Scanning Electron Microscopy, Transmission Electron Microscopy, X-ray Energy Dispersive Spectroscopy, X-ray Photoelectron Spectroscopy, and Atomic Force Microscopy. Thin film adhesion is also being tested. X-ray diffraction is being use to determine if the Hf films are amorphous or crystalline. Deposition rates are estimated to be on the order of 0.05 nm/pulse at a deposition rate of 20 pulses/s.

*This research was supported by an Applied Materials Graduate Fellowship.

FM 11 MAGNETICALLY ENHANCED PLASMAS

FM 12 Resolving the Plasma Sheath Layer in Two–Dimensional Magnetized Discharges* MARK CARTER, PHILIP RYAN, *Oak Ridge National Laboratory* DANIEL HOFFMAN, *Applied Materials* The nonlinear physics of sheaths is important to study, not only for the constructive use of sheaths in semi–conductor processing, but also for their destructive tenden-

cies in high power RF fusion applications. The disparity in device–to–sheath scale lengths often allows semi–analytical sheath models to be applied locally in a sheath layer, but whole–system models of realistic devices must be at least two–dimensional (2D) and require a consistent implementation of the sheath models. Whole–system models must also consider sources and transport of plasma outside the sheath layer, electromagnetic coupling throughout the entire RF circuit, and neutral gas flows through the system. In this paper, we present results from joining 2D models of plasma transport and RF power coupling (including static magnetic fields) with locally consistent sheath models using the Modular Oak Ridge RF Integeration Code (MORRFIC). Nonlinear power coupling is accounted for by modifying the local dielectric inside the sheath when resolving the layer. Relatively modest 64–bit computing facilities are used to iterate the RF sheath and nonlinear dielectric properties to be consistent with the RF global solution.

*Research sponsored under U.S. DoE contract DE–AC05–00OR22725.

FM 13 Biased substrate effects on ion characteristics in magnetized inductively coupled plasma* SANGHYUN JUN, HONG YOUNG CHANG, *Korea Advanced Institute of Science and Technology* Biased substrate can affect the plasma parameters related to ion heating. We suggest that bulk ions accelerated through sheath become energetic neutrals at the surface, and the neutrals may heat bulk ions again. DC bias is coupled to the substrate parallel and perpendicular to the magnetic field. The velocity distribution functions of the heated ions can be measured by diode LIF(Laser Induced Fluorescence) technique at 668.6nm for argon ion metastable LIF in magnetized ICP. We can take ion temperature, density and drift velocity from the velocity distribution functions.

*Sponsored by Korea Basic Science Institute (KBSI).

FM 14 Time-Resolved Optical Emission Studies of Pulsed DC Magnetron Plasmas* JOSE LOPEZ, WEIDONG ZHU, ABRAHAM BELKIND, *Stevens Institute of Technology* KURT H. BECKER, *Stevens Institute of Technology and Center for Environmental Systems* STEVENS INSTITUTE OF TECHNOLOGY, HOBOKEN, NJ, USA TEAM, CENTER FOR ENVIRONMENTAL SYSTEMS, HOBOKEN, NJ, USA TEAM Pulsed DC unbalanced magnetron sputtering is a well-developed deposition technique for coatings and thin films and is widely used in industry to deposit thin films such as alumina, Al_2O_3 and titania, TiO_2. The pulsed modulation of the direct current (DC) has been demonstrated to create plasmas that solve many of the arcing problems observed in DC magnetrons which can lead to non-uniform removal of material from the anode resulting in poor or unusable thin films for high-tech applications. The intense photon emission from the pulsed DC magnetron sputtering plasmas allows for the investigation of the optical plasma emissions with a fast intensified CCD (ICCD) camera. The non-intrusive diagnostic methods of time-resolved optical emission spectroscopy (TR-OES) and time-resolved imaging were used to study the temporal behavior of the various plasma species.

*Work supported by US Army and NSF.

FM 15 INDUCTIVELY COUPLED PLASMAS

FM 16 Model and Measurements for Closed Loop Control of an Inductively Coupled Plasma Source BERNARD KEVILLE, PETAR IORDANOV, DECLAN DOHERTY, *National University of Ireland, Maynooth, Ireland* MICHAEL B. HOPKINS, RONAN FAULKNER, *Dublin City University, Ireland* Process analysis and design and simulation of closed loop control algorithms require lumped parameter or low order models of plasma sources which reveal the essential dynamics of the system. Empirical models do not facilitate the simulation of process disturbances and hence an approach based on first principles is preferable. A physically-based, control-oriented model consisting of a global model of the plasma chemistry, together with a model of power deposition and models of the mass flow controllers and throttle valve has been used in the design and simulation of closed loop control algorithms for an inductively coupled plasma source with internal intenna. Multivariable closed loop control of an Argon/Oxygen plasma has been demonstrated experimentally and the use of a number of different sensors for feedback control has been investigated.

FM 17 Investigation of inductively coupled CF_4/O_2 discharges by Langmuir probe method and optical emission spectroscopy TAKASHI KIMURA, MASAHISA NOTO, *Nagoya Institute of Technology* The oxygen content dependence of the plasma parameters in inductively coupled CF_4/O_2 plasmas was investigated by Langmuir probe and optical emission spectroscopy. Plasma was produced in the cylindrical stainless steel chamber with 160 mm in inner diameter and 75 mm in length. Experiment was performed at three total pressures of 8m, 15m and 25 mTorr. The electron energy probability functions (EEPFs) were approximately Maxwellian at any oxygen content, although a slight enhancement of EEPF with respect to a Maxwellian distribution was observed at the energy region lower than 2-3 eV for the oxygen content lower than 70%. The electron density decreased in the oxygen content below 20%, beyond which it remained nearly constant. On the other hand, the measured electron temperature did not depend strongly on the content. The densities of fluorine and oxygen atoms were also investigated by actinometry method. The fluorine atom density increased markedly as oxygen was mixed to CF_4 discharges, and then reached the maximum around the oxygen content of 20 - 30%, beyond which it decreased with increasing oxygen content. The oxygen atom density increased with the increase in the oxygen content and saturated at about 50% oxygen content. A global model for electronegative plasma was used in order to study the dependence of the plasma parameters on the oxygen content assuming the Maxwellian electron energy distribution.

FM 18 Improvement in Uniformity of Linear Inductively Coupled Plasma for Large Area Processing S.M. CHOI, S.H. LEE, J.K. LEE, *Pohang University of Science and Technology, S.Korea* K.N. KIM, G.Y. YEOM, *Sungkyunkwan University, Korea* The external planar ICP sources with low pressure high density plasma have limited scale-up capabilities due to its high impedance accompanied with the large antenna size. The novel internal-type linear inductive antenna system (1020mm830mm437mm) is investigated to improve both the plasma density and the uniformity of LAPS for FPD processing.

Until now, we have observed the characteristics of LAPS under various conditions to overcome the problems stated above. The total length of antenna is comparable to the driving rf wavelength to cause the plasma non-uniformity and so the uniformity is improved by reducing the standing wave effect. We will show the effects of various antenna shapes and permanent magnet that reduce standing wave effect, electron loss to chamber wall and finally the effects of the parallel resonance antenna that controls the current at each segment of antenna with a variable capacitor. To describe the discharge phenomenon we have utilized a magnetized two-dimensional fluid simulation. [References] 1. S.E.Park, B.U.Cho, Y.J.Lee, and G.Y.Yeom, and J.K.Lee, ''The Characteristics of Large Area Processing Plasmas,'' IEEE Trans. Plasma Sci., Vol.31, No.4(2003) 2. K.N.Kim, S.J.Jung, Y.J.Lee, and G.Y.Yeom, S.H.Lee and J.K.Lee, ''Low-impedance internal linear inductive antenna for large-area flat panel display plasma processing,'' J. Appl. Phys. 97, 063302(2005).

FM 19 Chlorine atom measurements in Ar:Cl_2 discharges. F.G. MARRO, *Queen's University Belfast, Northern Ireland* W.G. GRAHAM, *Queen's University Belfast, Northern Ireland* Two-photon Laser Induced Fluorescence has been used to measure the chlorine atom density in an inductively coupled discharge. A 233.3nm beam was focused into a 130μm waist 2-3 cm above the lower electrode pumping the ground state $3s^23p^5(^2P^0_{3/2})$ to the excited level $3s^23p^44p(^4S^0_{3/2})$. From the three radiative decay channels at 725.6, 754.7 and 774.5nm, the strongest one, 725.6nm, was monitored. The UV photons were obtained from mixing an Nd:YAG fundamental (1064nm) and the second harmonic of a DYE laser. Relative and total measurements were performed in pure chlorine and in Ar:Cl_2 mixtures. A calibration based on CCl_4 photolysis was used. The estimated dissociation shows values as high as 33% near the transition between the capacitive and the inductive coupling. An unexpected decay of the atom density with power was observed in the inductive mode. The dependence of the atom density as chlorine is introduced into an argon discharge is linear. Doppler broadening was estimated from the line-shape, suggesting that the atomic temperature rises a few hundred Kelvin in the inductive mode. A kinetic model has been developed which shows that gas heating and the surface recombination coefficient have an important effect on the dissociation.

FM 20 Study of non-local electron kinetics in a low-pressure afterglow argon plasma* SERGEY GORCHAKOV, FLORIAN SIGENEGER, DIRK UHRLANDT, *INP Greifswald, F.-L.-Jahn-Str. 19, 17489 Greifswald, Germany* Non-isothermal pulsed plasmas are widely used for technological applications. The specific properties of these plasmas could be adjusted by appropriate choice of operation conditions. In particular, the switch-off period of a discharge has a strong influence on the time-averaged plasma properties. In this contribution results of theoretical investigations of the early afterglow, i.e. the range of few microseconds after switching off the power input, in an argon plasma of an inductively coupled discharge at pressures of few Pa are presented. Under these conditions the kinetic behaviour of the electron component dominates the plasma properties. The plasma is studied by means of a self-consistent model which includes the non-local electron kinetic approach taking, in particular, the impact of electron-electron collisions and of electron cooling due to ambipolar losses to the walls (diffusive cooling) into account. The results for temporal evolutions of the velocity distribution function, density and mean energy of electrons and the space-charge potential are discussed in comparison with recent experimental data. Good agreement has been found. The analysis confirms the significant influence of the diffusive cooling on the plasma properties and shows a marked impact of electron-electron collisions on the afterglow behaviour.

*Supported by Deutsche Forschungsgemeinschaft, project Uh 106/2-1.

FM 21 Optical emission and self mode transition of low frequency inductively coupled plasmas driven by crossed internal oscillating currents YUPING REN, PAVLO RUTKEVYCH,* JIDONG LONG, QIJIN CHENG, SHUYAN XU, *PSAC/NIE/NTU, Singapore* KOSTYA OSTRIKOV,† *School of Physics, The University of Sydney, Australia* Optical emission and self induced electrostatic (E)-to-electromagnetic (H) mode transition in a newly-developed plasma reactor are investigated. Volume uniform, high density Ar/N2 plasmas are generated by means of transverse unidirectional currents driven by a low frequency RF power of 460 kHz in a 23 cm height and 32 cm diameter reactor. Plasma properties are investigated using a high-resolution optical emission spectroscope. The measurements reveal that the spatial profiles of the excited atomic naturals and singly ionized ions feature a high degree of uniformity in radial and axial directions. A spatially homogeneous E-mode discharge is observed at a power level as small as 40 W. At RF power exceeding a transition threshold of 230 W, the integral emission intensity suddenly jumps to approximately one order of magnitude (H-mode). Further increase of RF power results in a gradual rise of the optical emission intensity. This phenomenon is reproducible for all discharges under the investigation. Furthermore, a spontaneous E-> H mode transition (''self-transition'') is observed at input power slightly below the conventional transition threshold value.

*Presenting author.
†Also with: PSAC/NIE/NTU, Singapore.

FM 22 Neutral gas collisional heating and the 0D/1D modeling in a semiconductor plasma reactor MASASHI SHIMADA, GEORGE R. TYNAN, *Department of Mechanical and Aerospace Engineering, University of California, San Diego* The significant neutral gas temperature increase has been observed in various noble gases in the center of an inductively coupled plasma (ICP) chamber and the actual neutral gas pressure has been obtained by considering the thermal transpiration effects with this neutral gas increase. A plate which consists of 8 vertical optical ports with collimating lens and a movable optical fiber probe have been developed and used to measure axial and radial profile of gas temperature in an inductively coupled plasma reactor respectively. The rotational temperature obtained from the second positive band of Nitrogen molecule has been compared with the Doppler broadening translational temperature of the noble gas (Ar/He) emission line in a various partial pressure of N_2 in Ar/N_2 and He/N_2 mixture, and both temperature have been observed to be in equilibrium in the conditions of our plasma experiment. 0D/1D neutral gas heating model have been developed and compared with experimental results. Monte Carlo simulation have been carried out to model the ion acceleration by pre-sheath electric field.

FM 23 PLASMA BOUNDARIES

FM 24 Consistent matching of plasma and sheath KARL-ULRICH RIEMANN, *Ruhr-University, D 44780 Bochum, Germany* Due to the sheath edge singularity, the asymptotic ($\epsilon \sim \lambda_D/L \rightarrow 0$) plasma- and sheath solutions cannot be matched smoothly. The sheath edge singularity, however, can be bridged by an intermediate scale analysis accounting in lowest order both for plasma processes (e.g. collisions, ionization, and non-planar geometry) and space charge. The possibility to construct a uniformly valid matched asymptotic expression from the plasma -, intermediate -, and sheath solutions was questioned in the literature. Problems arise from the asymptotic singularities and from the ionization eigenvalue problem of bounded plasmas (plasma balance). To clarify the topic we analyze the plasma-sheath problem both analytically and numerically. We show that the validity of the intermediate scale analysis is limited to a very narrow vicinity ($|\Delta\varphi| \leqslant 0.1$) of the sheath edge and formulate a matched asymptotic expression uniformly valid from the plasma core to the wall. The approximations obtained by matching are compared with exact solutions and discontinuities in the derivatives are investigated analytically.

FM 25 A bounded active magnetized plasma over a wide range of collisionality RAOUL FRANKLIN, *Open University, Oxford* At the last GEC Sternberg gave a treatment of this problem in the collisionless limit, and with the magnetic field at a variable angle to the wall. This is extended to include the effect of collisions on the ion motion in the constant collision frequency for momentum model ν_i. The relevant parameters are ω_{ci}, the ion cyclotron frequency, the plasma half size L, the central Debye length λ_{D0}, and the ionization frequency Z. For $\nu_i = 0$ the results of Sternberg and Poggie are recovered and the dimensionless quantities used in the description of the results here are λ_{D0}/L, ω_{ci}/Z, ν_i/Z and the angle Ψ. The eigenvalue is ZL/c_s. As ν_i/ω_{ci} becomes greater than 1 the effect of the magnetic field is nullified, as is to be expected on physical grounds. Sternberg N and Poggie J (2004) IEEE Trans. Plasma Science **32**, 2217.

FM 26 Investigation of a Planar Langmuir Probe Orientated Parallel to the direct of Flow in a Laser Ablation Plasma PETER SHEERIN, MILES M. TURNER, *Dublin City University, Ireland* BRENDAN DOGGETT, JAMES G. LUNNEY, *Trinity College Dublin, Ireland* Langmuir probes are a well established tool for investigating the characteristics of laser produced plasmas. Such plasmas typically take the form of highly directed plumes, with flow velocities that are supersonic with respect to the ion sound speed. The behaviour of planar Langmuir probes in such conditions are dependant on both the plasma parameters and the orientation of the probe with respect to the flow. The theory for such probes in supersonic flowing plasmas is not well developed. This limits their usefulness as diagnostic tools in the various applications where such conditions are encountered. The adaptations made to the associated theory of plasma ion implantation (PIII) to describe the I-V characteristics of the planar Langmuir probe in a flowing plasma are discussed. The resultant analytical theory when used in combination with one dimensional particle in cell simulations is shown to provide an excellent description of the behaviour of the planar Langmuir probe in a flowing plasma at early times.

FM 27 Energy Distributions of Ion Drift to the Cathode in a DC Microdischarge TSUYOHITO ITO, MARK CAPPELLI, *Stanford University* The cathode sheath serves many important functions in a discharge. A DC microdischarge has a relatively high ratio of cathode surface area to volume. Understanding the structure of the sheath and its associated physical phenomena is even more critical to the understanding of microdischarges. In this study, the ion energy distributions (IED) in the cathode sheath of a DC microdischarge were measured. The pressure-gap distance product was fixed at 1 cmTorr with a pressure from 2 Torr to 20 Torr. The measured IED was analyzed by the expanded theory of Davis and Vanderslice. The results indicate that a scaling law of pressure-normalized current density is no longer applicable. The background gaseous temperatures expected from IED and the collisional Child law is seen to increase with increasing current. Moreover, the expected temperature shows good agreement with that estimated by Doppler broadening via laser absorption spectroscopy. Given this result, it is concluded that the expanded theory might accurately describe microdischarges at least over the discharge conditions studied here.

FM 28 Different modes of arc attachment at HID cathodes: Simulation and comparison to measurements OLIVER LANGENSCHEIDT, LARS DABRINGHAUSEN, STEFAN LICHTENBERG, JUERGEN MENTEL, PETER AWAKOWICZ, *Ruhr-University of Bochum* Based on a model for the plasma boundary layer of high intensity discharge (HID) cathodes simulations are performed and compared to experimental results. To solve the power balance of the cathode body 1D, 2D and 3D finite-element calculations are used. The simulations are done for cylindrical tungsten cathodes operated in different pure noble gas discharges (0.1.. 1.0MPa) and with currents between 0.5A to 10A. Under these conditions different modes of arc attachment are found both in simulations and experiments. For the diffuse mode of arc attachment an excellent quantitative agreement between measurements and the simulations is obtained reflecting an improved accuracy of measurements and of simulation. In addition different spot modes are found. At least one of these modes is also observed in the experiment. Also for this spot mode the agreement between measurements and simulation for the integral quantities is good but there are still some open questions concerning the spot mode of cathodic arc attachment. Evaluating the cathode fall characteristics regions of existence for the different modes are found, which are similar to the experiments.

FM 29 Studies of sheath physics in two ion species plasmas with diode laser LIF* GREG SEVERN, *University of San Diego* NOAH HERSHKOWITZ, *University of Wisconsin-Madison* M.M. TURNER, *Dublin City University, Dublin Ireland* USD-UW-DCU COLLABORATION Recent diode laser based Laser-Induced Fluorescence (LIF) measurements of Ar ion flows at the sheath-presheath boundary in single and multiple ion species plasmas have confirmed that the usual Bohm Criterion holds for the single ion species plasma but must be generalized for multiple ion species plasmas to include the possibility that the ions may reach the sheath edge traveling either faster or slower than its individual ion sound speed. These results are in accord with the Generalized Bohm Criterion and PIC code simulation results for the experimental case of two ion species plasmas which are relatively collisionless and of low temperature (ArI+HeI plasmas, $P_{ArI} \sim 0.1mTorr, 0 \leqslant P_{He}/P_{Ar} \leqslant 25$, and $\lambda_{Debye} \ll \lambda_{mfp}, T_e \leqslant 2eV$). Both experimental and numerical simulation results will

be presented concerning the details of the ion velocity distribution functions (ivdfs) near the sheath edge in two ion species plasmas for the cases of He and Xe ions as the other ion species besides Ar. Our goal is ultimately to diagnose both ion species in a two ion species plasma with diode laser LIF, some thing which is still difficult to do, but which would significantly extend the range of possible experiments that test existing theory.

*Work supported by DOE grant DE-FG02-03ER54728, and NSF grant CHE0321326.

FM 30 Effect of bombarding ion energy distribution on ion/surface interaction during fluorocarbon plasma etching* AMY WENDT, SHUNTEL WILLIAMS, YUK-HONG TING, *University of Wisconsin-Madison* SATOSHI HAMAGUCHI, *Osaka University* In earlier studies, etch rate measurements in fluorocarbon plasmas showed a surprisingly significant dependence of fluorocarbon etch/deposition rate on the energy *distribution* of bombarding ions (IED). Understanding this result has implications for the many etch processes that depend on selective fluorocarbon deposition to control etch selectivity. Toward this end, an analysis was conducted of the nonlinear effects resulting from ions of different energies interacting with a surface simultaneously. The analysis made use of available data on the interaction between fluorocarbon ion beams of single fixed energy interacting with a silicon surface. The outcome was a simple model that illustrates and quantifies an important nonlinear effect: specifically, that the effect of ions of a particular energy on the substrate is sensitive to the presence of ions of other energies. The etch/deposition rate resulting from ions of different energies reaching the substrate simultaneously is not just the linear combination of the rates resulting from ions of each energy interacting with the surface on their own. The nonlinearity arises from differences in the chemical composition of the interaction region at the surface of the substrate, resulting from changes in the IED.

*Supported by NSF award # ECS-0078522, and JSPS.

FM 31 Photoresist covered wafer charging effects in pulsed plasma assisted ion implantation JI HYUN HUR, GYUNG SOO KEUM, JAE HYUNG WON, JAE JOON OH, JAI KWANG SHIN, MATERIALS AND PROCESS DESIGN TG, CSE CENTER, SAMSUNG ADVANCED INSTITUTE OF TECHNOLOGY TEAM, FAB EQUIPMENT TECHNOLOGY GROUP, SAMSUNG ELECTRONICS TEAM Ion implantation is a process in which energetic, high flux ions are directly introduced into a substrate such as silicon, poly silicon, and photoresist covered wafers. As a wafer is being implanted, ions can lead to positive charge build-up on the wafer. Especially for a low conductivity wafer like silicon dioxide or photoresist covered wafer, charging issue becomes more severe. Such charge build-up can cause two major problems. One is altering plasma conditions which results in reduction of ion energy and ion flux so that implantation condition is shifted lower energy/current process. And the other is wafer surface arcing owing to the large potential difference between wafer surface and powered electrode. We studied wafer charging effects in pulsed plasma assisted doping(P2LAD) for photoresist covered wafers by means of fluid plasma simulations. The results are discussed in comparison with experimental results.

FM 32 GLOWS I

FM 33 A multi-beam model for low-current, very high E/N discharges in hydrogen. A.V. PHELPS, *JILA, University of Colorado and NIST* The multi-beam model of Helm and Störi[1] has been applied to the motion and reactions of H^+, H_2^+, H_3^+, fast H_2, and fast H in H_2 for a uniform electric field. Plots of most of our analytic expressions for the cross sections are available[2]. Elastic scattering of non-identical particles is modelled with an energy loss for backward scattering in center-of-mass and the elastic momentum transfer cross section. For identical particles, we use the energy loss for 90° scattering and the elastic viscosity cross section. Calculated rates of excitation of H_α and the uv continuum versus distance and pressure are compared with experiments[3,4]. Calculated ion and fast neutral fluxes at the cathode will be compared with calculations using Monte Carlo methods[5].

[1]D. Helm and H. Störi, J. Appl. Phys. **72**, 3330 (1992).
[2]A. Bogaerts and R. Gijbels, Spectrochim. Acta Part B **57**, 1071 (2002).
[3]H.A.M. Blasberg and F.J. de Hoog, Physica **54**, 468 (1971).
[4]Z.Lj. Petrović, B.M. Jelenković, and A.V. Phelps, Bull. Am. Phys. Soc. **37**, 1951 (1992).
[5]T. Simko, Z. Donkó, and K. Rózsa, 23rd Intl'l. Conf. on Ionization Phenomena in Gases, (Univ. Paul Sabatier, Toulouse, 1997), p. II-64.

FM 34 NO kinetics in pulsed DC low-pressure discharge: influence of TiO_2 surface LINA GATILOVA, OLIVIER GUAITELLA, ANTOINE ROUSSEAU, *LPTP-Ecole Polytechnique CNRS, Palaiseau, France* YURY IONIKH, *St. Petersburgh State University-Russia* STEFAN WELZEL, JURGEN ROEPCKE, *INP-Greifswald-Germany* NO, NO_2, N_2O are readily formed in air discharge plasma. The study of their formation and destruction in plasma are of interest for environmental protection from industrial emissions. This interest has stimulated extensive experimental and theoretical investigations devoted to studying of air plasmas kinetics. Recently, measurements performed in the afterglow of a pulsed DC discharge showed that NO density scales as a universal function of the averaged power for a very wide set of pulse duration, repetition rate and current; this was analysed using a simple model of the NO_x kinetics [1]: the main source of NO formation is the reaction of $N_2*(A^3\Sigma_u^+)$ with atomic oxygen O. In the present work, time-resolved absorption spectroscopy measurements of NO concentration were performed in-situ the positive column of a low-pressure pulsed DC discharge in order to validate this model. It is first shown that NO production during one single plasma pulse is a linear function of the Ixt product where I is the pulse peak current and t the pulse duration.Then, we show that the presence of porous semi-conductor material (TiO2) inside the plasma region leads to a strong decrease of the NO production. [1] A. Rousseau, L. Gatilova, J. Röpcke, A. V. Meshchanov, Y. Ionikh Appl. Phys. Lett 86, 211501 (2005).

FM 35 Benchmark simulations of electronegative discharges DEREK MONAHAN, MILES M. TURNER, *Dublin City University, Ireland* There has recently been much interest–and some controversy–concerning the structure of electronegative discharges. These discharges can exhibit complicated spatial struc-

tures including stratification into electropositive and electronegative regions. Moreover, there are appreciable differences between discharges where the dominant negative ion destruction mechanism is detachment and those where it is recombination. In this paper we present benchmark particle-in-cell simulations for discharges in Ar/O_2 mixtures. These simulations cover a wide range of conditions in terms of collisionality, electronegativity, and negative ion destruction mechanism. We will discuss the changes in the spatial structure of the discharge that occur as the conditions change, including the appearance of structures such as double layers.

FM 36 Critical Evaluation of the Global Model Approximation DEREK MONAHAN, MILES M. TURNER, *Dublin City University, Ireland* The assumptions and simplifications typically associated with volume-averaged, or global, plasma chemistry models greatly limit the parameter domain over which they may be reliably applied. Well defined boundaries to these domains, however, have not been established and often only minimal model validation is offered in the literature. The aim of this project is to critically evaluate the performance of a global model over a range of parameters and gas compositions by comparing such a model to a more elaborate one dimensional kinetic simulation. The motivation for this work has arisen from the need for reliable and computationally inexpensive qualitative models in real time freedback control applications. In this paper initial findings are presented. It is found, as expected, that the most significant limitation of such a model appears to be the assumption of a Maxwellian electron energy distribution. The propensity of capacitively coupled discharges to develop energy distributions which are significantly non-Maxwellian, is well known. However, we have observed similarly restrictive behaviour in PIC simulations of a low pressure inductively coupled argon plasma. In our simulations the electrons appear to develop a bi-Maxwellian like distribution as pressure is increased above $\sim$ 10 mTorr. The volume averaged mean electron energy is then found to rise slowly with increasing pressure beyond this point. This is in direct contradiction with simple global model arguments. The source of this high energy tail is currently being investigated.

FM 37 Characterization of pulsed discharges for next-generation plasma processes SANG-HUN SEO, SHIN-JAE YOU, *KAIST* DONG-SEOK LEE, *Samsung Electronics* SANG-WON LEE, *Plasmart Co.* HONG-YOUNG CHANG, *KAIST* LOW-TEMPERATURE PLASMA LAB. KAIST TEAM, PLASMART CO. COLLABORATION, SAMSUNG ELECTRONICS COLLABORATION, As the device size is rapidly shrunk, various issues have been encountered in plasma etching processes for manufacturing of semiconductor with feature size of few tens nm. In particular, the deep contact hole etching with high aspect ratio becomes more and more difficult with reducing the contact-hole size and the serious distortions of contact profile are observable. Although several mechanisms on the distortion of contact profile, especially bowing and necking, have been suggested, any solutions on the basis of these mechanism have not been proposed. In this study, we concerned about the local pressure around the etched hole and propose new mechanism on bowing, tilting, and necking. In small and high-aspect-ratio contact, ions incident to the contact hole can give an amount of pressure to the by- products which are formed inside the contact hole and pumped out outside the contact hole, resulting in the increase of local pressure around the contact hole. We call this the ion-pressure effect. For the relief of the ion pressure, we investigated the pulse-modulation of rf power in ICP and CCP as the preliminary work and found that the modulation of bias power instead of source power is needed to relieve the incident ion pressure.

FM 38 Observations of Ionization Waves in Argon Glow Discharges using a Microwave Hairpin Resonator NICHOLAS SIEFERT, BISWA GANGULY, *Air Force Research Laboratory WPAFB* We use optical and electrical diagnostic tools, as well as the hairpin resonator, to observe large-amplitude fluctuations in light emission, electric field and electron number density due to traveling ionization waves in argon glow discharges. The location of maximum production of ionization and the location of maximum electron number density are over 180^o out of phase in ionization waves under our discharge conditions. The production rates of electrons peaks where the electric field is greatest; however, the electrons accumulate where the electric field is near its minimum. To measure the changing electron number density in these waves, we have revisited the hairpin resonator technique [R.L. Stenzel Rev. Sci. Instrum. 47, 603 (1976)]. We solve the wave equation with electron-neutral collisions and show that correction to the electron number density is less than 5% for pressures at or below 1 Torr. The wave frequency varies from 2 kHz to 5 kHz, depending on pressure and current. The data shows that both the light emission and the electric field are in phase with each other, but they are out of phase with the electron number density by 185^o-265^o. This is consistent with the current continuity equation. The effect of pressure and current on both the phase difference and the peak electron number density will be presented.

FM 39 ELECTRON AND POSITRON COLLISIONS WITH ATOMS AND MOLECULES

FM 40 Benchmark calculations for electron collisions with FeII* OLEG ZATSARINNY, KLAUS BARTSCHAT, *Drake University* We have applied the *B*-spline *R*-matrix method [1] to study electron collisions with Fe^+ over an energy range from threshold to 10 Ry. A major challenge for this astrophysically important collision system is the very complex target structure, with a strong term-dependence in the individual orbitals. Using a multi-configuration Hartree-Fock method with non-orthogonal orbitals, we generated a target description of unprecedented accuracy in collision calculations. Our results for individual cross sections and effective collision strengths are in qualitative agreement with the predictions by Ramsbottom *et al.* [2]. A few significant discrepancies are found in the low-energy regime, which is dominated by resonance structures. [1] O. Zatsarinny and C. Froese Fischer, J. Phys. B **33**, 313 (2000). [2] C.A. Ramsbottom, C.J. Noble, V.M. Burke, M.P. Scott and P.G. Burke, J. Phys. B **37**, 3609 (2004).

*Work supported by the NSF under PHY-0244470 and PHY-0311161.

FM 41 Ground and Excited State Cross Sections for Electron Impact on Cesium* WILLIAM McCONKEY, MICHAL LUKOMSKI, TIMOTHY REDDISH, SEAN SUTTON, WLADEK KEDZIERSKI, *University of Windsor* We report some of the most interesting results of our ongoing [1,2] investigation of electron collisions with cesium atoms localized in a Magneto-Optical Trap (MOT). The trap loss technique used was pioneered by Lin and co-workers [e.g. 3], and does not require knowledge of the absolute target density. The choice of an appropriate pulsing scheme has enabled total cross sections for the ground (Cs $6\,^2S_{1/2}$) and $6\,^2P_{1/2}$ excited states to be determined. Furthermore, preliminary results of total ionization cross sections will also be presented. Our earlier studies [1] covered a 100-400eV energy range for the incident electrons. Recent significant modifications to the apparatus have resulted in a more efficient data acquisition rate and have enabled us to extend the energy range down to 5eV. This low energy capability is important as in this region the discrepancies with other experimental work and with theory become apparent. [1] J. A. MacAskill et al, J. Elect. Spect. and Rel. Phen., **123**, 173 (2002). [2] M Lukomski et al, J Phys B, **38**, (2005), Submitted. [3] R. S. Schappe et al, Europhys. Lett., **29**, 439, (1995).

*Supported by NSERC, CFI and OIF.

FM 42 Optical potential calculation of elastic electron scattering from heavy noble gases ALLAN STAUFFER, *York University, Toronto, Canada* ROBERT McEACHRAN, *Australian National University, Canberra, Australia* We have developed a complex optical potential within the framework of the Dirac equations to account for the absorption of flux into the inelastic channels for electron scattering at intermediate energies. We have used Dirac-Fock wave functions to represent the fine-structure excited states of the atomic target. Detailed results will be given for elastic scattering from argon, krypton and xenon.

FM 43 A New, High-Resolution Positron Beamline JAMES SULLIVAN, VIOLAINE VIZCAINO, JENS HUFT, GERARD ATKINSON, *Australian National University* ADRIC JONES, *Flinders University* STEPHEN BUCKMAN, *Australian National University* AUSTRALIAN POSITRON BEAMLINE FACILITY TEAM A new positron beamline has been constructed based on the techniques established by the Surko group at UCSD. The beamline uses a buffer gas trap system to trap and cool positrons before producing a pulsed high resolution positron beam, for the study of atomic and molecular collision processes [1]. The system has been designed to take advantage of the techniques developed in San Diego for studying scattering in a magnetic field, which have revolutionised the study of low energy positron collisions. However, experiments on helium are impossible on the San Diego system, due to the use of cryopumps for maintaining vacuum. To allow for experiments on helium, the new experiment uses turbopumps. In addition, a charge sensitive detection system is also in place, enabling the use of electrons in the system. This not only provides for a direct comparison with well known electron cross sections, but also will allow the new techniques to be applied to electron scattering, in particular with regards to total excitation cross sections, where measurements have been difficult using conventional scattering techniques. [1] Gilbert et al., Appl. Phys. Lett. **70**, 1944 (1997).

FM 44 Elastic and Vibrational Cross Sections in Methane and Cyclopropane MICHAEL ALLAN, *University of Fribourg* There is a general agreement about the elastic cross sections in methane in the literature, but substantial discrepancies exist about the vibrational cross sections. This work measures absolute differential elastic and vibrational cross sections from nearly threshold to 20 eV. The cross sections are measured over a large angular range using the magnetic angle changer. All four vibrations are resolved at low energies. Earlier relative measurements {(M. Allan and L. Andrić, *J. Chem. Phys.* **105**, 3559 (1996)} have revealed large differences in the shapes of the cross sections in propane and cyclopropane due to an $l = 3$ shape resonance made possible by the C_3 axis in cyclopropane. The present work extends the existing measurements and presents absolute cross sections.

FM 45 Measurement of the Elastic and Vibrational Cross Sections in N_2 Over a Wide Angular Range MICHAEL ALLAN, *University of Fribourg* The poster will report on the recent improvements of the techniques to measure elastic and inelastic electron-molecule cross sections. Emphasis will be given on the measurement of the cross sections as a function of scattering angle over a large angular range using the 'magnetic angle changer' (MAC) invented by Frank Read and co-workers and on the measurements at low energies. It will be shown that measurement of cross sections in general and the use of the MAC device in particular require complex strategies to control instrumental drift and to determine the instrumental response function over wide ranges of energies and scattering angles, and that the results may to some degree depend on the details of these strategies. The procedures will be illustrated with measurement of elastic and vibrational cross sections in N_2. The $v = 0 \rightarrow 1$ cross section in the resonance region was measured in the full angular range $0° - 180°$, elastic cross sections were in the range of about $10° - 180°$, the lower limit being dependent on the electron energy. The results agree well with the high quality theoretical results of Morrison, Sun and Hao. The integral and momentum transfer cross sections derived from the differential data agree well with swarm data.

FM 46 Rydberg-Like Feshbach Resonances in Dissociative Electron Attachment to Amines and Alcohols MICHAEL ALLAN, BOGDAN IBANESCU, SVETLANA ZIVANOV, OLIVIER MAY, PATRIC OULEVEY, *University of Fribourg* The dissociative electron attachment (DEA) spectra of saturated compounds (*i.e.*, without double and triple bonds) containig the O and N atoms have recently been shown to be generally dominated by Feshbach resonances with double occupation of Rydberg-like orbitals around a cationic core {T. Skalický and M. Allan, *J. Phys.* B **37**, 4849 (2004)}. The Feshbach resonance serves as a doorway state anf is predissociated by a repulsive valence state of the anion. These resonances shift to lower energies with alkyl substitution, in contrast to the shape resonances, and are found at surprisingly low energies in amines because of their low ionization energies. Feshbach resonances have been identified already earlier as being responsible for DEA in water, amonia, and other molecules. We continue this work with the aim of gaining fundamental insight into the dynamics of dissociation of saturated organic compounds by electron impact. We study the dependence of the dissociation patterns on the energy of the resonance and the type of alkyl substitution of the amines.

FM 47 A method for measuring optical cross sections for electron impact excitation from metastable states* C.A. DEJOSEPH, JR., *Air Force Research Laboratory, Wright-Patterson AFB, OH* V.I. DEMIDOV, *UES, Inc., Dayton, OH* We present a method for determining optical cross sections of states which are excited by electron impact from metastable levels. The method

utilizes the afterglow of a low pressure, pulsed (100% modulated) rf-driven plasma. Following termination of the rf power, the average electron energy decreases rapidly to a few tenths of an eV, which, for the rare gases, is well below the inelastic threshold for excitation from the ground and metastable states. At the same time, metastable atoms can react to create fast electrons through pooling reactions, which produce ionization, and collisions of the second kind with slow electrons. The energy of these fast electrons depends on the specific production mechanism. These fast electrons can, in tern, collide with metastables leading to excitation and subsequent optical emission from higher lying states. At the low pressures of this experiment (~ 20 mTorr) emission from three body recombination is negligible. We demonstrate the method using a pulsed ICP in argon over the pressure range of 10-20 mTorr. Specifically, we present relative data for a number of lines from the Ar $3p^5 4p$ manifold, where optical cross sections have been measured, and from the $3p^5 5p$ manifold, such as the 420.1 and 419.8 nm lines where measurements are unavailable.

*This work supported by the Air Force Office of Scientific Research.

FM 48 A global (volume averaged) model of a nitrogen discharge JON T. GUDMUNDSSON, NARFI T. SNORRASON, *Science Institute, University of Iceland, Reykjavik, Iceland* SUNGJIN KIM, MICHAEL A. LIEBERMAN, *Department of Electrical Engineering and Computer Sciences, University of California, Berkeley, CA 94720-1770* We use a global (volume averaged) model to study the dissociation of the nitrogen molecule and the role of metastable species in a low pressure (1 - 100 mTorr) high density nitrogen discharge. The collisional energy loss per electron ion pair created is evaluated for the nitrogen atom and the nitrogen molecule. The dissociation mechanism in the nitrogen discharge is investigated as a function of power and pressure. The dissociation fraction is of the order of a few precent and increases with increased applied power. Furthermore, we explore and compare the reaction rates for the creation and destruction of the positive ions N^+ and N_2^+ .

FM 49 Electron excitation coefficients in oxygen ŽELJKA NIKITOVIĆ, VLADIMIR ŠAMARA, GORDANA MALOVIĆ, ZORAN PETROVIĆ, *Institute of Physics, POB 68, 11080 Zemun, Belgrade, Serbia and Montenegro* We have presented measurements of electron excitation coefficients for the level leading to 777 nm radiation of oxygen. Measurements were performed in a drift tube. The drift tube consists of a pair of plane electrodes, with a diameter of 79 mm at a distance of 14.7 mm, placed inside a close fitting quartz tube. The cathode was made of stainless steel and the anode of graphite so that backscattering of electrons from the anode is minimized. The self-sustained Townsend discharge between 600 Td and 24000 Td was maintained by running low current discharges at pressures between 2.2 Torr and 0.09 Torr, respectively. The absolute electron excitation coefficients were determined from the measurements of the optical signal at the anode. The spatial profiles of emission provide us with information on heavy particle excitation, on non-hydrodynamic behaviour of the discharge and on the reflection of electrons from the anode. The absolutely calibrated spatial profiles of emission may be used to separate the effects of electron and heavy particle excitation at high E/N values and obtain the cross sections for fast neutral excitation.

FM 50 HIGH PRESSURE PLASMA PHYSICS AND CHEMISTRY

FM 51 Experimental study on atmospheric pressure RF capacitive He/O_2 discharges TAKASHI KIMURA, YOSUKE HATTORI, TAKAMASA HANAI, *Nagoya Institute of Technology* The discharge voltage-current characteristics, and the densities of the active species such as oxygen atom and ozone were investigated in the capacitively coupled RF (13.56MHz) He/O_2 discharges at atmospheric pressure. The discharges were produced between two planar aluminum electrodes of 40mm-ϕ in the discharge gap range from 0.5mm to 2.0mm. The flow rates of helium and oxygen were controlled using the mass flow controllers, keeping the total flow rate at 10.0 ℓ/min. The oxygen content was changed from 0 to 5%. With increasing the applied voltage, the discharge current and the power dissipated in the discharge monotonically increased until the glow discharges turned into the arc discharges. But the slope of the voltage with respect to the current was less than linear. The small amount of argon (=10 sccm) was fed into the discharge in order to estimate the density of oxygen atom by the actinometry method, where the optical emission intensities of 844.6 nm and 750.4 nm were used. The ozone concentration was detected by an optical absorption of 254 nm line using the Lambert-Beer law. The oxygen atom density was higher than the ozone density. The densities of oxygen atom and ozone were on the order of 10^{15} - 10^{17} cm^{-3} in the power range lower than 100 W. This work is partially supported by Grant-in-Aid from the Japan Society for the Promotion of Science.

FM 52 Gas Temperature and Metastable Density Measurements in Ar/H_2DBD Using Diode-Laser Absorption Spectroscopy ROBERT LEIWEKE, BISWA GANGULY, *Air Force Research Laboratory WPAFB* Short-pulse excited DBDs are viable sources of UV, VUV radiation and radical flux at low gas temperatures for material processing applications. In this work, a 20% H_2/Ar short-pulse (15 ns FWHM) excited DBD was operated between 5-50 Torr, 6-8 kV, and 5 kHz repetition rate. Diode-Laser Absorption Spectroscopy was used to obtain Ar $1s_3 \rightarrow 2p_2$ transition profiles near 772.4 nm for bulk gas temperature and metastable line density measurements which are important for estimating both the power deposition efficiency into electronic states and the E/n. Absorption profiles obtained below 30 Torr were used to extract gas temperature, collisional Lorentzian linewidth, and absolute Ar line densities using standard iterative lineshape fitting techniques. In accordance with Lindholm-Foley $T^{0.3}$ scaling law for van der Waals interactions, we used the Lorentzian linewidths to obtain the pressure broadening coefficient for this gas mixture, which was found to be in agreement with the value for pure argon. Temperature and Ar* density were extracted from the pressure-broadened 50 Torr profile using an accurate method which self-consistently incorporates knowledge of the collisional line broadening parameter, the Doppler component, and the Voigt linewidth. At 50 Torr, we also estimated the energy deposition efficiency of direct electron impact metastable production based upon time-resolved power measurements and absolute Ar metastable line density.

FM 53 Two-dimensional numerical study of atmospheric pressure glows in helium* PENG ZHANG, UWE KORTSHAGEN, *Department of Mechanical Engineering, University of Minnesota* Atmospheric pressure glow discharges (APGs) have attracted significant attention due to their spatially homogenous plasma properties. Unfortunately, at atmospheric pressure a glow discharge has a strong tendency to transform into a non-uniform filamentary dielectric barrier discharge (DBD). The transition between filamentary DBDs and uniform APGs is studied by a two-dimensional fluid model. The results show that the discharge structure is affected by many operating parameters, including the dielectric constant and the thickness of the barriers, the driving frequency, and the voltage amplitude. For instance, an increase in the applied low-frequency voltage leads to an increase in the number of plasma filaments. In addition, the influence of the gas properties such as the ionization coefficient, and the mobility and diffusion coefficients of charge carriers is investigated. It is found that a uniform glow discharge is more easily achieved in a gas with higher ionization coefficient at a relatively low electric field. The ion transport properties have a larger influence on the discharge structure than those of the electrons.

*This work is supported by the Department of Energy under grant DE-FG02-00ER54583 and by the University of Minnesota Supercomputing Institute.

FM 54 On the mechanism of hollow-needle to plate atmospheric-pressure DC discharge* MILAN SIMEK, *Institute of Plasma Physics, Academy of Sciences of the Czech Republic, Za Slovankou 3, 18221 Prague 8, Czech Republic* STANISLAV PEKAREK, *Czech Technical University, Faculty of Electrical Engineering, Technick 2, 166 27 Prague 6, Czech Republic* Hollow needle to plate electrical discharge at atmospheric pressure with a supply of gaseous medium through the needle electrode is frequently studied for a variety of ecological applications. We explored various combinations of the mass flow and DC driving voltage in order to find limits of stable discharge operation. In pure nitrogen, we observed only two basic discharge modes. In the case of the needle biased negatively and at low energy dissipated between electrodes, the discharge is restricted to the small area surrounding the needle cathode. It takes the shape of a short continuous luminous jet, which is directed towards anode. At higher dissipated energy, the discharge is more complex. The luminous jet becomes longer and, simultaneously, the gap between the tip of the jet and the anode surface is frequently bridged by very thin filamentary discharges. In the case of the needle biased positively and at low dissipated energy, the discharge resembles a diffuse weekly luminous cone bridging completely the gap. With increasing energy, the continuous cone is superimposed with pulsed luminous filamentary discharges.

*Work supported by a Grant Agency of the Academy of Sciences of the Czech Republic, contract n. A1043403.

FM 55 Experimental and computational study of gas temperature characteristics for atmospheric-pressure microgap discharge AKIHIRO KONO, TOMOYUKI SHIBATA, MITSUTOSHI ARAMAKI, *Nagoya University* We are studying microwave-excited atmospheric-pressure high-density nonthermal plasma produced in the microgap between knife-edge electrodes, aiming at an application to VUV light source. The gas temperature is an important parameter for such an application and has been studied experimentally (from optical emission) and computationally for air and He discharges. In a previous presentation [1], we reported that a gas dynamic simulation indicates the existence of strong convection caused by a large temperature difference between the plasma center and the wall. However, detained reanalysis indicated that this convention was an artifacts caused by a particular discretization method of the pressure term. Here, we show, reanalysis of the previous results by a new code and extend the work to include Ar plasmas as well as to include the case of using new electrode system, in which gas blows out from the edge of the electrode. (Work supported by Grant-in-aid 15075205 from MEXT Japan) [1] A. Kono, GEC2004, Bul. Am. Phys. Soc. 49, 76 (2004).

FM 56 Time-Resolved Studies of Fast-Pulsed Dielectric Barrier Discharges* JOSE LOPEZ, *Stevens Institute of Technology, Hoboken, NJ, USA* ROBERT J. LEIWEKE, *US Air Force Research Laboratory, Propulsion Directorate, WPAFB, OH, USA* PETER BLETZINGER, JAMES M. WILLIAMSON, *Innovative Scientific Solutions, Inc., Dayton, OH, USA* ABRAHAM BELKIND, *Stevens Institute of Technology, Hoboken, NJ, USA* KURT H. BECKER, *Center for Environmental Systems, SIT, Hoboken, NJ, USA* BISWA N. GANGULY, *US Air Force Research Laboratory, Propulsion Directorate, WPAFB, OH, USA* Dielectric Barrier Discharges (DBDs) produce highly non- equilibrium plasmas that allow for the effective generation of ions, excited species, and radicals from energetic electron-driven processes. In an effort to improve the production of the excited species, radicals, and UV radiation, which is strongly influenced by the reduced electric field, it is more effective to use a pulsed high voltage of very short duration, particularly if the aim is to keep the gas temperature low. In order to better understand this physical phenomenon, time-resolved electrical measurements in conjunction with the established methods of time-resolved optical emission spectroscopy (TR-OES) and time-resolved diode laser absorption spectroscopy (TR-DLAS) were utilized to characterize the fast-pulsed discharge. As an additional investigative method, an ICCD camera was used for time-resolved imaging studies.

*Work supported by AFOSR

FM 57 Electrical properties of TiO_2 in a dielectric barrier discharge OLIVIER GUAITELLA, ANTOINE ROUSSEAU, *LPTP - Ecole Polytechnique - Palaiseau France* The efficiency of plasma and photocatalyst (TiO_2) combination for volatile organic compounds removal is now proved in atmospheric pressure DBD in air [1]. This efficiency may be due to chemical activity of TiO_2 as well as geometry of the surface or electrical properties of this material. A complete study of electrical properties is performed to check how TiO_2 changes discharge current in a DBD. The average injected energy is compared in plasma, plasma + UV lamp, plasma + TiO_2, plasma + TiO_2 + UV. Then, a statistical study of current peak amplitudes is carried out at different times during one period of the sinusoidal power supply (50Hz). Several populations of current peaks are observed during the positive half period and the negative one. These populations change with and without TiO_2 even for the same averaged injected energy and may be a reason for the depolluting efficiency of plasma/TiO_2 combination. [1] Kang et al, Journal of Molecular Catalysis (**2002**)

FM 58 Microdischarge-assisted ignition of large volume dielectric barrier atmospheric pressure glow (DB-APG) discharge JICHUL SHIN, LAXMINARAYAN RAJA, *University of Texas at Austin* Ignition of large-volume dielectric-barrier discharge (DBD) in the presence of dc microdischarges is studied with pure helium and pure nitrogen gas. A hybrid configuration that consists of a classical parallel-plate DBD and an array of microdischarges is used in this study. Microdischarges provide seed species (charged and radical) that allow for a low voltage (non-classical) breakdown of the dielectric-barrier gap. With microdischarges being turned on, both helium and nitrogen DBD ignite with a confined discharge that is localized above the microdischarge holes at as low as 50 % of breakdown voltage without the presence of microdischarges. In nitrogen gas, the localized discharge is much more confined than helium. Intensified CCD image provides an understanding of the structure of localized discharge. I-V characteristics suggest that the localized discharge has a glow-like character, with estimated electron densities ($\sim 10^{17}$ m^{-3}) that are typical of a regular DB-APG discharge. Higher microdischarge power makes the localized discharge slighly more intense and the geometric configuration of microdischarge array gives some effect with increasing packing densities of localized discharge resulting in a lower DBD breakdown voltage. This study suggests that low-voltage (less than a regular DB-APG), large-volume operation of DB-APG is possible using an array of microdischarges that covers the entire electrode plane.

FM 59 Secondary ionization coefficient and electron reflection coefficient of MgO electrode SUSUMU SUZUKI, HARUO ITOH, *Chiba Institute of Technology* Secondary ionization coefficient γ of MgO in Ar was determined using the Townsend's criterion[1] and the starting voltage of self- sustaining discharge between MgO electrodes in the plasma display panel (PDP) cell. Electron transport characteristics in the cell were also investigated under the driving condition of the PDP cell by the Monte Carlo Simulation (MCS). In this condition, the nonequilibrium electron energy distributions were recognized in the results. Therefore, the secondary ionization coefficient was about 20% larger than that in the case of energy equilibrium. In addition, γ slightly became small with an increase in initial energy of electron emitted from the cathode[1]. The secondary ionization coefficient was defined as the product of the secondary electron emission coefficient in vacuum and the electron transmission coefficient *T*in gases. We investigate on the influence of the electron reflection at the cathode and anode on the secondary ionization coefficient and electric power injection in the PDP cell. The result is shown that the secondary ionization coefficient is independent of the electron reflection at the electrode. Furthermore, the increases in electron reflection coefficient at the cathode and the anode give high values of the electric power injection and the delay of the time response of the electron flux at the anode, respectively. [1] S.Suzuki and H.Itoh: Jpn.J.Appl.Phys., **43**, 10 (2004) 7234-7239.

FM 60 Observation of N_4^+ recombination at near atmospheric pressure* S.F. ADAMS, C.A. DEJOSEPH, JR., *Air Force Research Laboratory, Wright-Patterson AFB, OH 45433* J.M. WILLIAMSON, *Innovative Scientific Solutions, Inc., Dayton, OH* We previously reported our initial modeling results of the $N_4^+ + e^-$ recombination observed by monitoring the time-resolved N_2 emission (GEC03, paper SRP 24). The N_2 2nd positive ($C\ ^3\Pi_u - B\ ^3\Pi_g$) and N_2^+ 1^{st} negative ($B^2\Sigma_u^+ - X^2\Sigma_g$) emission was measured following laser resonance-enhanced multi-photon ionization (REMPI) of N_2 at near-atmospheric pressure. N_4^+ is produced by the three-body association reaction of $N_2^+ + N_2$ which occurs rapidly at these pressures. Two types of fluorescence are observed following irradiation of N_2 by the laser pulse. A ''prompt'' fluorescence composed primarily of emission from the N_2^+ 1^{st} negative system ($B\ ^2\Sigma_u^+ - X\ ^2\Sigma_g$) followed by a ''delayed'' fluorescence form the aforementioned N_2 (C-B). The preliminary modeling presented previously has been extended to include other key N_2 neutral and ionic species as well as the important loss channel of N_4^+ by laser photodissociation which had been neglected. The improved model along with additional N_2^+ LIF and N_4^+ UV photolysis results will be presented.

*This work supported by the Air Force Office of Scientific Research.

FM 61 Control of ionic species composition in complex plasmas dominated by charge exchange collisions KOSTYA OSTRIKOV, *School of Physics, The University of Sydney, Australia* A generic approach towards tailoring of ion species composition in reactive plasmas used for nanofabrication of various functional nanofilms and nano-assemblies, based on a simplified model of a parallel-plate rf discharge, is proposed. The model includes a reactive plasma containing two neutral and two ionic species interacting via charge exchange collisions in the presence of a microdispersed solid component (''dust''). It is shown that the number densities of the desired ionic species can be efficiently controlled by adjusting the dilution of the working gas in a buffer gas, rates of electron impact ionization, losses of plasma species on the discharge walls and surfaces of fine particles, charge exchange rates, and efficiency of three-body recombination processes in the plasma bulk. The results are relevant to plasma-assisted fabrication of ordered patterns of carbon nanotip and other carbon-based nanostructures.

FM 62 Kinetic Modeling of Electric Discharge in a Preformed Air-Plasma Channel TZVETELINA PETROVA, *Naval Research Laboratory* HAROLD LADOUCEUR, *Naval Research Laboratory* ANDREW BARONAVSKI, *Naval Research Laboratory* Recent experimental studies of atmospheric discharges in a pre-existing plasma show that electrical breakdown occurs at relatively low electric fields ($\sim$ 5.7 kV/cm). This breakdown at such low fields cannot be explained in terms of the classical Paschen theory. To understand the physical mechanism of this phenomenon an extensive self-consistent collisional-radiative model for air plasma was developed. The model is based on the electron Boltzmann equation for the electron energy distribution function self-consistently coupled with the electron balance equation. The balance equations for various nitrogen and oxygen species in ground and excited states, as well as various atomic and molecular ions are incorporated. The model includes a variety of chemical reactions and plasma processes such as direct excitation and de-excitation, quenching, dissociation, ionization, attachment and detachment, charge exchange, and radiation. This system of equations was solved in a quasi-stationary regime and the self-consistent breakdown electric field and other plasma parameters were determined as a function of the initial degree of ionization. NRC-NRL Postdoc Supported by Office of Naval Research.

FM 63 LIGHTNING PLASMAS

FM 64 Basic Study of Discharge Simulation with Relaxation Process of Electron Swarm for Plasma Display Panel YUKIO MURAKAMI, *NHK Sci. Tech. Res. Labs.* KEIICHI KONDO, *Gaseous Electronics Inst.* Plasma display panels (PDPs) with a thin profile and a wide screen are widely used in displays for digital high-definition television broadcasting, etc. For further popularization of PDPs, the vacuum ultraviolet (VUV) radiation mechanism in microdischarge cells is determined by discharge simulation with the aim of achieving a lower power consumption. Although in ordinary discharge simulations, a fluid model with local field approximation (LFA) is widely used, the possibility of new analysis considering the relaxation process of electron swarms for high-precision analysis under a markedly changing electric field in a cell- like alternating current (AC) type PDP or radio-frequency field is examined. The time-dependent Boltzmann equation, which is transformed to the matrix representation of the Burnett basis function, is used for the analysis of the relaxation processes. For rare and mixed gases, relaxation processes of electron energy distribution function (EEDF) and its swarm parameters, such as drift velocity and mean energy, in applying step and repetitive pulsed electric fields under the condition of conventional PDPs were calculated. Considering these relaxation processes in the near future, a high-precision simulation will be developed in which the analysis of the short time evolution of the EEDF is possible, and the VUV radiation mechanism will be clarified in detail expecting advancement in the search of the high-efficiency new discharge mode.

FM 65 Near IR Continuum Radiation From Metal Halide HID Lamps J.E. LAWLER, M.T. HERD, *University of Wisconsin* A recent study demonstrated that the near IR continuum from pure Hg High Intensity Discharge (HID) lamps is primarily due to electron- atom bremsstrahlung over a pressure range from 8 bar to more than 200 bar [1]. The study compared absolute spectroradiometric measurements to radiation transport simulations using new (larger) electron-Hg atom bremsstrahlung coefficients. The absence of significant molecular radiation in the near IR from 230 bar Ultra High Pressure lamps was unexpected. Near IR losses from Metal Halide (MH) HID lamps are typically 20 to 30% of input power. A quantitative, microscopic understanding of these losses is very desirable since MH lamps are more and more widely used for general illumination. The near IR from MH lamps is emitted by the arc core. It is composed of a strong continuum, many weak atomic lines, and negligible molecular radiation. In an effort to understand the Near IR losses from MH lamps, we are mapping the spatial and spectral dependence of this radiation. The maps are being compared to radiation transport simulations. Additives provide most of the free electrons in MH lamps, and additive segregation complicates the analysis of near IR emission. Our approach to this problem and progress to date will be described. [1] J. E. Lawler, A. Koerber, and U. Weichmann, J. Phys. D: Appl. Phys., in press (2005).

FM 66 Development of a compact arc discharge light source for measurement of radicals HARUHIKO ITO, *Nagoya Municipal Industrial Research Institute* SEIGO TAKASHIMA, *Nagoya Univ.* HIROYUKI KANO, *NU Eco-Engineering* MASARU HORI, *Nagoya Univ.* To measure the radicals in plasma processes by using ultraviolet absorption spectroscopy, the light source that has a continuous emission spectrum in ultraviolet range is necessary. However, the size of the light source that has been used so far is generally large. So, the installation of the measurement system to the process chamber was very difficult. Therefore, the miniaturization of the light source was required. In this study, the compact light source using an arc discharge has been developed. The size of the electrode of light source was 30mm or less in the diameter. The small slit on the cathode electrode could act as enhancement to keep arc discharge. However, when the arc discharge time became long, the fluctuation of arc discharge point at time was caused because the insulator was consumed, and stability was low. To improve the stabilization of the arc discharge, the insulator was removed. The decrease in the stability of the arc discharge caused by the consumption of the insulator could be evaded and so the stability of the light source was greatly improved.

FM 67 COMPUTATIONAL METHODS FOR PLASMAS

FM 68 Convergence of particle-in-cell simulations MILES M. TURNER, *Dublin City University, Ireland* Particle-in-cell simulations are widely used for benchmarking other simulation methods and other purposes where a highly accurate representation of the physics is desired. In such cases, it is necessary to establish, among other things, that the simulation is fully converged with respect to all numerical parameters. There are generally accepted criteria or rules of thumb for selecting the numerical parameters to be used in particle-in-cell simulation. In this paper, we show that there are cases where the usual rules of thumb do not deliver satisfactory convergence, and indeed that such convergence is difficult to achieve at all. These issues are associated with a degradation of the kinetic properties of the particle-in-cell simulation that occurs when Monte Carlo collisions are introduced. In particular, the rate of numerical thermalization is greatly increased when the frequency of Monte Carlo collisions is large. Since this thermalization rate is a function of the number of simulation particles, it follows that a much greater number of particles may be required than is commonly assumed.

FM 69 Spectroscopic characterization of an ultrashort laser driven Ar cluster target incorporating both Boltzmann and particle-in-cell models MANOLO SHERRILL, J. ABDALLAH, G. CSANAK, *Theoretical Division Los Alamos National Laboratory* E. DODD, *Applied Physics Division, Los Alamos National Laboratory* Y. FUKUDA, *Advanced Photon Research Center, Japan Energy Research Institute* Y. FAENOV, *Multicharged Ions Spectra Data Center of VNIIFTRI* A model that solves simultaneously both the electron and atomic kinetics was used to generate a synthetic He_α and satellite X-ray spectra to characterize a high intensity ultrashort laser driven Ar cluster target experiment. In particular, level populations were obtained from a detailed collisional-radiative model where collisional rates were computed from a time varying electron distribution function obtained from the solution of the zero dimensional Boltzmann equation. In addition, a particle-in-cell simulation was used to model the laser interaction with the cluster target and provided the initial electron energy distribution function (EEDF) for the Boltzmann solver.

This study suggests that an average high density of $N_a = 3.2 \times 10^{20}$ cm^{-3} was held by the system for a time of 5.7 ps, and during this time the plasma was in a highly non-equilibrium state in both the EEDF and the ion level populations. Finally, this work provides evidence that cluster targets could produce X-ray radiation in the 100 femtosecond time scale.

FM 70 PLASMA AND NANOSTRUCTURAL MATERIALS

FM 71 Nanofabrication of single-crystalline flat panel display microemitter arrays: a ''plasma-building unit'' approach KEN OSTRIKOV, *School of Physics, The University of Sydney, Australia* SHUYAN XU, *Plasma Sources and Applications Center, NIE, NTU, Singapore* This contribution is focused on PECVD systems used for nanofabrication of flat panel display microemitter arrays based on ordered patterns of single-crystalline carbon nanotip structures (CNSs). The fundamentals of the plasma-based nanofabrication of CNSs and other nanofilms and nanostructures are critically examined and compared with CVD processes. Specific features, challenges, and potential benefits of using the reactive plasma-based systems for relevant nanofabrication processes are analyzed by using the ''plasma-building unit'' approach that builds up on extensive experimental data on plasma diagnostics and nanofilm/nanostructure characterization, and numerical simulation of the species composition in the plasma (fluid models), ion interaction with ordered carbon nanotip patterns (MC simulation), and computations of chemical structure of single crystalline carbon nanotips (DFT technique). This approach is also applicable for nanoscale assembly of other carbon nanostructures, polymorphous silicon films, semiconductor quantum dot structures, and nanocrystalline bioceramics. Special attention is paid to control strategies of the building units in the plasma phase and on nanostructured deposition surfaces. The issues of tailoring the plasma and development of plasma nanofabrication facilities are also discussed.

FM 72 Simulation of ion deposition in nanofabrication of single-crystalline carbon nanotip electron field emitters IGOR LEVCHENKO, KEN OSTRIKOV, *School of Physics, The University of Sydney, Australia* Three-dimensional topography of microscopic ion fluxes in the reactive hydrocarbon-based plasma-aided nanofabrication of ordered arrays of vertically aligned single crystalline carbon nanotip microemitter structures is simulated by using a Monte-Carlo technique. The ion trajectories are computed by integrating the equations of motion in the electric field of a biased substrate. It is shown that the ion flux focusing onto carbon nanotips is more efficient under conditions of low potential drop U across the plasma sheath. Under low-U conditions, the ion current density onto the surface of nanotips is higher for higher-aspect-ratio nanotips and can exceed the mean ion current density onto the nanopattern in up to 5 times. This effect becomes less pronounced with increasing the substrate bias, with the current enhancement not exceeding 1.7. This value is higher in denser plasmas and behaves differently with the electron temperature depending on the substrate bias. When the substrate bias is low, the ion current decreases with the electron temperature, with the opposite tendency under high-U conditions. The results are relevant to the PECVD of ordered large-area nanopatterns of vertically aligned carbon nanotips, nanofibers, and nanopyramidal microemitter structures for flat panel display applications.

SESSION GT1: IONIZATION OF ATOMS AND MOLECULES
Tuesday morning, 18 October 2005; Pine, Doubletree Hotel at 8:00
T.N. Rescigno, Lawrence Berkeley National Laboratory, presiding

Invited Papers

8:00
GT1 1 Low-Energy Electron Impact Ionization of Helium.
J.G. CHILDERS, *California State University Fullerton*

Following the completion of the measurements of the doubly-differential cross sections (DDCSs) for the electron-impact ionization of atomic hydrogen, the simplest three-body Coulomb system, we applied the experimental techniques developed to the simplest four-body system, electron scattering from helium. Recently completed measurements of the absolute DDCSs for the electron impact ionization of helium at low incident energies will be presented. The measurements were taken using the moveable nozzle technique developed in our laboratory.[1] Data were taken at incident energies of 26 eV, 28 eV, 30 eV, 32 eV, 34 eV, 36 eV, and 40 eV. The results are compared to the theoretical convergent close-coupling (CCC) calculations of Bray *et al.*[2] and good agreement is observed. This work is funded by the National Science Foundation under grant # NSF-RUI-PHY-0096808. In collaboration with Murtadha A. Khakoo, California State University, Fullerton.

[1]M. Hughes, K. E. James, Jr., J.G.Childers, and M.A. Khakoo, *Meas. Sci. Technol.* **14**, 841 (2003)
[2]Igor Bray, Dmitry V.Fursa, and Andris T. Stelbovics *J. Phys. B* **36**, 2211 (2003), and private communication.

8:30
GT1 2 Time-dependent studies of ionization of atoms and molecules.
JAMES COLGAN, *LANL*

The time-dependent close-coupling method has been a successful and efficient method of calculating cross sections for many fundamental atomic processes including electron-impact excitation and ionization, multiple photon ionization and heavy-ion impact collisions. In the past decade this method has been applied to the electron-impact ionization of many atoms and ions. Beginning with studies of the electron-impact ionization of hydrogen, the time-dependent method has also been applied to multi-electron systems such as He, Li, Be, C, and O, as well as many of their ions. Also, electron-impact excitation cross sections have been calculated for many of these systems. Recently a program of work was initiated to apply these time-dependent techniques to the electron-impact ionization of small diatomic molecules. This work was motivated by the need for accurate cross sections for these molecules, as well as complementary work on photoionization of light molecules. In this talk an overview will be given of our time-dependent method, especially as applied to molecular systems. Recent results will be presented for electron-impact ionization cross sections of various atomic ions, and very recent results will be presented for the electron-impact ionization of H_2^+. Comparison will be made, where available, with previous theoretical and experimental results. This work is supported in part by grants to Auburn University from the U.S. Department of Energy. Work at Los Alamos National Laboratory is performed under the auspices of the U.S. Department of Energy. In collaboration with Michael Pindzola, Auburn University.

Contributed Papers

9:00
GT1 3 An Elementary Method for Averaging over Molecular orientations in the Calculation of Electron-Impact Ionization of Molecules JUNFANG GAO, DON H. MADISON, JERRY L. PEACHER, *Department of Physics of University of Missouri-Rolla* One of the difficulties associated with the calculation of fully differential cross sections (FDCS) for electron-impact ionization of molecules is that the experimental data typically do not resolve the orientation of the molecules which means that the theoretical approaches have to average over all orientations. This is not a problem for elementary approaches but it becomes an important constraint for more sophisticated approaches which require extensive computer time for a single orientation. A new method is proposed for averaging over molecular orientations which can be shown to be valid for gerade states if the S-basis function is dominate in the formation of the Molecular Orbital (MO). This method for averaging the orientations will be used to calculate FDCS in the DWIAOA (Distorted Wave Impulse Approximation Orientation Average) and 3DWOA (3- body Distorted Wave Orientation Average). Results will be presented for electron impact ionization of Hydrogen, Nitrogen and Water molecules over a wide range of incident-electron energies. The agreement with experimental data is good.

9:15
GT1 4 First-Principles treatment of molecular double photoionization* DANIEL A. HORNER, T.N. RESCIGNO, *LBNL* C.W. McCURDY, *LBNL, UC Davis* We have developed a new computational approach to solving molecular double photoionization problems. The approach combines both Gaussian functions and the grid-based, exterior complex scaling discrete-variable representation (ECS-DVR) in a hybrid basis. Gaussian functions are well established and ideal for expanding molecular electronic states and the ECS-DVR on a finite-element grid has had much success solving atomic electron-impact ionization and double photoionization problems. The hybrid Gaussian ECS-DVR

method allows us to extend our treatment of problems with two active electrons in the continuum to molecular targets. We have performed calculations of absolute fully-differential cross sections for the double photoionization of molecular hydrogen. Unlike other model calculations, this is a true *ab initio* approach.

*Work performed under the auspices of US DOE by Lawrence Berkeley National Laboratory and supported by DOE-OBES, Division of Chemical Sciences.

SESSION GT2: PLASMA PROPULSION AND COMBUSTION II
Tuesday morning, 18 October 2005
Cedar, Doubletree Hotel at 8:00
Toza Popovic, Old Dominion University, presiding

Contributed Papers

8:00
GT2 1 Simulation of microdischarge gas heating in electrothermal class of small satellite propulsion devices PRASHANTH KOTHNUR, LAXMINARAYAN RAJA, *University of Texas at Austin* Microdischarges have unique features such as high power density (kW/cm^3) and high gas temperatures (1000-2000K) that enable use in electrothermal plasma devices with highly controllable thrust levels in the mN range. Two-dimensional modelling is used to simulate a flow-through microhollow electrode geometry with helium as the operating gas. Bulk fluid conservation equations are solved using the semi-implicit pressure linked equations (SIMPLE) approach and coupled to a nonequilibrium self-consistent plasma model [1]. Results indicate that plasma parameters are relatively insensitive to the flow rate. Electron temperatures as high as 20eV near the cathode fall and gas temperatures of 1000-2000K depending on the pressure and current are observed. Low Reynolds numbers and large surface-to-volume ratios result in strong sensitivity of gas temperatures to wall conditions. It is shown that wall losses must be minimized for any significant heating of the flow downstream of the electrodes, emphasizing the need for new refractory and insulating materials. [1] P.S. Kothnur, and L.L. Raja, J. App. Phys. 97(2005), 043305.

8:15
GT2 2 Electron Kinetics in Helicon Discharge GUANGYE CHEN, LAXMINARAYAN RAJA, ALEXEY AREFIEV, BORIS BREIZMAN, *The University of Texas at Austin* The Variable Specific Impulse Magnetoplasma Rocket (VASIMR) project employs helicon discharge as a plasma source [1]. A self-consistent description of the helicon discharge requires a power balance analysis, which involves electron kinetics. A steady-state electron distribution establishes when electron Ohmic heating becomes balanced by electron energy losses on atom excitation. RF-electric field and plasma density are the key parameters that determine features of the steady-state electron energy distribution function. The electron distribution has been studied in four different heating regimes using the Direct Simulation Monte Carlo method. We have found that the electron distribution is significantly non-Maxwellian in the dense gas regime, when elastic electron-atom collisions dominate. The non-Maxwellian feature of the electron distribution function has a strong impact on the cost of ionization in the discharge. [1] F.R. Chang-Diaz, Sci. Am. **283**, 90 2000.

Invited Papers

8:30
GT2 3 Efficiency of Nanosecond High–Voltage Discharge in Ignition and Combustion Enhancement.
SVETLANA STARIKOVSKAIA, *Moscow Institute Physics and Technology*

The problem of a fast homogeneous ignition of a combustible mixture is topical. High electric field in a front of nanosecond discharge and behind it results in effective ionization, dissociation and excitation. Two topics will be discussed: the efficiency of nanosecond discharges as active particles generator for ignition and study of nanosecond barrier discharge influence on a flame. Experimental results of a shift of ignition delays under the discharge are obtained for a set of combustible mixtures with H2 or hydrocarbons (up to C5H12) in a temperature range of 700– 2300 K and pressure range of 0.1-1.5 atm, numerical modeling was performed for the same conditions. Comparative study of laser flash-photolysis and nanosecond discharge allowed us to make a conclusion about a role of excited atomic oxygen in the process of ignition. Experiments on plasma– assisted combustion with a nanosecond barrier discharge at atmospheric pressure have demonstrated that with energy input negligible in comparison with burner's chemical power, it is possible to obtain double flame blow-off velocity increase. The role of addition of different radicals and excited species by the discharge is discussed. The lecture will be based on works carried out at the Laboratory of Physics of Nonequilibrium Systems of MIPT. In collaboration with Ilya Kosarev, Eugene Mintoussov, Andrei Nikipelov, and Andrei Starikovskii of the Moscow Institute Physics and Technology.

9:00
GT2 4 Air plasmas sustained by repetitive high-voltage nanosecond pulses: fundamental kinetics and aerodynamic applications.*
SERGEY MACHERET, *Princeton University*

The paper reviews the recent studies of highly efficient generation of weakly ionized plasmas and their applications to supersonic/hypersonic flight. Plasmas can be used simply as means of delivering energy (heating) to the flow, and also for electromagnetic flow control and magnetohydrodynamic (MHD) power generation. Plasma and MHD control can be especially effective in transient off-design flight regimes. In cold air, nonequilibrium plasmas must be created, and the

ionization power budget determines the design and performance envelope of plasma/MHD devices. The minimum power budget is provided by electron beams or repetitive high-voltage nanosecond pulses, and the paper describes theoretical modeling of those plasmas. The models include coupled equations for non-local and unsteady electron energy distribution function (modeled in forward-back approximation), plasma kinetics, and electric field. The modeling is in good agreement with experimental studies of quiescent air plasmas sustained by 2-nanosecond, 5 kV/cm, high (100 kHz) repetition rate pulses, where the average energy cost per electron was found to be about 100 eV, two orders of magnitude lower than in quasineutral DC and RF plasmas. Detailed investigations of the plasma dynamics revealed a critical role of the cathode sheath that was found to take up most of the peak voltage applied to the electrodes. The extremely high E/N, much higher than the Stoletov's field at the Paschen minimum point, results in a very high ionization cost in the sheath. In contrast, the E/N in the quasineutral plasma is closer to that associated with the Stoletov's point, resulting in a near-optimal electron generation. The positive space charge in the sheath and its relatively slow relaxation due to the low ion mobility was also found to result in reversal of electric field direction in the plasma at the tail of the high-voltage pulse. Experimental studies at Princeton University have also successfully demonstrated stable diffuse plasmas sustained by repetitive nanosecond pulses in supersonic air flow, and for the first time have demonstrated the existence of MHD effects in such plasmas. As one potential application, cold-air hypersonic MHD devices are shown to permit optimization of scramjet inlets at off-design Mach numbers while operating in self-powered regime.

*The work was supported by the Air Force Office of Scientific Research. M.N. Shneider, R.B. Miles, and R.C. Murray are the co-authors of this work.

SESSION HT: GEC FOUNDATION TALK
Tuesday morning, 18 October 2005; Pine/Cedar, Doubletree Hotel at 10:00
Mark Kushner, Iowa State University, presiding

10:00
HT 1 "Plasma" and "Sheaths" — The Discharge Science of Irving Langmuir.
M.A. LIEBERMAN, *University of California, Berkeley CA*

"We shall use the name *plasma* to describe this region containing balanced charges of ions and electrons" [1]. With these words, Irving Langmuir named our field. The following year he explicitly introduced the separation of a discharge into bulk plasma and sheath regions: "The word 'plasma' will be used to designate that portion of an arc-type discharge in which the densities of ions and electrons are high but substantially equal. It embraces the whole space not occupied by 'sheaths' " [2]. His remarkable contributions include [3]: Child-Langmuir sheaths, Langmuir probes, Langmuir waves, Langmuir's paradox, Langmuir's condition for double layers, Langmuir's isotherm for adsorption-desorption kinetics, and Langmuir-Hinshelwood surface reactions. Langmuir's famous talk, "Pathological Science," touched our field shortly after the "discovery" of cold fusion in 1989 [4]. Langmuir's plasma-sheath separation, along with particle, momentum and energy balance, has been very useful. The quasineutral plasma is described using simple diffusion models or more elaborate kinetic models, depending on the type of gas and pressure regime. The space-charge sheaths are modeled as low or high voltage, collisionless or collisional, dc or rf-driven, as appropriate. Exact conditions for joining plasma and sheath are well-known, but simple methods often suffice in practice. The analysis determines, in a transparent way, important discharge properties, such as ion and neutral radical fluxes to electrodes and ion acceleration energy across electrode sheaths. In a similar manner, for his adsorption-desorption isotherm, Langmuir made "assumptions which are as simple as possible . . . to see whether the resulting equations can find a field of application" [5]. When extended to incorporate ion-induced desorption, one obtains a simple model for ion-assisted etching in terms of the fluxes and ion energies. These types of simple assumptions did not please some people. "Langmuir is the most convincing lecturer that I have ever heard . . . I have heard Langmuir lecture when I knew he was wrong, but I had to repeat to myself: 'He is wrong; I know he is wrong. He is wrong,' or I should have believed like the others" [6]. Hopefully, you will believe. References: [1] I. Langmuir, *Proc. Nat. Acad. Sci.* **14** 627 (1928). [2] I. Langmuir and L. Tonks, *Phys. Rev.* **33** 195 (1929). [3] *The Collected Works of Irving Langmuir,* 12 volumes, C. Guy Suits, ed., Pergamon Press, New York, 1960–62. [4] Available from www.cs.princeton.edu/ ken/Langmuir/langmuir.htm; see also I. Langmuir and R.N. Hall, *Physics Today* **42** 36 (1989). [5] I. Langmuir, Nobel Lecture, December 14, 1932. [6] W.D. Bancroft, *J. Phys. Chem.* **35** 1904 (1931).

SESSION JT: BUSINESS MEETING
Tuesday morning, 18 October 2005
Doubletree Hotel at 11:15
Greg Hebner, Sandia National Laboratories, presiding

11:15
JT 1 Business Meeting

SESSION KT: GENERAL COMMITTEE MEETING
Tuesday noon, 18 October 2005
Boardroom, Doubletree Hotel at 12:00
Greg Hebner, Sandia National Laboratories, presiding

12:00
KT 1 General Committee Meeting

SESSION LT1: ELECTRON-MOLECULE COLLISIONS
Tuesday afternoon, 18 October 2005; Pine, Doubletree Hotel at 13:30
Michael Brunger, Flinders University, presiding

Invited Papers

13:30
LT1 1 Low-Energy Electron-Molecule Collision Experiments.
MICHAEL ALLAN, *University of Fribourg*

The talk will report on the recent improvements of the techniques to measure elastic and inelastic electron-molecule cross sections. Emphasis will be given on the measurement of the cross sections as a function of scattering angle over a large angular range using the 'magnetic angle changer' (MAC) invented by Frank Read and co-workers, and on the measurements at low energies. It will be shown that measurement of cross sections in general and the use of the MAC device in particular require complex strategies to control instrumental drift and to determine the instrumental response function over wide ranges of energies and scattering angles, and that the results may to some degree depend on the details of these strategies. The procedures will be illustrated with measurement of elastic and vibrational cross sections in N_2. The $v = 0 \rightarrow 1$ cross section in the resonance region was measured in the full angular range $0° - 180°$, elastic cross sections in the range of about $10° - 180°$, the lower limit being dependent on the electron energy. The results agree well with high quality theoretical results of Morrison, Sun and Hao. The integral and momentum transfer cross sections derived from the differential data agree well with swarm data. The talk will then present applications of these experimental techniques to study elastic and vibrational cross sections in NO, CH_4, cyclopropane and other molecules. Emphasis will be given on threshold peaks and near threshold structures due to vibrational Feshbach resonances. The vibrational excitation of NO *via* the low-lying shape resonances will also be presented and compared to the recent theoretical results {C. S. Trevisan, K. Houfek, Z. Zhang, A. E. Orel, C. W. McCurdy, and T. N. Rescigno, *Phys. Rev.* A **71**, 052714 (2005)}.

14:00
LT1 2 New trends in low–energy electron collisions with molecules.
HIROSHI TANAKA, *Sophia University, Japan*

Experimental studies on electron-polyatomic molecular collisions are reviewed in connection with the plasma processing and environmental issues. Recent developments in electron scattering experiments on differential cross sections (DCSs) are summarized for various processes such as elastic scattering, vibrational, and electronic excitations, including the dissociative attachments as well as the radical formation. Three illustrative examples are described specifically as follows: 1) perfluocarbons as the main feed gases in the plasma etching industry and the need to replaced by alternative compounds that have low global warning potentials, e.g. COF_2, C_3F_6, and $l - C_4F_6$; 2) detection of non-emissive CH_3 radicals via the low-lying electronic states of CH_4 by electron impact; and 3) the electronic spectra of thymine by electron impact methods, also including H_2O. This work was supported by the Ministry of Education, Sport, Culture and Technology, the Japan Society for Promotion of Science, the Japan Atomic Energy Research Institute, and the CUP program between Japan and South Korea. In collaboration with Masamitsu Hoshino, Department of Physics, Sophia University, Chiyoda-ku, Japan; Casten Makochekanwa, Department of Physics, Sophia University, Chiyoda-ku, Japan, Graduate School of Sciences, Kyushu University, Japan; Hyuck Cho, Physics Department, Chungnam National University, South Korea.

14:30
LT1 3 Physics with Cooled and Trapped Molecular Ions.
DANIEL ZAJFMAN, *Weizmann Institute of Science, Rehovot, Israel and Max-Planck Institute for Nuclear Physics, Heidelberg, Germany*

Modern techniques developed during the last decade have open several new opportunities to study low energy collision processes between molecular ions and electrons, such as dissociative recombination and electron impact excitation, with the help of fast molecular ion beams. The heavy-ion storage ring technique, together with cold electron beams produced by cryogenically cooled photocathode allow to reach center-of-mass resolution of the order of 500 μeV, permitting the observation of well separated Rydberg resonances in the recombination process. Also, manipulation and probing of the vibrational and rotational excitation of the stored molecular ions is now made possible with these tools. Observation of the molecular dynamics taking place during theses collisions can be made via three-dimensional imaging detectors. In this lecture, several examples will be shown which demonstrate the advantages of these techniques for simple molecular ions such as HD^+ and H_3^+. Comparison with recent theoretical calculations will be presented as well. Also, the next generation of experiments which will be performed by the end of this decade using the Cryogenic Storage Ring (CSR) will be described.

Contributed Papers

15:00
LT1 4 Low Energy Electron Scattering from Formic Acid
VIOLAINE VIZCAINO, MILICA JELISAVCIC, JAMES SULLIVAN, STEPHEN BUCKMAN, *Research School of Physical Sciences and Engineering, The Australian National University*
Formic acid (HCOOH) is the simplest of the organic acids and it is thought that it could play a key role in the formation of simple biomolecules such as glycine and acetic acid in the interstellar medium. We have studied elastic electron scattering from formic acid using a crossed-beam electron spectrometer. Absolute cross sections are obtained using the relative flow technique. Flow rates for HCOOH, and the reference gas He, are measured at a number of temperatures, including both room temperature and 70°C, in order to investigate the effects of molecular dimers which are thought to dominate at room temperature. Measurements at energies in the range 10-50 eV will be presented at the meeting and compared, where possible, with recent theoretical calculations.

15:15
LT1 5 Resonance Processes in Electron-CF Collisions
CYNTHIA TREVISAN, ANN OREL, *University of California, Davis*
THOMAS RESCIGNO, *Lawrence Berkeley National Laboratory*
CF radicals are by-products of semiconductor processing reactant gas C_2F_4 under electron bombardment. Since they are highly reactive and difficult to isolate under laboratory conditions, theoretical calculations are the only practical source for electron-CF collision cross section estimates. We have carried out an extensive set of *ab initio* calculations aimed at quantifying the various resonant collision processes that could lead to significant vibrational excitation and/or ion production in e^--CF collisions. Near equilibrium geometry, CF and its negative ion states are similar to NO, which is isoelectronic with CF and which has been the subject of much recent theoretical and experimental study. The binding energy of CF, however, is significantly smaller than that of NO and, unlike NO, there are negative ion states that correlate with both F^-+C and $F+C^-$ (N^- does not exist). These differences make for some interesting comparisons and differences between e^--CF and e^--NO cross sections, which will be the focus of this work.

SESSION LT2: HIGH PRESSURE PLASMAS II
Tuesday afternoon, 18 October 2005; Cedar, Doubletree Hotel at 13:30
Biswa Ganguly, Air Force Research Laboratory, presiding

Invited Paper

13:30
LT2 1 Microcavity Discharge Devices and Arrays: A Photonic Platform for Photodetectors, Optical Amplifiers and Displays.
J. GARY EDEN, *University of Illinois*

Microcavity plasma is the term associated with the spatial confinement of a nonequilibrium plasma to a cavity having a characteristic dimension below nominally 500 μm. Recently, fabrication techniques developed largely by the semiconductor and MEMs communities have been adapted to realize a family of microcavity plasma (microplasma) devices with cross-sectional dimensions as small as $(10\ \mu m)^2$. Fabricated in a wide range of materials platforms, including Si, ceramics, and metal/dielectric multilayer structures, these devices exhibit a number of intriguing properties. These include: 1) the ability to operate on a continuous basis at pressures of one atmosphere and above, 2) specific power loadings of at least tens of kW-cm^{-3}, and 3) microcavity volumes of nanoliters or picoliters. This talk will summarize the properties of microcavity plasmas with characteristic dimensions in the 10-150 μm range, and operating at gas pressures up to $\sim$ 1200 Torr. Emphasis will be placed on the scientific opportunities afforded by: 1) the access provided by microcavity plasmas to a new region of parameter space, and 2) the ability to now interface a low temperature plasma with an electronic or optical material. Several examples of photonic structures and their applications will be presented, including the recent development of arrays of 250,000 (500×500) inverted pyramid microcavity devices fabricated in

silicon. Having an active area of 25 cm^2, this array has been operated in both the rare gases and Ar/N_2 mixtures, and yields luminous efficacies > 5 lumens/W when coupled with a commercial green phosphor ($Mn:Zn_2SiO_4$). Ceramic microchips offering a microplasma gain length of 1-2 cm have also been developed and gain on the 460.3 nm transition of Xe^+ has been observed. Applications of microplasmas in biomedical diagnostics and optics will also be discussed.

Contributed Papers

14:00

LT2 2 Combination of atmospheric pressure dielectric barrier discharge and photocatalysis for C_2H_2 oxidation FREDERIC THEVENET, CHANTAL GUILLARD, *LACE UCB-Lyon1 UMR CNRS 5634 blvd 11Nov.1918 69100 Villeurbanne France* OLIVIER GUAITELLA, ANTOINE ROUSSEAU, *LPTP Ecole Polytechnique 91120 Palaiseau* Non-thermal plasma and photocatalysis have attracted attention as energy-saving methods for VOCs destruction. TiO_2 photocatalysts are porous semiconductors activated by UV radiations. They are known for their ability to oxidize organic molecules with high CO_2 selectivity. It was shown recently that the coupling of dielectric barrier discharges (DBD) with photocatalysis improves oxidation efficiency and reduces undesirable by-products. Experiments were carried out in a closed DBD reactor containing photocatalytic surface, with C_2H_2 as a test molecule. First, TiO_2 influence on DBD deposited energy was investigated, as well as ageing of TiO_2 under DBD conditions. Then, air cleaning efficiency of coupling was investigated. Introduction of higher specific energy and addition of UV radiations increase the synergistic effect. Selectivity is clearly enhanced. The CO amount is reduced in presence of TiO_2. CO_2 formation is improved. Experimental data were fitted by kinetics models. Constants were calculated and reaction mechanisms are reported. Understanding of plasma-TiO_2 synergy has been improved by in situ and time resolved laser absorption experiment in the mid infrared region

14:15

LT2 3 Hydrogasification of Coal using Atmospheric Pressure Microwave Plasma* YONGHO KIM, HANS ZIOCK, LOUIS ROSOCHA, GRAYDON ANDERSON, DON COATES, GABRIEL BECERRA, ELIJAH MARTIN, VINCENT FERRERI, JAEYOUNG PARK, TSITSI MADZAWA-NUSSINOV, *Los Alamos National Laboratory* A clean coal technology is a newly highlighted research field because coal is America's largest domestic energy source and coal can be gasified to methane or hydrogen. However, the coal gasification process has encountered technical barriers because no reliable sulfur-tolerant chemical catalysts exist. Los Alamos National Laboratory has proposed a plasma catalyzed coal gasification concept, where plasma turns coal and reactant gases into highly reactive free radicals and excited species, which are believed to promote gasification reactions. We have developed an atmospheric pressure microwave plasma system using a 2.45 GHz magnetron. In this paper, we report the preliminary results on the hydrogasification of coal ($C + 2H_2 \diamond CH_4$). Stable plasma conditions will be explored with pulverized coal powders, as functions of hydrogen flow, and applied power. UV/IR spectroscopic measurements will be carried out to characterize the plasma properties and correlate these to hydrogasification reactivity.

*Work funded by LANL/LDRD.

14:30

LT2 4 Measurement of plasma properties in a cutting arc JOHN PETERS, JOACHIM HEBERLEIN, *University of Minnesota* JON LINDSAY, *Hypertherm Inc.* Plasma cutting utilizes a highly constricted arc to melt the material being processed. The processed material, or work-piece, serves as the anode, and arc constriction between the torch cathode and anode is attained using a small diameter nozzle together with a high velocity gas flow. This gas flow also assists in the cutting process by removing the molten material from the work-piece. The performance of the cutting system is related to the properties of the plasma jet. Temperature, electron density and the velocity of the jet are the properties used to characterize the plasma arc. Spectroscopic methods are used to measure radial and axial distributions of the temperature and electron density within the arc using several calculation methods as well as several emitting species. From these measurements the axial pressure variations due to the expansion of the underexpanded plasma jet are estimated. The validity of the assumption of LTE in different regions of the arc is also discussed. Finally, the effects of selected cutting process inputs such as current, flow rate and nozzle diameter on the plasma jet properties are evaluated.

14:45

LT2 5 A 2-Temperature Model for High Pressure High Temperature Thermal Plasmas NING ZHOU, *ESI CFD* The high pressure thermal plasmas due to its high temperature and high ionization degree, are generally modeled using equilibrium assumptions. As the results, many variables can be expressed as the functions of thermodynamic states. And in particular, the electric conductivity is measured and curve-fitted as the function of temperature, pressure for the given gas mixture. This model is attractive for its simplicity, but it neglects some important aspects of physics and is subject to the accuracy of the measured coefficients. A fluid model for high pressure high temperature thermal plasmas such as arc discharge, is therefore proposed. In this model, the thermal non-equilibrium effect is considered by solving the temperatures for electron and gas, respectively. The plasma chemical kinetics is modeled by the finite-rate reactions and the electron transport coefficients (mobility, diffusivity and electric conductivity) are calculated according to the electron collisions with heavy particles. Quasi-neutrality is assumed for the bulk of plasma and sheath model is employed to account for the near electrode phenomena. This model is validated for arc discharges at near equilibrium conditions, and the comparison with the equilibrium model is discussed.

15:00

LT2 6 Simulations of glow discharge phenomena for high-speed flow control THOMAS DECONINCK, SHANKAR MAHADEVAN, LAXMINARAYAN RAJA, *University of Texas at Austin* Plasma actuators offer a promising opportunity for high-speed flow control applications. The forcing of the flow occurs through three primary mechanisms: bulk heating of the flow, electrostatic forcing and Lorentz forcing (in the presence of external magnetic fields). In typical experiments with plasma actuators, several of these forces act simultaneously. By developing detailed computational models for the plasma and bulk flow we hope to

gain a better understanding of each of these factors. The plasma model we are using is based on a two-dimensional, self-consistent, multi-species continuum description of the plasma. A surface plasma actuator with two electrodes on a single plane is considered. A DC plasma is generated between the two exposed electrodes to produce body forces that perturb the flow. Results include maps of charge density, temperature and electric potential profiles. For an argon plasma at a pressure of 5 Torr and an applied voltage of 100 V, the sheath region in front of the cathode is about 1 mm thick. In this region where electrohydrodynamic effects are dominant, the electrostatic body force is $\sim$ 100 N/m^3. For a magnetic flux density of 1 Tesla and in a region $\sim$ 1cm thick above the electrodes, the resulting Lorentz force is $\sim$ 10 N/m^3. Relative contributions of the body forces as a function of geometry and operating conditions will be explored in this study.

15:15

LT2 7 An efficient algorithm for axisymmetrical 2D fluid ZORAN RISTIVOJEVIC, ZORAN PETROVIĆ, *Institute of Physics, POB 68, 11080 Zemun, Belgrade, Serbia and Montenegro* We have developed an efficient algorithm for steady axisymmetrical 2D fluid equations. The algorithm employs multigrid method as well as standard implicit discretization schemes for systems of partial differential equations. Linearity of multigrid method with respect to the number of grid points allowed us to use 256 $\times$ 256 grid, where we could achieve solutions in several minutes. Time limitations due to nonlinearity of the system are partially avoided by using multi level grids. In other words the initial solution on 256 $\times$ 256 grid was the extrapolated, steady solution from 128 $\times$ 128 grid which allowed using ''long'' integration time steps. The fluid solver is used as the basis for hybrid codes for DC discharges.

SESSION MT1: MATERIAL PROCESSING
Tuesday afternoon, 18 October 2005
Pine, Doubletree Hotel at 16:00
Helen Hwang, NASA/Ames CA, presiding

16:00

MT1 1 Diagnostics of a Supersonic Plasma Jet Reactor with Secondary Discharge JAMI McLAREN, *Department of Mechanical Engineering – University of Minnesota* LENKA ZAJICKOVA, *Department of Physical Electronics – Masryk University, Brno, Czech Republic* JOACHIM HEBERLEIN, *Department of Mechanical Engineering – University of Minnesota* We have used electrostatic probe measurements to determine values of floating potential, electron temperature, and ion density near the substrate in a supersonic plasma jet deposition system. This system involves a plasma jet expanding to supersonic speeds into a chamber at a pressure of 3 torr. To enhance the deposition, a secondary discharge is superimposed over the plasma jet by applying a bias to the substrate with respect to the grounded torch nozzle anode. Probe measurements have been executed for varying substrate bias, torch power, and plasma composition to determine how these deposition conditions affect the measured plasma parameters, which are assumed important for superhard B-C-N film deposition. The diagnostics reveal that ion density is enhanced by increasing torch power and positive substrate bias, the electron temperature is decreased by introducing hydrogen to the plasma jet, and the plasma floating potential increases linearly with positive substrate bias while remaining approximately constant with negative bias. The implications of these measurements for superhard film deposition in our system will be discussed.

16:15

MT1 2 High Frequency ICP Source for HDPCVD JEUNG-HOON HAN, DAEBONG KANG, JINHYUK YOO, *JUSUNG* We have developed the high frequency source with a parallel antenna for HDP CVD. In the high frequency source, we have obtained the following results. The low capacitive voltage applied to antenna could minimize capacitive damage and reduce particles from ceramic dome covering chamber. The high frequency source made lower electron temperature than low frequency (400 KHz or 2 MHz), which can minimize plasma damage on the wafer. The plasma density from this source is from 10E11 to 10E12 per cubic volume and the electron temperature is less than 4 eV in 13.56 MHz. And the antenna of the low impedance reached easy impedance matching in 13.56 MHz. This source can be easy plasma strike and stable operation at low pressure (under 1mTorr) because of using High Frequency Source. It has been proven that it was improved gap fill at lower pressure. This result is due to longer mean free paths at lower pressures. Lower pressure than 1mTorr can be made a high-conductance chamber. Also, it is important to have the symmetrical pumping system for improved gap fill performance within wafer. The process characteristic of HDP CVD has proven in 0.065 μm technology with AR (aspect ratio) 6:1 and will has expected that the gap fill solution of the next generation device.

16:30

MT1 3 Investigation of charge-up and ion reflection effects in SiO_2 etching using a three-dimensional charge-up simulation SUNG JIN KIM, *Pohang University of Science and Technology* HAE JUNE LEE, *Pusan National University* JAE KOO LEE, *Pohang University of Science and Technology* A charge-up damage is one of plasma process induced damages and comes from different motions of ions and electrons. We have performed a three-dimensional charge-up simulation [1] to examine charge-up effects. Kinetic results of particles obtained from 1D particle-in-cell simulations [2] are used as input parameters of the 3D charge-up simulation. Charge-up potential and etching rates are calculated according to ion energy distributions, aspect ratios of trenches, and secondary electron emission coefficients. In ion physical etching with etching rate less than 1 μm/min, since a charge-up potential saturated time is shorter than a one-atomic layer etched time, charge-up potential plays an important role in etching profile evolution. Ion reflection coefficients calculated by trim code and inequality of ion and electron fluxes on wafers are considered to investigate ion reflection, which creates undesirable etching profiles. This work is supported by Tera-level nanodevices in Korea Ministry of Science and Technology. [1] H.S. Park, S.J. Kim, J.K. Lee, IEEE Trans. Plasma Science, 31 (2003) 703 [2] H.C. Kim, J.K. Lee, Phys. Rev. Lett., 93 (2004) 085003.

16:45

MT1 4 Measurement and analysis on ultraviolet radiation damage during plasma processing KEUN HEE BAI, KYEONG-KOO CHI, KEN TOKASHIKI, CHANG-JIN KANG, HANKU CHO, JOO-TAE MOON, *Samsung Electronics* As the feature size of ULSI device shrinks, device becomes more sensitive to the plasma damages caused from the charged particles (charge-up

damage) or ultraviolet radiation in the plasma. Generally, the charge-up damage is due to the plasma nonuniformity, electron shading effect or the antenna effect. However, the charge-up causes less damage with scaling down of the gate oxide thickness as decreasing the feature size. On the other hand, the damage from ultraviolet radiation will become relatively important when the gate oxide thickness decreases. It is difficult to decrease the ultraviolet radiation damage because it depends on various plasma parameters such as the electron temperature and density as well as the gas species. In this presentation, the ultraviolet damage is quantitatively analyzed by measuring the shift of threshold voltage in a specially designed E^2PROM transistor (electrically erasable read-only memory transistor) and optical emission spectroscopy in various plasma conditions to analyze the dependence of the ultraviolet damage on plasma parameters. Also, the effect of ultraviolet radiation is correlated to the device which is kwon to be sensitive to the ultraviolet damage.

17:00

MT1 5 Effect of Species Density and Ion Scattering During Ashing on Ultra Low-κ Inter-Level Dielectric Films M.A. WORSLEY, S. BENT, N.C.M. FULLER, T.L. TAI, J. DOYLE, M. ROTHWELL, T.J. DALTON, *Stanford University* Results of experimental analysis of an ultra low-κ inter-level dielectric (ILD) after ashing together with a determination of key parameters in the plasma are presented. Optical emission (OE) actinometry is used to measure the absolute densities of reactive radical species in several plasmas, and modeling of sheath thickness and positive ion mean free path is used to estimate the significance of ion scattering. The densities of H, N, and O are determined as a function of pressure and percentage argon in Ar/H_2, Ar/N_2, and Ar/O_2 plasmas respectively. Modeling reveals that a bias power range of 0-350W allows the sampling of different scattering regimes. Patterned structures in a porous organosilicate glass (OSG) are ashed under the characterized plasma conditions and then analyzed using XPS. Data from the OE actinometry and modeling are combined with the XPS data to gain further insight into the mechanism by which modification of the OSG occurs in a patterned structure.

17:15

MT1 6 Etching with Electron Beam-Generated Ion-Ion Plasmas S.G. WALTON, D. LEONHARDT, M. LAMPE, R.F. FERNSLER, *US Naval Research Laboratory* The advantage of positive ion-negative ion (ion-ion) plasmas in etching processes is the delivery of anisotropic fluxes of itboth positive and negative ions to the substrate surface, which is thought to prevent device damage and isotropic etch profiles associated with surface charging. Unfortunately, the low electron temperature required for ion-ion plasma formation in halogen-based gases is typically found only in the afterglow of pulsed plasmas, thereby limiting the duration and magnitude of the useful flux. Electron beam–generated plasmas are characterized by low electron temperatures (< 1.0 eV) during all phases of plasma production and can thus provide a continuous ion-ion plasma. In this work, we discuss silicon etching using these ion-ion plasmas produced in Ar/SF_6 mixtures. System operation and diagnostics are presented and correlated to a theoretical model (See paper by M. Lampe et al.). Silicon etch rates as a function of various input parameters will also be discussed. This work was supported by the Office of Naval Research.

SESSION MT2: GLOWS I
Tuesday afternoon, 18 October 2005
Cedar, Doubletree Hotel at 16:00
T. Gans, Ruhr University, Bochum, presiding

Contributed Papers

16:00

MT2 1 Thomson scattering and simulation study of electron energy distribution near the dielectric plate of a planar surface wave plasma source A. KONO, T. OTSUKI, R. LEE, J. KOBAYASHI, M. ARAMAKI, *Nagoya University* Planar surface wave plasma (SWP) is expected to be a promising plasma source producing large-area low-electron-temperatures plasma for materials processing. To clarify the electron heating mechanism in SWP, Thomson scattering measurements and Monte-Carlo simulation study are carried out. A mechanism believed to be responsible for electron heating is the existence of a thin resonance layer near or in the sheath region where the local electron plasma frequency equals the microwave frequency and hence the microwave electric field is enhanced. In the simulation, first the microwave electric field is estimated by solving the fluid equations for electron motion and then carrying out Monte-Carlo simulation in the estimated electric field to obtain the electron energy distribution. The results of simulation indicate that average energy increases near the dielectric plate as observed in Thomson scattering measurements. The electron energy distribution obtained in the simulation (with the effect of Coulomb collision included) is nearly Maxwellian and does not show a high energy hump as reported in some probe studies. (Work supported by 21st Century COE Program from MEXT Japan)

16:15

MT2 2 Time-Resolved Studies of Pulsed Plasmas* JOSE LOPEZ, WEIDONG ZHU, *Stevens Institute of Technology* BISWA N. GANGULY, *US Air Force Research Laboratory, Propulsion Directorate, WPAFB* PETER BLETZINGER, JAMES M. WILLIAMSON, *Innovative Scientific Solutions, Inc.* ABRAHAM BELKIND, *Stevens Institute of Technology* KURT H. BECKER, *Center for Environmental Systems, SIT* A periodic reversal of the voltage applied to an electrode during the application of pulsed direct current (DC) power has been shown to diminish the buildup of charge due to the attraction of oppositely charged particles in the reverse pulse. This technique has been widely used to reduce arcing caused by charge buildup, especially in reactive magnetron sputtering of dielectric films. A more recent application has been the application of very short DC pulses of voltages much higher than the breakdown voltage to dielectric barrier discharges (DBD). The resulting very high, but short-lived electric fields can enhance radical generation and the intensity of UV radiation emitted by the plasma. In an effort to better understand the effects of frequency, pulse width, and duty cycle on magnetron sputtering and DBDs, time-resolved electrical measurements and optical plasma emission spectroscopy and imaging were carried out using a fast intensified CCD (ICCD) camera. The effects of the pulsed DC power on the physical processes of both types of plasmas will be discussed in this work.

*Work supported by AFOSR and NSF.

16:30
MT2 3 Shockwave interactions with ionization waves in argon glow discharges NICHOLAS SIEFERT, BISWA GANGULY, We report measurements of enhancement in both optical emission and electric field at the shock front of weak shock waves (M~ 2) propagating in a 2 Torr argon glow discharge. The enhancements depend on when the shockwave arrives at the observation point because of the electric field modulation by the ionization wave. The ionization waves create large-amplitude fluctuations of the electron temperature and electron number density, which are modulated out of phase in order to conserve discharge current. This creates a plasma where the local electron Debye length fluctuates by nearly an order of magnitude without changing global properties, such as Mach number, gas pressure, and gas temperature. Depending on the timing between the ionization wave and the shockwave arrival, the local electron Debye length at the shock front can fluctuate between being either greater than or less than the shock thickness. The shockwave-induced enhancement in optical emission intensity and the electric field were found to exceed the modulation caused by the ionization wave itself only if the shockwave arrives when the Debye length is a maximum in the ionization wave. These measurements shows that, under a certain range of electron Debye length, shock thickness, and electron-neutral collision mean free path, there is an increase in the already non-equilibrium energy of the electrons at the shock front.

16:45
MT2 4 Spectrometric analysis and kinetic modelling of an O_2-N_2 discharge CHANEL HAYDEN, DEREK MONAHAN, MILES M. TURNER, ANDREY ISLYAIKIN, ALBERT R. ELLINGBOE, *Dublin City University, Ireland* Low pressure O_2-N_2 plasmas are widely used in a number of industrial processes such as surface treatment, cleaning and polymer etching. In this paper we will present an experimental analysis of an ashing discharge via mass spectrometry and optical emission spectrometry. The equipment under analysis comprises of an upstream microwave-rf downstream configuration at an operating pressure of 850 mT. Diagnostics were applied to the downstream chamber and a number of measurements taken for a range of microwave-rf power values and varying gas fractions. Resultant neutral species present in the discharge (N, O, NO, N_2O, NO_2) were analysed throughout this range of physical conditions. A general global model, currently under development, was used to simulate the experiment by means of a complex chemistry data set. It was found that the model was very sensitive to chemistry inputs, as such resulting outputs may well be deemed unreliable. Further investigation of the reliability of chemistry sets through validation by experimental assessment is central to the relevance of data obtained from global models.

17:00
MT2 5 Balmer series emission in the afterglow of high-pressure, laser-induced hydrogen and hydrogen-argon plasmas LUTZ HÜWEL, *Wesleyan University* TOM MORGAN, *Wesleyan University* BILL GRAHAM, *Queen's University Belfast* The afterglow of photoionised plasmas created in hydrogen and hydrogen with a small fractional addition of Ar (3.5 %) has been studied by focussing a 15 ns, 10 Hz, 1064 nm laser pulse into gas that is at a pressure of 10^5Pa. At the focus, the laser power density is about 10^{11} W/cm^2. Light emission is dispersed by a 0.6 m monochromator, with a 1220 line/mm grating blazed at 500 nm and detected using an image-intensified linear diode. In pure hydrogen, Hα, Hβ, and Hγ emission was observed to about 4 μs. In the mixture, the peak emission intensity is enhanced by a factor of about 2, Hδ and Hε lines are also observed, and the emission of the Hα and Hγ was observable to about 6 μs. The electron density, determined from Stark-broadening, is found to have a complex temporal behaviour. From an initial value at 0.3 μs of about 3.5×10^{16} cm^{-3} in pure hydrogen and 6.5×10^{16} cm^{-3} in the H_2/Ar mixture, the density falls by an order of magnitude by 1.5 μs. Thereafter, in pure hydrogen, an increase in density by about 1×10^{15} cm^{-3} over a period of about 1 μs is observed, followed by a decrease. In the mixture, a plateau occurs in the density temporal behaviour. It is also found that the line emission intensity decay rate changes at about 1.5 μs (pure). WG was a Mellon Fellow at Wesleyan University.

17:15
MT2 6 Enhanced Plasma Transport due to Neutral Depletion* AMNON FRUCHTMAN, GENNADY MAKRINICH, *Holon Academic Institute of Technology* PASCAL CHABERT, JEAN-MARCEL RAX, *LPTP, Ecole Polytechnique* The dynamics of plasma and neutral-gas in pressure balance are solved self-consistently to reveal the impact of neutral depletion. Analytical relations that determine the electron temperature, the rate of ionization, and the plasma density are derived. For the governing nonlinear diffusion equation an analytical solution in the form of Kepler's equation is found. A generalized Schottky condition is derived in which the total number of neutrals, rather than the Paschen parameter, controls the electron temperature. It is shown that even if the plasma is weakly- ionized (typically 1%), neutral depletion dramatically modifies the discharge equilibrium. Due to the inherent coupling of ionization and transport, an increase of the energy invested in ionization can nonlinearly enhance the transport process. We show that such an enhancement of the plasma transport due to neutral depletion can result in an unexpected it decrease of the plasma density when power isit increased, despite the increase of the flux of generated plasma.

*Supported by CNRS and the Israel Science Foundation (grant no. 59/99).

SESSION NT: RECEPTION AND BANQUET
Tuesday Evening, 18 October 2005
Pine/Cedar, Doubletree Hotel at 18:00

18:00
NT 1 Reception and Banquet

SESSION PW1: LIGHTING AND LASERS
Wednesday morning, 19 October 2005; Pine, Doubletree Hotel at 8:00
Walter Lempert, Ohio State University, presiding

Invited Paper

8:00
PW1 1 High Power Extreme Ultra-Violet (EUV) Light Sources for Future Lithography.
JEROEN JONKERS, *Philips EUV, Steinbachstrasse 15, 52074 Aachen, Germany*

Extreme Ultra-Violet (EUV) lithography is most likely to be used for the production of semi-conductors from about 2009. This technology will use 13.5 nm radiation to image features of 32 nm and below. One of the potential showstoppers in the commercialisation is the availability of a compact, high power source. Roughly, 500 to 1000 W in 2π sr and within a 2% bandwidth is required. Moreover, the lifetime of the first collector mirror (located at 10 to 20 cm away from the light source) should exceed half a year in continuous operation. This paper gives an overview of the latest developments in plasma-based EUV sources. In this case, transition radiation of highly ionised atoms (like Li III, O VI, Xe XI and Sn VIII to XIII) is used. There are two different schemes to achieve the high plasma temperatures (20 to 40 eV), which are necessary to reach these ionization stages: laser-produced plasmas (LPPs) and discharges. The progress within the first category seems to be limited as LPPs are roughly at the same level as five years ago. In the field of gas discharges and vacuum sparks, a lot of progress has been made recently. Especially vacuum sparks seem to offer the possibility to meet the specifications for high-volume manufacturing.

Contributed Papers

8:30
PW1 2 Excitation of $O_2(^1\Delta)$ in Pulsed Radio Frequency Flowing Plasmas for Chemical Oxygen Iodine Lasers* NATALIA BABAEVA, *Iowa State University* RAMESH ARAKONI, *University of Illinois* MARK J. KUSHNER, *Iowa State University* In chemical oxygen-iodine lasers (COIL), oscillation at 1.315 μm ($^2P_{1/2} \rightarrow {}^2P_{3/2}$) in atomic iodine is produced by collisional excitation transfer of $O_2(^1\Delta)$ to I_2 and I. Plasma production of $O_2(^1\Delta)$ [eCOIL] is interesting to eliminate liquid phase generators. For the flowing plasmas used for eCOILs (He/O_2, a few to 10s Torr) self sustaining electron temperatures are 2-3 eV whereas excitation of $O_2(^1\Delta)$ optimizes with T_e = 1-1.5 eV. Lowering T_e is of interest to increase system efficiency. One method is the spiker-sustainer (S-S). A high power pulse (spiker) is followed by a lower power quasi-dc period (sustainer). Excess ionization produced by the spiker enables the sustainer to operate with a lower T_e. Results from global kinetics modeling suggest that S-S can raise yields of $O_2(^1\Delta)$-to over 30%. In this paper, results from a computational investigation of radio frequency (13, 27, 56 MHz) excited flowing He/O_2 plasmas will be discussed with emphases on S-S techniques. The model is a 2-dimensional plasma hydrodynamics simulation encompassing a solution of Navier Stokes equations for neutral flow dynamics. The efficiency of S-S methods generally increase with increasing frequency by producing a higher electron density, lower T_e and, as a consequence, a more efficient production of $O_2(^1\Delta)$.

*Work supported by Air Force Office of Scientific Research.

8:45
PW1 3 Plasma Kinetics of High Power Overtone Carbon Monoxide Lasers YURII UTKIN, MATTHEW GOSHE, IGOR ADAMOVICH, WALTER LEMPERT, J. WILLIAM RICH, *Ohio State University* Electric-discharge-excited carbon monoxide gas lasers, operating on either the fundamental vibrational bands (near 5 μ) or first overtone vibrational bands (near 2. 5 μ) are among the very few lasers operating at high efficiencies ($>$ 10%) that are scalable to truly high c.w. powers. We report the recent development of a small compact first overtone band CO laser, together with a plasma kinetic model of the laser. Model calculations show that it is possible to build a CO laser operating on the second and higher vibrational overtone bands, with high efficiencies and powers. The possibility of lasing over a very large bandpass, extending to short IR wavelengths, is discussed.

9:00
PW1 4 Color Rendering and Power Factor Trade-offs in Rare Earth Containing Ceramic Discharge Metal Halide Lamps RAY GIBSON, *Philips Lighting Company* Medium power ceramic discharge metal halide lamps that contain rare earth iodides have been designed to operate on existing pulse start metal halide magnetic ballast systems intended for quartz lamps that utilize the $NaI\text{-}ScI_3$ salt system. One problem encountered was that the rare earth containing ceramic lamps operated well below rated power on commercial ballasts with the consequence of lower luminous flux than expected. Lower power operation is characterized electrically as a lower lamp power factor. Experiments were carried out with several different discharge tube dimensions and salt chemistries, which showed a strong correlation between color rendering (CRI) and lamp power factor. Higher CRI lamps had lower power factors. One-dimensional modeling of the arc plasma using the Elenbaas-Heller equation confirmed that by increasing the radiation contribution from the rare earth salts to model a higher lamp CRI resulted in larger swings in the central arc temperature. Consequently, a high re-ignition voltage during current reversal occurs and the lamp power factor is lowered.

9:15
PW1 5 Model Study of Breakdown in Long Tubes W.J.M. BROK, J.J.A.M. VAN DER MULLEN, G.M.W. KROESEN, *Eindhoven University of Technology* EPG TEAM The mechanisms responsible for the propagation of ionization waves that occur in a straight discharge tube during breakdown are studied by means of a fluid model. The discharge tube contains a gas mixture of argon at 3.0 Torr and saturated mercury vapour. The electrodes are heated to thermal emission temperatures. These conditions are

similar to those found in fluorescent lamps. Firstly, operation at a dc applied voltage is investigated numerically and compared to experimental observations. Secondly, breakdown at a high frequency (tens of kHz) applied voltage is considered. It will be shown that during dc operation, the anode directed ionization wave charges the wall of the lamp and thereby shields it from outside influences on the electric field. When this wave reaches the anode, a conducting path is established between the electrodes. The subsequent cathode directed ionization wave increases the plasma density and redistributes the axial electric field towards the situation found in stationary operating discharges. During ac operation, depending on the frequency, these two processes alternate as the ionisation wave cannot cross the entire tube in a half-cycle of the applied voltage.

SESSION PW2: PLASMA SHEATHS
Wednesday morning, 19 October 2005
Cedar, Doubletree Hotel at 8:00
B. Graham, Queen's University-Belfast, UK, presiding

Contributed Papers

8:00
PW2 1 The plasma-sheath transition in the Tonks-Langmuir model KARL-ULRICH RIEMANN, *Ruhr-University, D 4470 Bochum, Germany* The plasma-sheath matching problem in the hydrodynamic plane Tonks-Langmuir model has attracted considerable interest during the last few years. It is complicated not only by the singular structure of the asymptotic ($\lambda_D/L \to 0$) plasma and sheath solutions but also by a coupling with the eigenvalue problem originating from the plasma balance. Due to these difficulties the existence of a matched asymptotic expression uniformly valid from the plasma core to the wall is widely questioned. The issue is clarified both analytically and numerically by the explicit construction of a matched asymptotic expression and comparison with exact solutions. Accounting for a shift in the ionization eigenvalue, the approximations obtained by consistent matching show an excellent agreement with numerical potential curves. The singularities of the asymptotic components are reflected by small discontinuities in the derivatives that vanish in the limit $\lambda_D/L \to 0$. Finally an outlook is given to the kinetic analysis of the same problem.

8:15
PW2 2 Electron sheaths in low-pressure weakly-collisional plasma* N. HERSHKOWITZ, *D* S. BAALRUD, B. LONGMIER, *Department of Engineering Physics, University of Wisconsin-Madison* The plasma potential in anode sheaths can be negative going measured from the anode (electron sheaths) or positive going (ion sheaths). In weakly-collisional low-pressure plasma, electron sheaths are normally only present near small probes when they are biased more positive than the plasma potential or at electron emitting surfaces. Electron sheaths created along the axis of a large positively biased plate (diameter = 10 cm) located in a multi-dipole argon plasma are described here. Experimental data show non-ambipolar electron loss in which the electron sheath collects almost all electrons produced by ionization if sufficient loss area is provided for ions at the chamber walls. Measurements of the plasma potential with emissive probes and Langmuir probes show potential dips form at the sheath edges to limit electron loss and increase ion energy. The use of electron sheaths for extracting electron beams from both dc and rf plasma will also be discussed.

*Work Supported by US DOE Grant No. DE-FG02-97ER 54437.

Invited Paper

8:30
PW2 3 Measurement of Electric Fields in Radio Frequency Argon Discharges.*
ED BARNAT, *Sandia National Laboratories*

We present a summary of our measurements of electric fields present in the sheath region formed between an electrode and a radio frequency generated argon plasma. Experimental calibrations for several Stark shifted argon Rydberg states are presented. Desired field resolution and field range are shown to be dependant on the choice of Rydberg level probed. For example, the 11d[1/2] level can be used for fields exceeding 5000 V/cm while the behavior of Rydberg states around 38n push detection sensitivities down to the V/cm level. Both spatial and temporal maps of the electric fields are presented for sheaths formed around several electrode configurations. Electrode configurations studied range from complex topologies present on a powered electrode to thin metallic wires (Langmuir probes) present in the bulk of the discharge. Discussion will be offered on the effect of the electrode structure on the resulting field structure as well as the resulting behavior of the discharge around the electrode. When possible, comparison between the measured sheath structure and expected sheath structure will be made. This work was supported by the Division of Material Sciences, BES, Office of Science, U. S. Department of Energy and Sandia National Laboratories, a multiprogram laboratory operated by Sandia Corporation, a Lockheed Martin Company for the United States Department of Energy's National Nuclear Security Administration under contract DE-AC04-94AL85000.

*In collaboration with Greg Hebner, Sandia National Laboratories.

Contributed Papers

9:00
PW2 4 Measurements of the Sheath Capacitance using a Tunnel Diode Oscillator in Inductively Coupled Plasmas SEJIN OH, MINHYONG LEE, PYUNGWOO LEE, CHINWOOK CHUNG, *Division of Electrical Engineering, Hanyang University* A tunnel diode oscillation method is one of techniques to measure the sheath capacitance in plasmas. [B.M Oliver et. al., J. Physics. E. 5, 718] Using this method, we investigated the sheath capacitance of a ring probe in an Inductively Coupled Plasmas (ICPs). The effects of the RF fluctuation and the noise on the sheath capacitance were considered. We measured the change in the tunnel diode oscillation frequency to acquire the sheath capacitance of the probe. The probe was biased with probe potentials ranging from 0V to -45V. The result agreed well with that calculated from a Child- Langmuir theory when the probe was highly negative biased with respect to the probe floating potential. However, it was found that the measured sheath capacitance increases rapidly than that from the Child-Langmuir theory as the bias potential increases. This is understood by the Bohm sheath theory.

9:15
PW2 5 Investigation of anodes for high intensity discharge lamps OLIVER LANGENSCHEIDT, LARS DABRINGHAUSEN, STEFAN LICHTENBERG, MARCO REDWITZ, JUERGEN MENTEL, PETER AWAKOWICZ, *Ruhr-University of Bochum* To optimize the electrodes of high intensity discharge (HID) lamps a detailed physical understanding of the interaction between the arc column and the cathode and anode has to be achieved. In the Bochumer model lamp the anodic behaviour of electrodes for high intensity discharge lamps was characterized by pyrometric, electric and spectroscopic measurements. The lamp was operated with currents between 0.5A to 10A in pure noble gases at pressures up to 1MPa and pure or doped tungsten electrodes of different sizes. The temperature and power losses of the anode were determined by pyrometric measurements, the anode fall by Langmiur-probe measurements. Spatially resolved spectroscopic measurements yield the electron temperature and density in front of the anode. It is found that the plasma in front of the anode consist of a contraction zone with enhanced power input and an anodic boundary layer which converts thermal power into electrical power. The temperature of the anode shows a stronger current dependency than the cathodic tip temperature. In AC operation it is possible to pre-heat the electrode during the anodic phase and therefore to influence the subsequent type of cathodic arc attachment.

SESSION QW1: ELECTRON AND POSITRON COLLISIONS
Wednesday morning, 19 October 2005; Pine, Doubletree Hotel at 10:00
Murtadha A. Khakoo, California State University-Fullerton, presiding

Invited Papers

10:00
QW1 1 High-Precision Cross Sections for Electron-Atom Collisions in Laser and Lighting Applications.* KLAUS BARTSCHAT, *Drake University, Department of Physics and Astronomy, Des Moines, IA 50311*

In recent years, much progress has been achieved in calculating reliable cross-section data for electron scattering from atoms and ions. In particular, the ''convergent close-coupling'' (CCC) [1] and ''R-matrix with pseudo-states'' (RMPS) [2] methods have been extremely successful in describing elastic scattering as well as electron-impact excitation and ionization of light quasi-one and quasi-two electron targets, such as atomic hydrogen, helium, the alkalis, and the alkali-earth elements. However, accurate calculations of electron collisions with more complex targets, notably the heavy noble gases Ne − Xe, heavy quasi-one electron targets such as Zn, Ba, or Hg, and transition metals such as Fe or Mo [3], continue to be a major challenge. We have recently further developed a new version of the R-matrix (close-coupling) method, using a B-spline basis with non-orthogonal sets of term-dependent orbitals [4]. This method allows us to generate target descriptions of unprecedented accuracy in collision calculations. Example results [5-7] for some of the systems mentioned above illustrate that the flexibility of the B-spline R-matrix (BSR) method to describe both the N-electron target and the $(N + 1)$-electron collision problems is of crucial importance for obtaining highly accurate cross sections, particularly in the low-energy near-threshold regime, which is often dominated by resonance structure. [1] I. Bray, D.V. Fursa, A.S. Kheifets, and A.T. Stelbovics, J. Phys. B **35** (2002) R117. [2] K. Bartschat, Comp. Phys. Commun. **114** (1998) 168. [3] K. Bartschat, in *Atomic and Molecular Data and Their Applications*, D.R. Schultz, P.R. Krstic, and F. Owbny (eds.), AIP Conf. Proc. #636 (2002) 192. [4] O. Zatsarinny and C. Froese Fischer, J. Phys. B **33** (2000) 313. [5] O. Zatsarinny and K. Bartschat, J. Phys. B **37** (2004), 2173 and 4693. [6] O. Zatsarinny and K. Bartschat, Phys. Rev. A **71** (2005), 022716. [7] O. Zatsarinny, K. Bartschat, L. Bandurina, and V. Gedeon, Phys. Rev. A **71** (2005) 042702.

*This work was performed in collaboration with Oleg Zatsarinny and supported by the NSF under grants PHY-0311161 and PHY-0244470.

10:30
QW1 2 Ionization of Simple Molecules by Ion or Electron Impact in a Reaction Microscope.*
CHRISTINA DIMOPOULOU, *Max-Planck-Institut für Kernphysik, Heidelberg, Germany*

We have studied single ionization of simple molecules by fast charged particle impact in a reaction microscope. By measuring the momenta of the emitted electron and the recoil ionic fragment in coincidence, channel-selective low-energy electron spectra have been recorded. For non-dissociative ionization of H_2 by 6 MeV protons, the electron energy distribution agrees well with a CDW-EIS prediction [1] except for $E_e < 1$ eV where an significant enhancement is observed. It is due to the autoionization of rovibrational levels of Rydberg states of H_2, which occurs by converting vibrational energy into kinetic energy of the emitted electron. First fully differential cross sections have been obtained bearing the ''signature'' of this molecular mechanism, which lies beyond the Born-Oppenheimer approximation [2]. Recently, considerable interest has been raised by the observation of two-center interference effects in the electron emission from H_2, in analogy to Young's double-slit experiment [3]. They are predicted to be more pronounced if one could fix the orientation of the molecular axis at the instant of the collision [4]. For dissociative ionization of H_2 by 6 MeV protons we had access to this information. Molecular-frame angular distributions of the emitted electrons have been compared to the CDW-EIS calculation [5]. Argon dimers as well as atomic Ar, both present in the same gas-jet, are ionized by 1keV electron impact in a kinematically complete experiment carried out in an upgraded reaction microscope. The obtained electron spectra for Ar_2 and Ar are compared directly in order to identify interference structures, which are expected to be much more visible than for H_2 since the interatomic distance of Ar_2 is comparable to the de Broglie wavelength of the emitted electron. [1] M.E. Galassi et al., Phys. Rev. A **66**, 052705 (2002) [2] C. Dimopoulou et al., Phys. Rev. Lett. **93**, 123203 (2004) [3] N. Stoltherfoht et al., Phys. Rev. Lett. **87**, 023201 (2001) [4] G. Laurent et al., J. Phys. B **35**, L495 (2002) [5] C. Dimopoulou et al., J. Phys. B **38**, 593 (2005)

*Coauthors: R. Moshammer, A. Dorn, D. Fischer, P.D. Fainstein, M. Dürr, C. Höhr and J. Ullrich.

Contributed Papers

11:00
QW1 3 Low Energy Proton Impact Ionization M. FOSTER, D.H. MADISON, J.L. PEACHER, M. SCHULZ, *University of Missouri - Rolla* LABORATORY FOR ATOMIC, MOLECULAR AND OPTICAL RESEARCH COLLABORATION Recent experiments have measured fully differential cross sections (FDCS) for single ionization of helium by 75 keV proton impact for fixed ejected electron energies and different momentum transfers. These measurements show major discrepancies in the absolute magnitude between the experiment and the theoretical, 3DW (three-distorted-wave) model. The 3DW model is a fully quantum mechanical calculation that has accurately predicted FDCS for higher energy C^{6+} impact ionization of helium. However, the 3DW model treats the collision as a three-body process (projectile, ion, ejected electron). The lack of agreement between the 3DW model and experiment for low energy collisions suggests that a three-body model may not be appropriate for lower collision energies (especially, when considering that a proton with energy of 75 keV is equivalent to electron energy of 40 eV, which is only 15 eV above the ionization threshold for helium). These experiments further demonstrate the fact that the fundamental physics governing a simple collision process is still not well understood. Consequently, we will present a complete four-body model known as the 6DW (six- distorted-wave) model. The 6DW model takes all two particle Coulomb interactions (six in total) into account on equal footing.

11:15
QW1 4 Excitation of H_2 by electron impact* YONG-KI KIM, *NIST, Gaithersburg, MD* M. ASGAR ALI, *Howard Univ., Wash. DC* Cross sections for the excitation of H_2 by electron impact from its ground electronic state to the first two dipole- and spin-allowed electronic states (B and C) have been calculated by modifying plane-wave Born cross sections (BE scaling) as was done successfully for neutral atoms.[1] The scaled cross sections are in good agreement with the experimental data by Khakoo and coworkers.[2] [3] Calcualtion of BE scaled excitation cross sections for other molecules is in progress, and the results will be presented at the conference.

*Work at NIST was supported in part by the Office of Fusion Energy Sciences, USDOE.

[1]Y.-K. Kim, Phys. Rev. A **64**, 032713 (2001).
[2]M.A. Khakoo and S. Trajmar, Phys. Rev. A **34**, 146 (1986).
[3]J. Wrkich et al. J. Phys. B **35**, 4695 (2002).

11:30
QW1 5 Positron-molecule annihilation, Feshbach resonances and bound states* J.A. YOUNG, C.M. SURKO, *University of California, San Diego* Positron-matter interactions are unique as the positron has no exchange interaction with electrons, is repelled by nuclei, can form positronium and can annihilate with electrons. Using monoenergetic positrons from a trap-based beam, we have been able to measure the first energy-resolved, positron-on-molecule annihilation spectra below the positronium formation threshold [1,2]. Strong peaks in annihilation rate are observed at energies just below the vibrational modes of various molecules. These peaks are due to vibrational Feshbach resonances (VFR) and provide evidence of positron-molecule binding. In alkanes, the binding energy grows linearly and the annihilation rate exponentially with molecular size. In this paper, the properties of these VFR are further explored. The dependence on target morphology is studied for the ring hydrocarbons, benzene, cyclohexane and cyclopropane. A comparison is presented of positron-annihilation and infrared-absorption spectra. Finally, evidence is presented for a second, ''positronically excited'' bound state in largest alkane molecules studied. [1] S. J. Gilbert, et al., Phys. Rev. Lett., **88**, 043201 (2002). [2] L. D. Barnes, et al., Phys. Rev. A **67**, 032706 (2003).

*This work is supported by NSF.

11:45

QW1 6 Positron transport in argon M. SUVAKOV, Z. LJ. PETROVIC, *Institute of Physics, POB 68, 11080 Zemun, Belgrade, Serbia and Montenegro* S.J. BUCKMAN, *Australian National University* We have compiled a complete set of cross sections for positrons in argon based on recent measurements and theory. All aspects of the positron transport differ significantly from that of electrons. The positronium channel leads to a loss of positrons and therefore will be analogous to electron attachment in electron transport. At the same time ionization is treated as an inelastic, conservative process. A Monte Carlo program has been used to calculate positron transport coefficients. The most significant feature is the effect of positronium formation at low E/N. The transport coefficients show a huge effect of non- conservative collisions as the bulk drift velocity becomes almost two orders of magnitude smaller than the flux drift velocity. At higher E/N, however, the two drift velocities have the same order of magnitude.

SESSION QW2: INDUCTIVELY COUPLED PLASMAS
Wednesday morning, 19 October 2005
Cedar, Doubletree Hotel at 10:00
T. Makabe, Keiou University, presiding

10:00

QW2 1 2D Fluid Simulation of VHF_ICP Source with Parallel Resonance Antenna for Next Generation Etch Processing SUNG HEE LEE, JAE KOO LEE, *Department of Electronics and Electrical Engineering, Pohang University of Science and Technology, S.Korea* *G.C.KWON, *J.W.SHON COLLABORATION Inductively coupled plasma is known for high-density material processing at low pressure. In addition to high density and low pressure, a next generation of plasma sources are needed to control the ion flux and ion-bombarding energy for wafer of over 300mm diameter. However the conventional ICP source with a spiral antenna have a problem of non-uniformity due to large inductance. To overcome the non-uniformity problem, the antenna is segmented and three segments are connected in parallel. The antenna with three segments connected in parallel also causes the non-uniformity problem due to the difference of inductance for each segments. The current in outer segment is larger than that of other segments and it causes the non-uniformity of plasma in radial direction. To reduce the problem, the variable capacitor is connected in series with outer segment. After all, we can overcome the problem of non- uniformity by the proper distribution of current among three segments with variable capacitor. To investigate the discharge phenomenon in the VHF(Very High Frequency-)_ICP source that consists of the parallel resonance antenna, we have used a two-dimensional fluid simulation and the results from our simulation are compared with experimental data. * Jusung Engineering Co, Gwangju-Gun, Gyeonggi, S.Korea

10:15

QW2 2 Numerical Study of Hysteresis Phenomenon in an Inductively Coupled Plasma in Ar TOSHIKAZU SATO, TOSHIAKI MAKABE, *Keio University* As is well known, there exist two sustaining mechanisms in inductively coupled plasmas (ICPs), capacitive coupling mode (E mode) and inductive coupling mode (H mode)[1][2]. Especially in H mode, ICP in Ar is sustained by direct ionization and stepwise ionization of metastables. The ratio of these two processes significantly depends on the external conditions. A large amount of metastables in an ICP reactor gives a strong hysteresis of the plasma density as a function of input power, because high density plasma can be sustained by way of the stepwise ionization even at low power supply. In this paper, we numerically investigate the role of Ar metastables in the sustaining mechanism and the hysteresis characteristics in an Ar-ICP. The contribution of the stepwise ionization of Ar metastable to the total plasma production considerably depends on the gas pressure. The plasma density shows a strong hysteresis under the presence of metastables at 50 mTorr. We will also discuss the dependence of the hysteresis characteristics on gas pressure. [1] Y. Miyoshi et al, IEEE Trans. Plasma Sci., 30, 130 (2002). [2] Y. Miyoshi et al, J. Phys. D: Appl. Phys., 35, 454 (2002).

10:30

QW2 3 Investigations on an inductively coupled magnetic neutral loop discharge* DEBORAH O'CONNELL, DRAGOS CRINTEA, MARTIN BRENNSCHEIDT, TIMO GANS, UWE CZARNETZKI, *Institute for Plasma and Atomic Physics, Ruhr-University Bochum, Germany* An inductively coupled magnetic neutral loop discharge (NLD) was designed and has been investigated using various diagnostic techniques. Coaxial coils produce a magnetic field vanishing along a ring in the discharge - the so called neutral loop (NL). An oscillating rf electric field along the NL is induced through a planar four turn ICP antenna operated at 13.56 MHz. Stochastic electron heating in the NL allows for plasma operation at extremely low pressure, down to 10^{-2} Pa. These conditions are ideal for anisotropic etching, while uniform plasma surface treatment can be achieved by varying the NL diameter. Langmuir probe measurements, revealing electron densities up to $10^{12} cm^{-3}$ and electron temperatures up to 10 eV, are in good agreement with global model predictions. Phase resolved optical emission spectroscopy (PROES) allows us to distinguish the different power coupling mechanisms in the discharge. PROES is used to probe the high energy tail of the electron energy distribution function (EEDF), while the low energy part of the EEDF can be measured using phase resolved Thomson scattering.

*The project is funded by the DFG in the frame of SFB 591.

10:45

QW2 4 Electrical and Plasma Parameters of Distributed ICP Driven by Ferromagnetic Core Array WONKI LEE, CHINWOOK CHUNG, *HanYang University* V.A. GODYAK, *OSRAM Sylvania* Two distributed plasma sources were explored and results were compared with corresponding data obtained in a conventional ICP with flat coil driven at 13.56 MHz. The first source was driven with six toroidal ferromagnetic cores at 400 kHz. This source was able to operate in a wide range of the input rf power. In reported experiments, the rf power delivered to plasma was up to 4 kW at the input rf voltage less than 300 V and high power factor and power transfer efficiency. The second source driven with eighteen toroidal inductors at fixed rf power has demonstrated an exceptional plasma uniformity measured near the discharge chamber bottom. Due to mainly resistive input impedance, the power factor of both ICP sources was close to 1 and the input voltage and current are order of magnitude less than in the similar wattage conventional ICP system operating at 13.56 MHz. Plasma parameters, the plasma density and electron temperature were obtained as appropriate integrals of the measured electron energy distribution functions. A twice less the plasma

potential (15 V) was found in ICP driven with ferromagnetic cores at 400 kHz than that in the conventional ICP driven at 13.56 MHz. It seems that ICP with ferromagnetic cores has a great potential as a plasma sources for next generation plasma processing.

11:00
QW2 5 Investigations of the E-H transition in an inductively coupled plasma using phase resolved optical emission spectroscopy* DEBORAH O'CONNELL, TIMO GANS, UWE CZARNETZKI, *Institute for Plasma and Atomic Physics, Ruhr University Bochum, Germany* Inductively coupled plasmas (ICPs) can be operated in capacitive mode (E-mode) or inductive mode (H-mode) depending on the RF power. At relatively low powers the electron density is not sufficient to sustain H-mode operation and the RF antenna acts as an electrode, therefore the discharge operates in E-mode. Phase resolved optical emission spectroscopy (PROES) can be used to distinguish between E- and H-mode. In pure H-mode the emission is modulated sinusoidally with twice the RF frequency while in E-mode the various excitation mechanisms are non- sinusoidal with one emission maximum per RF cycle. A Fourier analysis of the phase resolved emission, therefore, allows us to distinguish different power coupling mechanisms. Measurements in a pulsed ICP show that the discharge ignites in E-mode before turning to stable H-mode. In the transition from E- to H-mode instabilities can occur. In this instability regime strong plasma inhomogeneities, so called plasmoids, are also investigated.

*The project is funded by the DFG in the frame of SFB 591.

11:15
QW2 6 Comparison of Model and Experiment for Ar/O_2 Inductively Coupled Plasmas C.C. HSU, M.A. NIERODE, J.W. COBURN, D.B. GRAVES, *University of California at Berkeley* A detailed comparison has been made between measurements and a fluid model of an inductively coupled plasma in mixtures of argon and O_2. Measurements include electron density, electron energy distribution function, positive ion wall flux and composition, and O, Ar and O_2 densities measured at the chamber wall. The inductively coupled power ranged from 150 to 500W, the pressure from 5mT to 80mT, and the $O_2/(Ar+O_2)$ inlet flow rate ratio varied from 0 to 1. The overall gas flow was kept at 33.5sccm. Model equations are solved with a commercial finite element package (FemLab^{TM}). The fluid model is shown to capture all trends in mean electron energy, neutral densities and the positive ion flux to the wall, as well as the electron density radial profile over the conditions investigated. The model predicts that the O_2-containing plasmas are weakly electronegative over the conditions studied. The measured eepf is nearly Maxwellian at high O_2 concentrations, and under these conditions the model prediction for T_e are in good quantitative agreement with measurements. The stainless steel chamber walls are effective for O recombination, resulting in relatively low degrees of dissociation and strong gradients in O atom concentration, even at the lowest pressure. Model limitations will be discussed.

11:30
QW2 7 Plasma Characteristics of Industrial Transformer Coupled Plasma L. OKSUZ, A.R. ELLINGBOE, *Dublin City University Physics Department* Langmuir probes, double probes and capacitive probes are used to characterize an industrial transformer coupled plasma (TCP). Process gasses are mixtures of $Ar/O_2/C_4F_8$, such chemistry is similar to used in the etching of ULK materials. The obtained results are valuable for optimizing conditions for plasma processing for TCP. The plasma characteristics are investigated for varying gas mixtures, TCP power, substrate bias power and pressures for SiO_2 etching. Optimum etching process is strongly dependent on main power, O_2 flow rate or partial pressure of O_2, and pressure. The plasma density is found to drop with increasing partial-flow of either molecular gas up to 10% flow of the molecular gas. Further addition of molecular gas has almost no affect on plasma density and electron temperature. The results are understood by a global model.

11:45
QW2 8 Comparison of ICP with and without ferromagnetic core VALERY GODYAK, BENJAMEN ALEXANDROVICH, *Osram Sylvania* In spite of common operational principles, there are fundamental differences in electrical properties of a conventional transformer and a conventional inductively coupled plasma, ICP. Due to a strong coupling between primary and secondary circuits provided by a ferromagnetic core with high permeability, a conventional transformer behaves very closely to an ideal transformer, where the primary impedance is merely the load impedance times square of the primary winding turns. Experimental results of comparative study of ICP operated with and without ferromagnetic core are reported here. Electrical characteristics and power transfer efficiency of ICP with air core and different kinds of ferromagnetic cores have been measured in ICP of Kr/Hg mixture operating at 0.4 and 2.5 MHz in the discharge power range between 2 and 200 W. The comparison was made for discharges having the same geometry, gas fill and discharge power. It has been shown that ICPs enhanced with ferromagnetic core have significantly larger primary power factor and power transfer efficiency that those operated without ferromagnetic core. An extremely high power transfer efficiency (99%) has been demonstrated for ICP with ferromagnetic core that corresponds to 1% power loss in antenna with ferromagnetic core. This number is an order of magnitude better than that in the best helicon plasma sources having reputation of the most efficient plasma source.

SESSION RW1: CAPACITIVELY COUPLED PLASMAS
Wednesday afternoon, 19 October 2005
Pine, Doubletree Hotel at 13:30
P. Chabert, Ecole Polytechnique, France, presiding

Contributed Papers

13:30
RW1 1 Breakdown in dual frequency capacitive discharges MILES M. TURNER, *Dublin City University, Ireland* There are two classical mechanisms of breakdown. At low frequencies, an ion-controlled Townsend mechanism prevails, and at high frequencies, there is an electron-controlled breakdown. Among other points, these mechanisms differ in the character of the particle orbits. At low frequency, no particle orbits close within the plasma volume. At high frequency, nearly all particle orbits do so. In this paper we show that there is a third breakdown mechanism at intermediate frequency, where ion orbits are mainly closed and electron orbits are mainly open. In this regime, the dominant ionization mechanism is via electrons produced by fast neutral im-

pacts on the electrodes. We will show that this intermediate frequency mechanism is likely the dominant breakdown process in dual frequency discharges, with the surprising implication that the discharge is initiated by the lower frequency in typical cases.

13:45

RW1 2 Phase resolved optical emission spectroscopy on a dual frequency capacitively coupled rf discharge* TIMO GANS, JULIAN SCHULZE, UWE CZARNETZKI, *Institute for Plasma and Atomic Physics, Ruhr-University Bochum, Germany* MILES M. TURNER, *National Centre for Plasma Science and Technology, Dublin City University, Ireland* Dual frequency capacitively coupled rf discharges are frequently used in technological applications. The principle of these discharges is to allow separate control of the ion energy and ion flux impinging on the substrate surface. The ion flux is mainly controlled by the high frequency component while the ion energy is predominantly determined by the low frequency voltage. We present experimental investigations on a confined industrial discharge (Exelan, Lam Research Inc.) operated with two frequencies, 1.94 MHz and 27.12 MHz, applied simultaneously to one electrode. Phase resolved optical emission spectroscopy (PROES), resolving both the high and low rf frequencies, gives insight into the electron impact excitation dynamics. Measurements reveal a strong coupling of both frequencies. The discharge is well confined resulting in similar excitation mechanisms in front of the powered and grounded electrodes.

*Funding from: Lam Research Inc. and the European Union in the frame of FP5 and FP6.

14:00

RW1 3 Frequency dependent spatial distributions of the electrons in a 300 mm diameter VHF capacitively coupled plasmas GREG HEBNER, *Sandia National Laboratories* E. BARNAT, P. MILLER, A. PATERSON, J. HOLLAND, T. LILL, SANDIA NATIONAL LABORATORIES TEAM, APPLIED MATERIALS TEAM The characteristics of VHF capacitively coupled Argon plasmas produced in a modified 300 mm diameter chamber have been investigated. The chamber had a 14-inch diameter upper electrode (source) that was driven at 10 to 196 MHz. The spatial distribution of the electrons is observed to change with the frequency of the applied rf drive. As the frequency was increased, the electron spatial distribution went from approximately uniform across the electrode diameter to peaked in the center. These results will be compared with our previous measurements of the line integrated electron density obtained from microwave interferometry and Abel inverted optical emission measurements. Scaling of the plasma parameters with frequency, power and pressure, and implications to energy deposition models will be discussed. This work was supported by Applied Materials and Sandia National Laboratories, a multiprogram laboratory operated by Sandia Corporation, a Lockheed Martin Company for the United States Department of Energy's National Nuclear Security Administration under contract DE-AC04- 94AL85000.

14:15

RW1 4 *E* to *H* transition in very high frequency capacitive discharges. PIERRE LEVIF, PASCAL CHABERT, JEAN-LUC RAIMBAULT, JEAN-MARCEL RAX, *LPTP, Ecole Polytechnique, France* MICHAEL A. LIEBERMAN, *Department of Electrical Engineering and Computer Science, University of California, Berkeley, USA* Large area capacitive discharges driven at frequency higher than the usual industrial frequency of 13.56 MHz have attracted recent interest for materials etching and thin film deposition on large area substrates. However, electromagnetic effects, become significant if the excitation wavelength λ and the plasma skin depth δ are not infinite and can be important limitations for plasma processing uniformity. A self-consistent electromagnetic-transmission line model valid in the entire range of λ and δ of practical interest is solved. We find that the plasma may either be sustained by the usual capacitive (E) field or by an inductive (H) field, and that the discharge experiences E to H transitions as the voltage and frequency between the electrodes are raised. At low pressure, the transition is global whereas at high pressure the transition is local, the centre is in the E mode while the edges are in the H mode.

Invited Papers

14:30

RW1 5 PIC and fluid simulations of capacitively coupled plasmas for dielectric etchers and microplasmas. JAE KOO LEE, *Pohang University of Science and Technology, South Korea*

Fluid, particle-in-cell and hybrid models are the numerical simulation techniques are overviewed. The three modelling techniques are benchmarked by comparing simulation results in different plasma systems (plasma display panels [1], capacitively coupled plasmas [2]) with experimentally measured data. The potential profile and the electron kinetic information such as electron energy distribution and temperature are important for understanding the PDP striation phenomena. Kinetic 1d particle-in-cell/Monte-Carlo-collision modeling of the single- and dual-frequency capacitively coupled plasma (CCP) sources was also carried out in the wide parameter range. In particular, as the low- frequency current increases for the fixed high-frequency current in low-pressure dual radio-frequency argon discharges, the electron energy distribution function (EEDF) changes from Druyvesteyn to bi-Maxwellian type, along with the significant drop in the effective electron temperature. The EEDF evolution was shown to be attributed to the transition of the electron heating mode from collisional to collisionless heating in dual-frequency CCP [2]. *In collaboration with HC Kim (now at UC Berkeley), N Babaeva (now at Iowa State Univ.), F Iza, SS Yang, SJ Kim, M Radmilovic-Radjenovic, HJ Lee (Pusan National Univ.) [1] Plasma Display Review, J.K. Lee and J. Verboncoeur, in Low Temperature Plasma Phys. ed. by R. Hippler et al., p. 367 (Wiley- VCH 2001). [2] Mode Transition Induced by Low-frequency Current in Dual-frequency Capacitive Discharges, H.C. Kim and J.K. Lee, Phys. Rev. Lett. 93, 085003 (2004).

15:00
RW1 6 Analysis of Triple-Frequency Capacitive Systems for Plasma Processing.
DAN HOFFMAN, *Applied Materials, Inc.*

Dual- and triple-frequency capacitive systems are becoming more common among dielectric plasma etch systems in the industry today. Frequencies range from < 1MHz to ~ 200 MHz. The choice of frequencies is governed primarily by the relative effects desired with respect to density creation, average ion energy, and ion energy spread. At frequencies below 15 MHz, the dominant effect of mixing capacitive systems is seen in changes in ion energy and spread, with density affected to a lesser degree. At frequencies between 15 and 100 MHz, a trade-off exists between density creation and energy spread, particularly when these frequencies are combined with one or more frequencies below 15 MHz. When frequencies exceed 100 MHz, density formation dominates, with changes in ion energy getting progressively smaller at higher frequencies. In this paper, we explore practical density, energy, and spreads achievable for various combinations of frequencies using a physics DOE based on RF measurements of a triple-frequency system, and transform the results into process parameters proportional to density, energy, and spread.

SESSION RW2: BIOLOGICAL APPLICATIONS OF PLASMAS
Wednesday afternoon, 19 October 2005; Cedar, Doubletree Hotel at 13:30
Uwe Kortshagen, University of Minnesota, presiding

Invited Papers

13:30
RW2 1 Biological Application of Plasma: Sterilization, Surface Treatment, and Tissue Engineering.
ALEXANDER FRIDMAN, *Drexel University*

The presentation reviews modern achievements in using non- thermal plasma for different applications in biology and medicine. Specific features of non-equilibrium atmospheric pressure discharges attractive for biological and medical applications are to be discussed. Primary attention will be focused on such discharges as: dielectric-barrier discharge (DBD) in homogeneous and streamer modes; RF atmospheric pressure glow discharges (RF APG); corona and pulsed corona discharges; gliding arc discharges. Especially novel discharges in liquids efficient for bio-medical applications are to be discussed. Specific non-thermal plasma applications in biology and medicine will be subdivided into three major groups: different kind of sterilization processes; surface treatment and tissue engineering processes; direct cold plasma applications in medicine. Sterilization processes are to be considered separately for treatment of different surfaces, treatment of air, and treatment of water (and other liquids). Specifics related to bacteria, viruses, spores will be addressed. Disinfection is to be compared with low-temperature burning out and complete disintegration. Major sterilization mechanism related to atoms and radicals (OH et al.), ozone, UV, charged particles, excited molecules (singlet oxygen et al.), micro-shocks are to be discussed. Kinetic modeling of plasma sterilization processes will be demonstrated. Surface treatment and tissue engineering applications will be discussed using as an example DBD bio-printer experiments. Direct plasma-medical applications are to be considered using as examples: non-thermal plasma cauterization and blood coagulation; non-thermal plasma treatment of wounds; and non- thermal plasma treatment of skin deceases. Mechanisms of the non-thermal plasma effects in medicine will be discussed; detailed kinetic modeling of the plasma-medical processes is to be compared with experiments.

14:00
RW2 2 Electron attachment to molecules of biological relevance.
VERENA GRILL, *Institut für Ionenphysik, Technikerstr. 25, A-6020 Innsbruck*

Free electron attachment to biomolecules in the electron energy range from about 0 – 15 eV has been studied. The experiments have been carried out using a homebuilt crossed electron/neutral beams apparatus in combination with a quadrupole mass spectrometer described in detail in [1]. The electrons are monochromatized in a high resolution hemispherical electron monochromator with an energy resolution of about 110 meV in the present experiments. The biomolecules under study include thymine, alanine, glycolaldehydes, thymidine, uridine and uracil. In this presentation we want to focus on one particular experiment, where bond-selective H- ion abstraction by electron attachment to thymine has been studied [2]. This study has been performed using partially deuterated thymine to enable the measurement of electron attachment to certain bonds in the molecule. The results are particularly interesting as certain sites of the isolated molecules are not available (or even not present) when they are incorporated in the DNA structure. Therefore the present results can be used to evaluate the previously reported DEA to isolated undeuterated bases concerning their importance for real DNA environments. In particular the radiation damage due to (dissociative) anionic resonance states are assumed to be critical intermediates leading to DNA strand breaks. To support the experimental results we have also

performed quantum chemical studies using the G2(MP2) method. In collaboration with Stephan Denifl, Sylwia Plasinska, Michael Probst, Paul Scheier, and Tilmann Maerk, Institut für Ionenphysik, Leopold-Franzens-Universität Innsbruck. Financial support from the FWF, ÖAW, and ÖNB (Vienna) and the EU Commission (Brussels) through the EPIC Network is gratefully acknowledged. [1] D.Muigg, G. Denifl, A. Stamatovic, T.D.Märk, Chem. Phys. 239 (1998) 409. [2] S. Ptasinska, S. Denifl, V. Grill, T.D. Märk, P. Scheier, S. Gohlke, M.A. Huels and E. Illenberger, Bond-Selective H^- Ion Abstraction from Thymine. Angew. Chem. Int. Ed. **44** (2005) 1647–1650.

Contributed Papers

SESSION SW: POSTER SESSION II
Wednesday afternoon, 19 October 2005
Fir/Oak, Doubletree Hotel at 16:00

14:30

RW2 3 Spatial and Temporal Behavior of Repetitive Plasma Discharges in Saline Solutions KENNETH STALDER, *Arthro-Care Corp.* GAGIK NERSISYAN, WILLIAM GRAHAM, *Queen's University Belfast* Plasmas formed around multielectrode devices submerged in saline solution were investigated using fast, intensified charge-coupled detector imaging techniques. The images show that synchronous, bipolar, moderate-voltage ($<$ 300 volts rms) square-wave pulses at 100-kHz frequency applied to the electrodes cause intense and transient plasma regions to form randomly in both space and time on short (10 microsecond) time scales, even though they appear to be more stationary and constant on longer (seconds) time scales. Images from progressively longer exposures show that there is an increasing probability that the electrodes closest to the common ground electrode will develop discharges sometime during this period, but there is also a large variation in the intensity of the discharges surrounding each electrode. These observations support the notion that the dynamic and varying behavior of the thin vapor layer developed around the electrodes influences the nature of the microdischarges.[1]

[1]K. R. Stalder, D. F. McMillen and J. Woloszko, J. Phys. D: Appl. Phys. **38** 1728-1738 (2005).

14:45

RW2 4 Electron-impact total ionization cross sections of DNA sugar-phosphate backbone and an additivity principle WINIFRED HUO, *NASA Ames Research Center* CHRISTOPHER DATEO, *ELORET Corporation* The improved binary-encounter dipole (iBED) model [W.M. Huo, Phys. Rev. A64, 042719-1 (2001)] is used to study the total ionization cross sections of the DNA sugar-phosphate backbone by electron impact. Calculations using neutral fragments found that the total ionization cross sections of C3′- and C5′-deoxyribose- phospate, two conformers of the sugar-phosphate backbone, are close to each other. Furthermore, the sum of the ionization cross sections of the separate deoxyribose and phosphate fragments is in close agreement with the C3′- and C5′- deoxyribose-phospate cross sections, differing by less than 10%. The result implies that certain properties of the DNA, like the total singly ionization cross section, are localized properties and a building-up or additivity principle may apply. This allows us to obtain accurate properties of larger molecular systems built up from the results of smaller subsystem fragments. Calculations are underway using a negatively charged sugar-phosphate backbone with a metal counter-ion.

SW 1 CAPACITIVELY COUPLED PLASMAS

SW 2 Study of a capacitive discharge driven by three frequencies using inline RF metrology STEVEN SHANNON, *Applied Materials Incorporated* JOEL BLACKBURN, *Advanced Energy Incorporated* DANIEL HOFFMAN, VALERY GODYAK, JANG GYOO YANG, *Applied Materials Incorporated* STEPHEN ROSENBLUM, *Advanced Energy Incorporated* A capacitive discharge driven by a combination of 2MHz, 13.56MHz, and 60MHz is analyzed using voltage, current, and phase measurements taken at the interface between the electrode and the matching network. The electrode measurements are taken at 2MHz and 13.56MHz using an Advanced Energy Z-Scantrademark RF sensor. Using these measurements and combining rigorous RF characterization of the process chamber, discharge impedances are calculated. These impedances are input into a discharge model to calculate electron density and time averaged sheath thickness above the electrode. Over 450 combinations of pressure and power were measured to study the interaction of these three frequencies with regard to plasma parameters. Trends in electron density and sheath parameters over this experiment matrix, with particular attention to the impact of mixing of the 2MHz and 13.56MHz, will be presented.

SW 3 Diagnostics of a large size cylindrical CCP reactor NEVENA PUAČ, *Institute of Physics, POB 68, 11080 Zemun, Belgrade, Serbia and Montenegro* GORDANA MALOVIĆ, *Institute of Physics, POB 68, 11080 Zemun, Belgrade, Serbia and Montenegro* ANTONIJE DJORDJEVIĆ, *School of Electrical Engineering, Bulevar Kralja Aleksandra 73, 11000 Belgrade, Serbia and Montenegro* ZORAN PETROVIĆ, *Institute of Physics, POB 68, 11080 Zemun, Belgrade, Serbia and Montenegro* Cylindrical CCP reactor was built for treatment of textile, biological samples and polymers. It is a cylinder 1.2 m in diameter and 2 m long. Central electrode is powered and it is 2 cm in diameter. A stable uniform plasma is produced at 13.56 MHz and for powers in the range from 20 W to several hundred watts. We have used current and voltage probes to measure voltage and current waveforms and obtain the real power transmitted to the plasma. We will show how these waveforms depend on the power, gas, and pressure. In a smaller chamber of a similar geometry increasing the power led to a smaller percentage of the power transmitted to the plasma while in this case the percentage of transmitted power is constant and reasonably high.

SW 4 Secondary electron effects in dual frequency discharges MILES M. TURNER, *Dublin City University, Ireland* Secondary electron effects are often characterized by an effective emission coefficient for each ion arriving at an electrode surface. This approach acknowledges that processes such as the photoelectric effect and fast neutral impact may be important, without representing them explicitly. However, the relative importance of these processes may vary with time during a radio-frequency period and may change as the discharge conditions change. In such cases, a fixed effective secondary emission coefficient is not satifactory. In this paper, we present particle-in-cell simulations including a detailed secondary emission model [1]. These simulations show that under typical dual-frequency capacitive discharge conditions, these issues are significant. Among other things, the effective secondary emission coefficient varies greatly with time, and can reach a maximum of 0.6, which considerably exceeds the values usually assumed. Consequently, secondary emission effects are of considerable significance and have a large effect on the discharge parameters. [1] A. V. Phelps and Z. Lj. Petrovic, Plasma Sources Sci. Technol. 8, R21 (1999).

SW 5 Measurements of power dissipation in a capacitive sheath DAVID GAHAN, MICHAEL B. HOPKINS, ALBERT R. ELLINGBOE, *Dublin City University, Ireland* An experimental system is presented to investigate collisionless power coupling through a capacitively coupled rf sheath. An electrode is mounted in the downstream region of an inductively coupled discharge and driven using a separate power source. The frequency of the power delivered to the electrode is sufficiently different to that of the plasma power source to avoid interference. A DC power supply is used to bias the electrode slightly more negative than the self bias and hence alter the sheath electron density profile to exclude losses at the end of the rf cycle. This enables comparison with theoretical collisionless heating models which assume no electron loss [1] and a recent model [2] which suggests that there is a significant difference in power coupling if electron loss is included or not. The power absorbed by the plasma is measured using a customised current / voltage sensor which enables both time averaged and phase resolved power measurements. Initial results show that the collisionless power decreases as electrons are retarded while the rf electrode voltage is held constant. The phase resolved measurements confirm that the drop in power occurs in the region where electron loss is expected, consistent with the latter model mentioned above. References: [1] M. A. Lieberman, IEEE Trans. Plasma Sci., vol 16, p. 638, 1988. [2] G. Gozadinos *et al*, Phys. Rev. Lett., vol 87(13), 2001.

SW 6 Ignition conditions for peripheral plasma in a grounded chamber connected to a dual frequency capacitive discharge SUNGJIN KIM, M.A. LIEBERMAN, A.J. LICHTENBERG, *University of California, Berkeley* J.T. GUDMUNDSSON, *University of Iceland, Reykjavik, Iceland* A capacitive discharge connected through a slot to a peripheral grounded pumping region is a configuration of both theoretical and practical interest. It is used in commercial dual frequency capacitive discharges with one frequency higher than the usual industrial frequency of 13.56 MHz, with application to dielectric etching. In some configurations a dielectric slot surrounding the substrate separates the main plasma from a peripheral pumping region. Ignition of the peripheral plasma produces detrimental effects on processing performance. Discharge models for diffusion and plasma maintenance in the slot have been developed to obtain conditions for ignition of the plasma in the periphery. We found that, depending on the discharge conditions, either maintenance of the slot plasma or the periphery plasma determines the loss of confinement in the system. An experiment has been constructed to compare with and validate theoretical predictions of ignition conditions. We observed a significant hysteresis in the loss of confinement and ignition of the peripheral and slot plasmas, which can be explained qualitatively by our model theory. Support provided by Lam Research, the state of California MICRO program, NSF Grant ECS-0139956, and UC Discovery Grant from IUCRP.

SW 7 Stochastic heating in RF capacitive discharges* E. KAWAMURA, M.A. LIEBERMAN, *University of California Berkeley* There are two main mechanisms for heating electrons in RF capacitive discharges: ohmic and stochastic heating. Plasma resistivity due to electron-neutral collisions leads to ohmic heating while momentum transfer from high voltage moving sheaths leads to stochastic heating. Thus, ohmic heating is mainly a bulk phenomena while stochastic heating is localized in the sheaths areas. We try to understand the nature of stochastic heating and how it depends on various parameters such as pressure, sheath velocity, frequency and density profiles. We are particularly interested in the case of dual frequency discharges in which the high frequency controls the ion flux while the low frequency controls the ion mean energy. We conduct a series of fixed ion particle-in-cell simulations of RF capacitive discharges in order to investigate the electron heating mechanisms.

*This work was supported by NSF Grant ECS-0139956, and a UC Discovery Grant on Feature Level Compensation and Control.

SW 8 Modeling of a 2f-CCP in SF_6/O_2 for high-speed MEMS processiong FUKUTARO HAMAOKA, TAKASHI YAGISAWA, TOSHIAKI MAKABE, *Keio University* MEMS (Micro Electro Mechanical Systems) device processing has been developed on the basis of the techniques utilized in microelectronic device fabrications. For a MEMS processing, Si etching with high-speed ($>$ 100 μm min^{-1}) and high-selectivity ($>$ 100) is required due to the large scale of trench/hole profiles with several hundred μm in width and depth, as compared with semiconductor devices. In the etching of a large scale structure on a wafer, the sheath tends to wrap around the corner of the structure (plasma molding), which strongly affects the ion flux, energy and angular distribution. In the present study, a self-consistent modeling of a 2f-CCP in SF_6/O_2 practically used in industry will be performed at 300 mTorr. We will mainly focus on the 2D-t structures SF_6/O_2 plasma under the presence of large scale structure on a wafer. We use a small spatio-mesh at the vicinity of the wafer in order to predict the distorted sheath structure in a self-consistent system of 2f-CCP. That is, the sheath is distorted on the large-scale trench corner and is radially nonuniform on the wafer.

SW 9 Driving frequency effect on the heating mode transition in capacitive discharge SHINJAE YOU, *KAIST* SUNGSIK KIM, *KBSI* HONGYOUNG CHANG, *KAIST* The evolution of the electron energy distribution function (EEDF) with various driving frequencies is investigated in capacitive discharge. While increasing the driving frequency, a significant change of the EEDF is found, the bi-Maxwellian electron energy distribution changes drastically to the Druyvesteyn-like one. This observed result can be understood as an electron heating mode transition from the collisionless to collisional heating induced by driving frequency.

SW 10 Time resolved investigations of hydrogen DFC-CCP plasma sheaths in afterglow discharge CEZAR-MIHAI GAMAN, ALBERT R. ELLINGBOE, *Dublin City University, Ireland* This paper reports the results of time resolved measurements of ion energy distribution function in an afterglow discharge for a hydrogen DFC-CCP (dual-frequency confined capacitively coupled plasma). The experiments were carried out in the CIRIS device which consists of two flat, parallel-plate electrodes. The plasma is confined in the volume between the powered and grounded electrodes by a quartz tube, which shields the plasma from the grounded chamber walls, resulting in a symmetric discharge. In the grounded electrode is mounted a energy resolved mass spectrometer. The experiment was performed in a dual frequency mode (2~ Mz and 27.12 MHz). The pressure range was 5 – 25 Pa and the working domain of the power of radio frequency in on phase was 15 – 150 W. We have measured IEDFs (Ion Energy Distribution Functions) of the dominant ion in this discharge – H_3^+ , in the afterglow with steps of 1 μs. Further into the afterglow, we find that the sheath potential does not fully collapse to zero, and, after a transient phase, a constant ion energy of about 5 eV is maintained. This suggests that the electron temperature does not full collapse in the afterglow, but is maintained at approximately 1 eV.

SW 11 Mechanism of Electron Heating in Radio Frequency (RF) Capacitive Discharges ALAN WU, Using a fixed ion background to focus on the electron physics, an investigation is conducted to examine the heating mechanisms of the electrons using PIC simulation. The pressure is varied and after running the simulations to steady-state, necessary data are gathered in order to calculate the effective collision frequency. The pressure dependence of collision frequency depends upon the heating mechanism: ohmic heating results in a collision frequency proportional to pressure, and stochastic heating results in a collision frequency independent of pressure. The heating mechanism that occurs is important in understanding how to control the heating in the plasma. Results are as expected for normal operating ranges, with abnormalities that must be resolved at really high and low pressures.

SW 12 Optical Emission Measurements of Dual Frequency Capacitively Coupled Plasmas ERIC BENCK, KRISTEN STEFFENS, *National Institute of Standards and Technology* Dual frequency capacitively coupled plasma sources are becoming increasingly important in semiconductor manufacturing processes. By having the two frequencies separated sufficiently far apart, it is possible to essentially independently control the plasma density and ion energies impacting wafers. This significantly increases the operating range and etching control over that of a single frequency CCP. An imaging spectrometer combined with a high speed intensified CCD camera is utilized to obtain spatially and temporally resolved measurements of the optical emissions from dual frequency fluorocarbon plasmas created in a Gaseous Electronics Conference (GEC) reference reactor. Plasma behavior is characterized for a variety of operating conditions. In particular, the influence of a single vs. multiple powered electrodes will be presented.

SW 13 Electron density measurement in a dual frequency confined capacitive coupled plasma (DFC-CCP) processing tool using a floating hairpin resonance probe S.K. KARKARI, A.R. ELLINGBOE, *Plasma Research Laboratory, NCPST, School of Physical Sciences, Dublin City University, Dublin-9, Ireland* The DFC-CCP's are widely used in industries for etching metals, insulators and semiconductor materials. In a symmetric DFC-CCP plasma tool [Exelanregistered, Lam Research Corporation] the discharge is electro-statically confined within a narrow gap (12 mm), which causes large plasma potential oscillation (1KV) of the two fundamental frequencies and their harmonics with the mean potential floating at several hundreds of volts above the ground. Therefore for plasma diagnostics, the RF compensated Langmuir probes are not suitable since appropriate resonant filters are practically difficult to design and also the bulky probe construction highly perturb the discharge. To overcome such limitations, we have designed a ''floating hairpin probe'' for measuring the electron density in Exelanregistered. This technique is based on Piejak's directly coupled hairpin probe operated in the reflection mode [presented in the 56^{th} and 57^{th} GEC conference], however with the hairpin probe electrically isolated from the loop antenna. Using this probe we have measured the time-averaged electron plasma density at the mid-plane of the discharge electrodes in $Ar/O_2/C_4F_8$ gas mixtures. The spatial and the phase-resolved measurements of the electron densities are presently being carried out and the results shall be presented in the conference.

SW 14 PLASMA DIAGNOSTICS II

SW 15 Asymmetry reversal of ion collection by Mach probe in flowing unmagnetized plasma* EUNSUK KO, XU WANG, NOAH HERSHKOWITZ, *Dept. of Engineering Physics, University of Wisconsin - Madison* GREGORY SEVERN, *Dept. of Physics, University of San Diego* Mach probes derive ion drift velocity in flowing plasma from the asymmetry of ion current collection by measuring upstream and downstream flux. Intuitively it is expected that the ion flux density on the upstream side of the Mach probe is higher compared to the downstream side. Hutchinson's numerical calculation[1] of a sphere in unmagnetized plasma found unexpected result that the downstream flux was higher than the upstream flux for relatively low drift velocity v_d, comparable Debye length λ_D to the probe size r_p, high probe bias V_p. We found experimental evidence for such a reversal when $\lambda_D/r_p \sim 0.18$, $v_d < 2.7c_s$, where c_s is the ion sound velocity, and $V_p > 20T_e$. The experiments were performed in a double plasma system with $v_d \leq 4.5c_s$ and Ar pressure range of $0.3 \sim 0.6$mTorr and a plasma density range of $10^8 \sim 10^{10}cm^{-3}$. The supersonic ion drift was determined from ion beam detection[2] using the upstream planar Mach probe, and the ion beam energy was found to agree with Ion energy analyzer measurements.

*Work Supported by US DOE grant no. DE-FG02-97ER 54437.

[1]I. H. Hutchinson, Plasma Phys. Control. Fusion **45**, 1477 (2003).
[2]Wim. J. Weber, Richard J. Armstrong, and Jan Trulsen, J. Appl. Phys. **50** (7), 4545 (1979).

SW 16 Plasma Potential Fluctuation Measured by an Emissive Probe in Processing Plasma* DONGSOO LEE, NOAH HERSHKOWITZ, *Department of Engineering Physics, University of Wisconsin-Madison* Measuring the plasma potential is very important not only to the fundamental understanding of plasma parameters but also to industrial development of plasma systems such as semiconductor etchers because the plasma potential determines the ion energy to wafers. One weakly perturbing technique for measuring the plasma potentials is the use of emissive probes for evaluating the inflection points of the I-V characteristics in the limit of zero emission. When RF power is coupled to the plasma, difficulties can arise in the measurement due to potential fluctuations by harmonic RF fields and deposition on the probe by reactive gases. In this study, we provide experimental data of plasma potential fluctuations measured in an inductive and a helicon processing tool using a fluorocarbon gas (CF_4). The fluctuations give the minimum and maximum values of the fluctuating plasma potential. Deposition effects on the probes are also investigated.

*Work Supported by US EPA grant no. RD-83145901-0.

SW 17 Electron Number Density Decay in Nitrogen Afterglow Using a Microwave Hairpin Resonator NICHOLAS SIEFERT, BISWA GANGULY, *Air Force Research Laboratory WPAFB* GREG HEBNER, *Sandia National Lab* AIR FORCE RESEARCH LABORATORY COLLABORATION A microwave hairpin resonator probe has been built to measure the decay of the electron number density in nitrogen afterglow (p = 0.25 & 0.75 Torr). In order to operate at these pressures, it was necessary to make corrections for both sheath and collisional damping. In order to measure the change in electron number density in the afterglow, it was necessary to convert the hairpin resonator probe from a steady-state diagnostic tool into a time-dependent one. The results presented in this work will show that both the steady state and time dependent electron density measurements are reasonably accurate up to a pressure of 0.75 Torr, but only over a limited range of electron number densities ($5x10^8$ cm^3 < n_e < $5x10^9$ cm^3). For pressures at or below 0.75 Torr, the error due to electron-neutral collisions is less than three percent. Using the e-folding decay time of the electron number density, we solve the ambipolar diffusion equation to determine the mean electron temperature in the afterglow. We estimate that the electron temperature stays between 0.7 eV and 1.3 eV for up to a few hundred microseconds after the discharge is switched off.

SW 18 Electric field measurements by fluorescence-dip Stark spectroscopy ERIK WAGENAARS, GERRIT KROESEN, *Eindhoven University of Technology, The Netherlands* MARK BOWDEN, *The Open University, United Kingdom* We used Stark spectroscopy with fluorescence-dip detection to quantitatively measure electric field strengths in the sheath region of a dc glow discharge in xenon. Our laser spectroscopic technique is based on the observation of Stark mixing of Rydberg energy levels in an atom due to external electric fields. In order to quantify the electric field strength, the measured spectra are matched to a theoretical calculation. A 2+1 photon excitation scheme is used to excite xenon atoms from the ground state, through an intermediate 6p state, to high-lying Rydberg levels. During this two-step process, fluorescence light at 828 nm is measured. When scanning the wavelength of the second laser, a reduction (dip) of the fluorescence intensity indicates excitation to a Rydberg state. The theoretical calculation of the Stark shifts and splitting of xenon energy levels is based on solving the Schrödinger equation of a system with a perturbation due to the dipole interaction of the atom with an electric field. In order to test our experimental arrangement we used a simple dc glow discharge. This consisted of two parallel electrodes separated by a 1 cm gap in 800 Pa xenon gas. The applied dc voltage was about 300 V. Axial profiles of the electric field strength in the sheath region were determined by measuring Stark spectra of several *ns* and *nd* levels of xenon atoms in the discharge.

SW 19 Population Distribution of Atmospheric Pressure Argon Discharge Based on CR Model HIROSHI AKATSUKA, *Tokyo Tech.* We carried out numerical study on the population densities of excited states of argon atoms under atmospheric pressure discharge for the basis of OES measurement of electron temperature and density. As a numerical code, we applied collisional radiative model (CR model) to calculate excited populations as a function of the electron temperature, density, gas temperature and total pressure. As a preliminary stage, we assumed the EEDF to be Maxwellian in the present study. The CR model included not only electron collisional/radiative processes but also atomic collisional processes and optical escape factors. We found that the highly excited states for the recombining plasma are not in the state of LTE, which were generally considered to be the case for the low-pressure discharge. Excitation temperature became closer to the gas temperature when we applied the levels with the same principal quantum number. On the other hand, it became closer to the electron temperature when the levels with the same angular momentum states were used. Consequently, there is possibility to obtain electron temperature by line intensity measurement.

SW 20 Measurement of Radical Density in an Atmospheric Plasma by Molecular Beam Mass Spectrometry YOLANDA ARANDA GONZALVO, ALAN REES, PETER HATTON, DAVE L. SEYMOUR, IAN D. NEALE, *Hiden Analytical Ltd., 420 Europa Boulevard, Warrington, WA5 7UN, England* Radical species produced in an atmospheric discharge have been measured by appearance potential mass spectrometry (APMS) using a Hiden EQP differentially pumped mass/energy analyser. The non-thermal discharge was generated by a radio frequency driven atmospheric plasma source.[1] Species were sampled from atmospheric pressure using a triple stage differentially pumped molecular beam inlet system. The discharge was generated mainly in Helium and, for the present investigation, different percentages of Oxygen, Nitrogen, Nitrous oxide, Carbon dioxide and Carbon monoxide gases were added to the plasma discharge. Radical densities produced in the atmospheric discharge were studied as a function of the power and the distance between the plasma source and the entrance to the analyser. Other species observed from the Oxygen/ Helium and Nitrogen/Helium mixtures were NO radicals formed by recombination.

[1]E. Stoffels etit al., Plasma Sources. Sci. Technol.11(2002) 383-388.

SW 21 Measurement of electric fields in plasma using Stark spectroscopy of krypton atoms TAO JIANG, *Eindhoven University of Technology* M.D. BOWDEN, *The Open University, UK* E. WAGENAARS, G.M.W. KROESEN, *Eindhoven University of Technology* The electric field is one of the most important discharge parameters. In glow discharges, it is the driving force behind many processes at the plasma boundary. But it is difficult to measure, because of perturbation problems. We report a spectro-

scopic method for the measurement of the electric field in a glow discharge in krypton. The method to determine the electric field is based on the comparison of the results of experimental laser optogalvanic (LOG) spectra and theoretical calculations, obtained by solving the Schrdinger equation of krypton atoms in an electric field. For high electric fields, there is a good agreement between experiment and calculation for excitation from 5s to f states of krypton atoms in an electric field. For lower electric fields, the resolution of the technique is lower using f state. However, excitation from 5s to p-states results in a larger LOG signal and larger Stark shifts were observed. Therefore, the resolution of the technique is better using p-states for low electric fields.

SW 22 Biased hairpin probes NICHOLAS BRAITHWAITE, FRED HAAS, JAFAR AL-KUZEE, *The Open University* A hairpin probe is an open, quarter-wave transmission line. When immersed in a plasma its resonant frequency can directly and immediately provide a measure of local electron density, through the plasma's dielectric response. The sheath around the hairpin wires can be relatively large, either at low electron density or when deliberately baised to several times the mean electron energy. A model the hairpin resonance has been developed incorporating sheaths with positive and negative bias, including electron space charge in the former and taking account of the radial geometry. To date, in using the hairpin is has been presumed that its behaviour is well modelled without any independent test, though comparisons with Langmuir probes are certainly favourable. The variation of resonant frequency with bias is an important test of the hairpin concept. Calculations show that, as expected, negative bias lowers the resonant frequency monotonically. Positive bias shows a different trend with an initial sharp increase in resonant frequency at small bias settling into a weakly declining trend at larger bias. The latter behaviour is traced to radial convergence of electrons near the probe wires. Experimental results show similar trends with notable differences that highlight the shortcomings of the model.

SW 23 GLOWS II

SW 24 Self-consistent kinetic study of abnormal glow discharge plasmas FLORIAN SIGENEGER, DETLEF LOFFHAGEN, *INP Greifswald, F.-L.-Jahnstr. 19, 17489 Greifswald, Germany* The axial structure of abnormal glow discharge plasmas is analysed by means of a self-consistent hybrid approach. The investigations have been performed in plane parallel geometry for inert gases at pressures of some Torr. This approach couples the solution of Poisson's equation and a fluid description of electrons, ions and excited atoms with a kinetic treatment of the electron component. The system of Poisson's and time-dependent fluid equations is solved by a semi-implicit method. Using the electric field course determined from Poisson's equation and the excited atom densities from the fluid equations, the space-dependent electron Boltzmann equation is solved. This approach avoids the separation in fast and slow electrons and yields the axial profiles not only of rate coefficients but also of the transport coefficients. Starting from a space-independent electric field, the fluid and kinetic parts of the model are iteratively solved until a stationary state is reached. The results show a distinct separation between the cathode fall with a strongly decreasing electric field and the negative glow with a very low or even reversed electric field. The pronouncedly non-local behaviour of the electrons in this strongly changing field results in remarkable spatial alterations of their collision rate and transport coefficients.

SW 25 Optical and Electrical Characteristics of AC Glow Discharge Plasma in N_2O H. MARTÍNEZ, *Centro de Ciencias Físicas, UNAM* F.B. YOUSIF, *Facultad de Ciencias, UAEM* A. ROBLEDO, *UAM, Acopotzalco* F. CASTILLO, *Instituto de Ciencias Nucleares, UNAM* A.B. MONDRAGÓN, *Facultad de Ciencias, UAEM* CCF-UNAM TEAM, FC-UAEM TEAM, UAM-ACOPOTZALCO TEAM, ICN-UNAM TEAM This paper considers the optical and electrical characterization of AC glow discharge plasma in the abnormal glow mode used for optical emission spectroscopy. The total discharge current and applied voltage are measured using conventional techniques. Optical emission spectroscopy was used to determine the main emission lines of the glow discharge plasma of N_2O at pressures between 0.5 and $4.0 Torr$. It shows that the discharge emission range is mainly within $300 - 400\ nm$. The emission lines at 315.98, 337.55, 354.20, 357.24, 380.09 and 391.42 nm corresponding to NO, O_2, and O_2^+ are the dominant lines in the glow discharge plasma in the present study. Intensity of the emission lines show linear increase with the discharge current up to 0.6 A followed by saturation at higher currents. The emission consists of NO, O_2^+ and O_2 narrow peaks. No emission lines were identified with the atomic oxygen leading us to conclude that the atomic oxygen is produced either in the $O(^5S)$ state that is sufficiently energetics and most likely is lost collisionally, or produced in its ground state $O(^3P)$ or themetastable state $O(^1D)$ that is quenched in collisions with N_2 resulting in $O(^3P)$.

SW 26 Dispersion of a Stationary Acoustic Shock in a Supersonic Flowing Afterglow DERETH JANETTE DRAKE, REZA BIAZARAN, SVETOZAR POPOVIC, LEPOSAVA VUSKOVIC, *Old Dominion University* Experimental studies of shock wave dispersion in weakly ionized gas have been mostly performed on traveling shock waves [1,2]. Inability to fully characterize transient phenomena in the shock layer interacting with electric discharge has produced some ambiguity in the interpretation of the phenomenon of dispersion. In the attempt to elucidate the role of excited states in the dispersion, we employed a supersonic microwave flowing afterglow apparatus with a blant solid body suppressing the flow to generate a stationary shock. Commercial microwave generator, operating in S-band, was used to sustain a cylindrical cavity discharge in argon and nitrogen at power density between 3.5 and 7 W/cm^3. The discharge was sustained downstream of the cavity by the traveling microwave field using the quartz tube as the wave guide. Therefore, this plasma generator differs from conventional d.c. flowing afterglow in the ability to sustain ionized gas over a longer distance. As a consequence, electron density was higher, in the range of (1-3)$\times$ 10^{13}cm^{-3}, which was determined by the Stark broadening technique. Gas temperature was constantly below 800 K that was determined by thermocouple measurements, Doppler component of the observed line profiles, and rotational spectra of nitrogen molecules. Excited state population in argon was measured with combined emission and absorption spectroscopy using the absolute intensities of (4p-4s) spectral lines. Dispersion effect was observed in the form of a

double- peaked distribution of intensities in front of the model. Interpretation of the results will be presented at the conference. [1] P. Bletzinger, B. N. Ganguly, Phys. Lett. A **258** (1999) 342. [2] S. Popovi and L. Vuškovi, Physics of Plasmas **7** (1999) 1448.

SW 27 Investigations of argon hollow cathode discharge with iron cathode J.F. BEHNKE, H. SCHEIBNER, *Institut of Physics, University of Greifswald, Germany* H. KERSTEN, *Institute of Low Temperature Plasma Physics, 17489 Greifswald* H. LIEDER, *OSRAM GmbH, D-81536 Munich, Germany* The formation of argon metastable and resonance state densities and of iron ground state densities by ion sputtering are studied experimentally by absorption spectroscopy and LIF in the plasma of a cylindrical hollow cathode discharge (Fe, R = 0.4 cm l = 3.0 cm, p0 = 160 Pa argon). The intensity of iron spectral lines has been measured by means of the emission spectroscopy. The EEDF in the negative glow were determined from the second derivative of the probe characteristic and the charge carrier density from the ion saturation probe current. The densities of the sputtered iron atoms in the ground and excited states in dependence of discharge current have been calculated by a simple model of the sputter process and the excitation kinetic via measured EEDF and electron densities. The discharge current characteristics were calculated via the POISSON equation in the cathode fall region considering the electron multiplication and secondary emission of electrons by ions and resonance photons at the cathode.

SW 28 Investigation of a Micro-Hollow Cathode Discharge stability in different gases XAVIER AUBERT, ANTOINE ROUSSEAU, *LPTP-Ecole Polytechnique-Palaiseau France* Micro-hollow cathode discharge (MHCD) are of interest for the plasma generation near atmospheric pressure at a relatively low voltage [1-3]. MHCD are generated in the hole (typically few hundreds of micrometers) made in a conductor-dielectric-conductor sandwich. We report the characterization of such plasmas in argon, helium and air and show that the electrical behaviour is different from air to noble gases. Current/ voltage characteristics performed under various hole diameter and gas pressure show that highly reproducible self pulsing regime exists when the plasma expends towards the backside cathode region. The influence of such a self-pulsing regime on the discharge stability in a multi-hole configuration is also reported. Finally, the possibility of generation of a microplasma in a three electrodes configuration is studied. Production of oxidized species such as nitrogen oxides in air is also reported. [1] K. H. Schoenbach, R. Verhappen, T. Tessnow, F. E. Peterkin, W. W. Byszewski, Appl. Phys. Lett. 68 (1996) 13. [2] D.D. Hsu and D. B. Graves J. Phys. D: Appl. Phys. 36 (2003) 2898. [3] J. P. Boeuf, L. C. Pitchford, K. H. Schoenbach, Appl. Phys. Lett. 86 (2005) 71501.

SW 29 Dynamics of striations formed in a hollow anode covered by a dielectric layer V.N. KHUDIK, *Plasma Dynamics Corp., MI* A. SHVYDKY, C.E. THEODOSIOU, *University of Toledo, OH* The dynamics of the charging of a cylindrical hollow anode (covered with a dielectric layer) by an electron current is studied via 3-dimensional Particle-in-cell/Monte-Carlo kinetic simulations. For the first time, it is shown that this process is accompanied by the successive formation of striations in the plasma created by the electron impact ionization of the background noble gas. The dynamics of the formation of striations can be quite different depending on the gas pressure, the cylinder radius, the thickness of the dielectric layer, and the magnitude of the current from the emitter. A number of specially designed numerical experiments are performed to further explore the nature of this phenomenon. An experimental set-up where this type of striations should be observed is suggested.

SW 30 Expansion of a Dynamic Cathode Fall along the Dielectric Surface A. SHVYDKY, *University of Toledo, OH* V.N. KHUDIK, V:P. NAGORNY, *Plasma Dynamics Corp., MI* C.E. THEODOSIOU, *University of Toledo, OH* The dynamics of the expansion of a cathode fall along the plane cathode covered with dielectric layer is studied via Particle-in-cell/Monte-Carlo kinetic simulations. It is shown that the spreading progresses in a wave-like manner with a quite pronounced wave front where most of ionizations of the background noble gas take place. Different mechanisms of the ionization wave propagation are discussed. The role of the electron and ion diffusion is elucidated. It is found that the wave propagates over very thin dielectrics as well as very thick ones. The dependence of the wave velocity on the dielectric layer parameters and on the potential difference between the plasma and the cathode is determined.

SW 31 PLASMA DIAGNOSTICS I

SW 32 Imaging spectrometer based on Fabry-Perot interferometer ALEKSANDR KRAVCHENKO, ANATOLY KHAKHAEV, LIDIA LUIZOVA, ALEKSEI SOLOVEV, The aim of this work is to construct a research complex, which will allow to investigate spatial distribution of parameters of inhomogeneous plasma such as distribution of atomic temperature, density of atoms in different states and others by spectrum line profiles in certain parts of plasma; and then to investigate real plasma sources to determine their parameters and internal processes. In our setup, the light from the source, placed in a focus of focusing lenses, passes through the Fabry-Perot interferometer. The superposition of a source image and interference rings is drawn by the drawing lenses on the entrance slit of the spectrometer. In this setup, the spectrometer is used for picking out a definite spectral line. Having carried out the experiment with interferogram obtainment, we try to model interferograms obtained in the experiment. We set desired plasma characteristics using models with few parameters and calculate light intensity distribution along the entrance slit of the spectrometer taking into account the spread function of the Fabry-Perot interferometer. Varying parameters, we achieve the best agreement between experimental and calculated light intensity distribution.

SW 33 Experimental Details on Air-Plasma Measurements of Electron Density and Ozone Concentration ROBERT VIDMAR, *University of Nevada, Reno* KENNETH STALDER, *Stalder Technologies and Research* MEGAN SEELEY, *University of Nevada, Reno* Details on the measurement of electron density and ozone concentration in air plasma are presented. Air plasma is generated by a 100-kV10- 20 mA electron beam for approximately 1 ms in a 400-liter test cell filled with air under atmospheric

conditions from sea level to 300,000 ft. An electron-density measurement technique based on RF absorption and phase shift at X-band using a null-based differential measurement system is used. A White's cell topology is used to measured ozone concentration using absorption at 254 nm. System sensitivity, time response, engineering details, and representative data for both systems are quantified. This material is based on research sponsored by the Air Force Research Laboratory, under agreement numbers FA9550-041-1-0015 and FA9550-04-1-0444.

SW 34 A measurement of F metastables by laser absorption spectroscopy in a two frequency CCP KENJI HAYASHI, TAKESHI OHMORI, TAKUMI AKAIKE, *Keio University* TAKESHI KITAJIMA, *National Defense Academy* TOSHIAKI MAKABE, *Keio University* KEIO UNIVERSITY TEAM, NATIONAL DEFENSE ACADEMY TEAM Fluorine-containing plasmas are used in SiO_2 etching. The degree of dissociation of CF_4 is a critical factor for bottom etching and sidewall polymer deposition and determines the absolute density of F atom. Relative density is of F atom in metastables and grand state are experimentaly reported in an ECR plasma[1]. In the present study, we have observed the absolute density of F metastables by using a tunable diode laser absorption spectroscopy(LAS) in a capacitively-coupled plasma (CCP) in Ar/CF_4. The transition line used for absorption spectroscopy of F metastables is $3s4p_{3/2} - 3p4D_{5/2}$ at 690.25nm. The metastable density, $6.0 \times 10^9 cm^{-3}$ on the center of electrodes is measured at conditions that the CCP is sustained at 100MHz with 50W and a pressure of 100mTorr. Consequently we performed a measurement of absolute density of F metastables in the low and middle-density plasma. [1]Kazuki Takizawa, Koichi Sasaki and Kiyoshi Kadota. Jpn. J. Appl. Phys. Vol40(2001)pp. 5130-5133

SW 35 Optical emission CT for an effect of LF-bias voltage on a 2f-CCP for etching TAKUMI AKAIKE, TAKESHI OHMORI, KENJI HAYASHI, MIKIO ISHIMARU, *Keio University* TAKESHI KITAJIMA, *National Defense Academy* TOSHIAKI MAKABE, *Keio University* KEIO UNIVERSITY TEAM, NATIONAL DEFENSE ACADEMY TEAM It is essential to control and optimize 2-dimensional ion velocity and radical distributions under a strong sheath dynamics in front of an oxide wafer biased deeply by a low frequency source in a 2f-CCP, because high energy ions have a responsibility for oxide etching in RIE. In our previous work, we have performed a design of the functional separation in a 2f- CCP sustained at VHF and biased at LF source. Experimental evidence was limited to a low bias voltage of the LF at the wafer[1]. In this work, by using the CT image of the optical emission from the short-lived Ar($2p_1$) and Ar($2p_9$) as the probe of the transport of electrons with energy greater than 13.48 eV and 1.53 eV, we spatiotemporally investigate the influence of the high voltage LF bias on the 2f-CCP in Ar. The degree of a collapse of electrons from the bulk plasma at the instantaneous anode phase, and that of an ionization growth of the secondary electrons emitted at the wafer by high energy ions at the instantaneous cathode are experimentally shown in the CT images as a function of 2D space and time. [1] T.Kitajima, Y.Takeo, N.Nakano and T.Makabe : J. Appl. Phys. 82, 5928 (1998)

SW 36 Investigation of Pulse-Modulation Effect in Electron Beam Excited Plasma with Time Resolved Optical Emission Spectroscopy KEIGO TAKEDA, *Graduate School of Eng., Nagoya Univ.* TAKAYUKI OHTA, MASAFUMI ITO, *Faculty of Systems Eng., Wakayama Univ.* MASARU HORI, *Graduate School of Eng., Nagoya Univ.* Micromachining of optical devices attracts much attention. In the process, the fast atomic-beam etching or the ion-beam etching has been employed, since the conventional reactive plasma etching can't be employed as the radio-frequency self-biasing is not efficiently supplied to the thick dielectric materials. However, a pulse-modulated electron-beam-excited plasma (EBEP) has a potential to realize the high etching rate without any additional bias power supply. Therefore, we have investigated the effect of pulse-modulation of EBEP using time resolved optical emission spectroscopy. Plasma was generated at a pressure of 0.27Pa and the fed gases were C_4F_8/Ar, a discharge current of 25A and an electron acceleration-voltage of 65V with a pulse-modulation frequency of 50kHz. It was found that CF_2 optical emission intensity at the 50%-duty ratio was involved in two lifetimes of $\tau_1 = 3$ and $\tau_2 = 19.8\mu s$ compared with Ar optical emission intensity. Moreover, CF_2 radical density was evaluated by using Actinometry in order to compare with F atom density. F atom density increased with the increase of duty ratio, but CF_2 radical density decreased. Therefore, the dissociation degree of C_4F_8 was controlled by the duty ratio of electron acceleration voltage.

SW 37 F^- detection by CRDS in a dual-frequency capacitive plasma in Ar/C_4F_8/O_2 CORMAC CORR, GARRETT CURLEY, JEAN-PAUL BOOTH, *LPTP, Ecole Polytechnique, 91128 Palaiseau, France* Dual-frequency capacitively coupled plasmas in Ar/fluorocarbon mixtures are widely employed for etching of holes in SiO_2-based dielectrics in integrated circuit manufacture. Negative ions can dominate the structure and dynamics of discharges if their density is high enough, yet no experimental data is available for dual-frequency plasmas. They may also play a role in etching if they can reach the surface. The determination of the negative ion density via the detection of photo-detached electrons is difficult to implement in such reactors due to the large RF fluctuations of the plasma potential. Therefore we have implemented the cavity ring-down spectroscopy (CRDS) technique to measure the density of fluorine negative ions in a customized industrial dual-frequency capacitive etch reactor operating with Ar/C_4F_8/O_2. A pulsed laser beam from a tuneable dye laser was scanned over the wavelength range 340 to 360 nm and injected into an optical cavity formed by two high-reflectivity concave mirrors ($>$ 99.95 %). The temporal behaviour of the decaying pulse at the cavity exit allows the density of absorbing F^- ions to be determined from the known photo-detachment cross-section. The negative ion density will be investigated as a function of input power and gas mixture.

SW 38 Characterization of the Lam 9100TCP plasma through atomic argon spectral lines VLADIMIR MILOSAVLJEVIC,* ALBERT R. ELLINGBOE, *Dublin City University, Ireland* Argon as one of most frequently used gas in RF discharge. Determination of plasma parameters through analysis of argon emission would be a powerful tool. Four argon lines have been measured from two different transitions. From the 4s–4p transition the 750.387 nm and 751.561 nm spectral lines are recorded and also from 4p–4d transition the 687.129 nm and 751.041 nm Ar I spectral lines are recorded. These four Ar I spectral lines each belong to the differ-

ent multiplets and therefore have the different upper energy level. The difference of upper energy levels among these argon spectral lines is greater than 1.5 eV. Also, the 751.041 nm spectral line of Ar I have an upper energy level very close to ionized limit for atomic argon. Data is collected for a range of operator contribution in an Ar-O_2–C_4F_8 gas mixture discharge, by high resolution spectrometers Carl Zeiss PGS–2 with 60 pm instrumental width. The emission strengths and profile shapes are found do be dependent on RF power settings, gas mixture and pressure. Correlation of plasma internal state will be presented.

*Also at University of Belgrade, Serbia.

SW 39 Local Stochiometry Distortions in a Rotatable Magnetron Sputter Source measured by True 2D Imaging Spectroscopy TILL WALLENDORF, SWEN MARKE, *IfU Diagnostic Systems GmbH* FALK MILDE, *Von Ardenne Anlagentechnik GmbH* Reactive sputter processes are widely being used for large scale optical glass coating. Even though there is a strong push towards the use of ceramic target materials at the moment, also in the future reactive sputtering will play an important role. Process control is of very high importance for reactive sputtering especially for the transition mode, where working points are not stable by nature. By use of a new type true 2D imaging spectrograph we demonstrate, how to acquire the spatial intensity distribution of selected emission lines. This true 2D imaging spectrograph combines wide wavelength range, excellent wavelength resolution, and good spatial resolution with a short sample time. The observations presented in this paper may serve as a starting point for systematic optimization of the appropriate choice of position and properties of the optical collimation hardware.

SW 40 Magnetic field measurements for N_2 and H_2 discharges from a low frequency RF inductively coupled plasma source CHANDAN KUMAR CHAKRABARTY, *University Tenaga Nasional* The electric field due to a strong capacitive coupling between the induction coil and the walls of the plasma chamber is quite large despite the discharge being in the H-mode in N_2 and H $_2$ gases. And as such, this field will interfere with the measurement of the magnetic field thus causing a higher degree of measurement error. This paper hence describes the use of a centre-tapped coiled magnetic probe for the measurement of magnetic field profiles in 1-D in the low frequency RF inductively coupled plasma source. From these profiles, an independent method to determine the average electron density is shown.

SW 41 BIOLOGICAL, ENVIRONMENTAL, AND OTHER INNOVATIVE APPLICATIONS

SW 42 Investigation of Bacterial Biofilm Destruction Using Gas Discharge Plasma N. ABRAMZON, J. BRAY, J.C. JOAQUIN, G. BRELLES-MARIÑO, *California State Polytechnic University, Pomona* Biofilms are bacterial communities embedded in an exopolysaccharidic matrix with a complex architectural structure. Bacteria in biofilms show different properties from those in free life thus, conventional methods of killing bacteria are often ineffective with biofilms. The use of plasmas potentially offers an effective alternative to conventional sterilization methods since plasmas contain a mixture of charged particles, chemically reactive species, and UV radiation. 4 and 7 day-old biofilms were produced using two bacterial species. Gas discharge plasma was produced by using an AtomfloTM reactor (Surfx Technologies) and bacterial biofilms were exposed to it for different periods of time and different plasma conditions. For each plasma condition, cell counts were plotted against the time of treatment, which allow us to calculate D-values and compare various plasma treatments quantitatively. Optical emission spectroscopy was used to study plasma composition and temperature which was then correlated with the effectiveness of killing. This Work was supported partly by CSUPERB.

SW 43 Investigation of Sporicidal Effect of Gas Discharge Plasma SHAWN TSENG, WEI-JEN LIN, NINA ABRAMZON, *California State Polytechnic University, Pomona* Bacteria spores are the most resistant form of life and have been a major threat to public health and food safety. In this study, helium- based plasmas were used to treat spores of various bacteria including it Bacillus and itClostridium. Gas discharge plasma was produced by using an AtomfloTM reactor (Surfx Technologies). The spore species tested include itB. subtilis, itB. stearothermophilus C. sporogenes, C. perfringens, and it C. difficile. Also, the bactericidal effects of plasmas are tested against vegetative cells of itB. subtilis, the gram positive rods, and the gram negative rods, itEscherichia coli. The D-values for spores range from 2 to 10 minutes, in comparison with the D-values of vegetative cells, ranged from 20 to 50 seconds. Our results show the effectiveness of using plasmas to sterilize vegetative bacterial cells as well as bacterial spores of various types. Optical emission spectroscopy was used to study plasma composition which was then correlated with the effectiveness of killing. The sporicidal mechanisms of various plasma species will be characterized morphologically and molecularly in future studies. This Work was supported partly by CSUPERB.

SW 44 Purification of Gaseous Pollutant using Secondary Emission Electron Beam generated by Wire Discharge Plasma Source* MASATO WATANABE, YUSUKE SAKAI, EIKI HOTTA, *Tokyo Institute of Technology* It is well known that the non-thermal plasma processes using electrical discharge or electron beam are effective for the environmental pollutant removal. Especially, the electron beam can efficiently remove pollutant, because a lot of radicals which are useful to remove pollutant can be easily produced by high-energy electrons. We have developed a compact 100kV secondary emission electron gun to apply several gaseous pollutant removals. The device offers several inherent advantages such as compact in size, wide and uniform electron beam. Besides, the device offers good capability in high repetition rate pulsed operation with easy control compared with glow discharge or field emission control cathode guns. In present study, the NOx removal characteristics have been studied under the increased gun voltage, varied pulsed electron beam parameters such as current density and pulse width as well as gas flow rate. The experimental results indicate a better NOx removal efficiency comparing to other high-energy electron beam and electrical discharge processing.

*This research was partially supported by the Ministry of Education, Science, Sports and Culture, Grant-in-Aid for Scientific Research (B).

SW 45 Infrared laser diagnostics of the plasma-photocatalyst interaction in a pulsed low pressure discharge OLIVIER GUAITELLA, FREDERIC THEVENET, ANTOINE ROUSSEAU, *LPTP-Ecole Polytechnique CNRS, Palaiseau, France* CHANTAL GUILLARD, *LACE-Lyon-France* GABI STANCU, JURGEN ROEPCKE, *INP-Greifswald-Germany* The combination of a plasma with a porous semi-conductor surface (TiO_2 photocatalytic material) has been recently reported to oxidize volatiles organic compounds (VOC) at a low energy costs [1]. However, activation mechanisms of the photocatalytic surface by the plasma are not clearly identified to the day. In order to improve the understanding of the synergy of the plasma-photocatalysis combination for C_2H_2 removal, time resolved in-situ measurements of infrared laser absorption spectroscopy are performed in a low pressure pulsed DC discharge in air containing less than 1000 ppm of C_2H_2. The time resolution of the infrared lead-salt diode laser is about 1ms. Time resolved measurements are carried out during a series of single pulses (10 to 100 ms) in a closed plasma reactor. It is shown that the combination of TiO_2 with external UV irradiation leads a strong enhancement of the C_2H_2 oxidation rate under plasma exposure. Similarly, adsorption/desorption characteristic time of C_2H_2 on TiO_2 is modified by the presence of the plasma. [1] S. Futamura, H. Einaga, H. Kabashima, L.Y. Hwan, Catal. Today 89, 89 (2004).

SW 46 Production of Syngas via Biomass Pyrolysis in Thermal Hydrogen/Oxygen Plasma MILAN HRABOVSKY, MICHAL HLINA, MILOS KONRAD, VLADIMIR KOPECKY, *Institute of Plasma Physics AS CR, Prague* DEPARTMENT OF THERMAL PLASMA TEAM The plasma reactor for pyrolysis of waste materials with dc arc gas/water plasma torch was operated at arc power up to 140 kW using wood as a model substance. High enthalpy, low-density hydrogen/oxygen plasma generated in the torch interacted with a flow of treated material in a reactor volume. The experimental results prove that homogeneous heating of volume of plasma reactor and proper mixing of plasma with treated material was ensured despite of very low plasma mass flow rate and constricted form of plasma jet. The conditions within the reactor ensured complete destruction of tested substance. Synthetic gas with high content of hydrogen and carbon monoxide and low concentration of carbon dioxide was produced. Due to composition of plasma and its very low mass flow rate the composition of reaction gases was close to stechiometric composition of cellulose fully dissociated to hydrogen and carbon monoxide with their concentrations exceeding 40%. The authors gratefully acknowledge the support of this work by the Grant Agency of the Czech Republic under the project No. 202/05/0669.

SW 47 Spectroscopic study for abatement system for the global warming gases using VAWP* JIANKUN WANG, RYOHEI ITATANI, TOHRU YASUDA, *Adtec Plasma Technology Co. Ltd, 5-6-10, Hikinocho, Fukuyama, Hiroshima, Japan* A unique abatement system for the global warming gases such as PFCs, HFCs and CFCs was developed. This, called as VAW(Vertical Aqua Wall) plasma system, consists of a vertical straight tube, from the top of which the target gases are introduced with the water covering the inner wall of the tube. A stable long arc in atmospheric pressure is produced between a cathode above the tube and an anode covered by thin water film in the lower part of the tube through which the arc current flows. More than 99% of decomposition efficiency with 300sccm CF4 diluted by 15slm N2 was achieved by this system. Here, in order to investigate the structure of this exotic plasma, we observe the distribution of OES along both vertical and radial directions of the plasma column. The results will be shown in the presentation.

*This study is sponsored by New Energy and Industrial Technology Development Organization of Japan.

SW 48 Model Study of the Pulsed Discharge Nozzle W.J.M. BROK, B.H.P. BROKS, J. REMY, J.J.A.M. VAN DER MULLEN, *Eindhoven University of Technology* EPG TEAM The characteristics of the plasma generated by a pulsed discharge slit nozzle (PDN) are investigated. The PDN source was designed to produce and cool molecular ions, creating an astrophysically relevant environment in the laboratory. A discharge model is applied to this system to provide a qualitative as well as a quantitative picture of the plasma. We find that the plasma's properties and behaviour are characteristic of that of a glow discharge. The model describes the electron density and energy, as well as the argon ion and metastable atom number density. The results reveal a high abundance of metastable argon atoms in the expansion region, which is more than one order of magnitude higher than the abundance of electrons and ions. These findings confirm experimental observations, which concluded that large molecular ions are dominantly formed through Penning ionization of the neutral molecular precursors seeded in the supersonic expansion of argon gas. The simulations presented here will help optimise the yield of formation of molecular ions and radicals in the PDN source; they will also provide key physical insight into the characteristics of interstellar molecules and ions analogs in laboratory experiments.

SW 49 Surface dielectric barrier discharges as actuators for flow control Y. LAGMICH, G. HAGELAAR, L.C. PITCHFORD, J.P. BOEUF, *CPAT, CNRS and Univ P Sabatier, Toulouse, France* Surface discharges created in Dielectric Barrier Discharge (DBD) configurations have been proposed as actuators for flow control in aerodynamic applications. Using a two-dimensional model of the surface dielectric barrier discharge in pure nitrogen we study the time evolution of the plasma and calculate the electrohydrodynamic force acting on the gas flow. The results show that this force is due to the momentum transfer from the ions to the neutral molecules in the sheath that propagates along the dielectric layer surface. The calculations also confirm that the asymmetry of the electrode configuration is responsible for the existence of a non-zero averaged force parallel to the surface. We present a parametric study of the discharge and calculated electrohydrodynamic force as a function of geometry and applied voltage. We also discuss the possible effect of photoemission from the dielectric surface on the discharge properties. Finally, the discharge model is coupled to the Navier Stokes equations for the gas flow to evaluate the effect of the surface discharge on the boundary layer.

SW 50 Measurement of the Absolute Concentration of Molecular Oxygen in a Capacitively-Coupled RF Discharge in a Martian Simulant Gas* GEORGE BROOKE, *Department of Physics and Astronomy, Virginia Military Institute, Lexington VA 24450* We will be presenting the results of an experiment to measure the absolute concentration of molecular oxygen in a capacitively-coupled RF discharge in a Martian simulant gas using cavity ring-down spectroscopy (CRDS). The goal of this work is an efficient, low-power oxygen generator for use on the surface of Mars. Previous experiments have demonstrated the ability to pro-

duce and extract molecular oxygen using an RF discharge but were unable to measure the absolute concentration within the discharge volume. Using the CRDS technique we have measured the absolute concentration of molecular oxygen in the discharge with respect to RF power and two different electrode configuration (planar and solonoidal) at a fixed pressure of 5 Torr.

*This work is supprted by the Thomas F. Jeffress and Kate Miller Jeffress Memorial Trust.

SW 51 ARCS AND BREAKDOWN

SW 52 Model Study of Breakdown in Low-Pressure Argon between Parabolic Electrodes W.J.M. BROK, E. WAGENAARS, J.J.A.M. VAN DER MULLEN, *Eindhoven University of Technology, The Netherlands* M.D. BOWDEN, *The Open University, United Kingdom* EPG TEAM Breakdown between two electrodes in argon at 3.5 Torr is investigated by means of a fluid model and a fluid-particle hybrid model. The cylindrically symmetric electrodes have a parabolic cross section and are placed in a vacuum chamber with their axis aligned and tips separated by 3.3 mm. Experimental observations of visible emission have shown a pre-breakdown light flash near the anode before the applied voltage reached the static breakdown voltage of the setup. After the breakdown voltage had been reached, an ionisation wave was observed to travel from anode to cathode and subsequently to envelope the cathode. The phenomena related to the pre-breakdown flash are investigated with a fluid-particle hybrid model and the results account for the stratified emission near the anode. By modelling this setup with a fluid model, the observed breakdown phenomena can be explained by means of buildup of space charge and the resulting evolution of the electric field.

SW 53 Experimental study of breakdown in low-pressure argon between parabolic electrodes ERIK WAGENAARS, NIELS PERRIËNS, GERRIT KROESEN, *Eindhoven University of Technology, The Netherlands* MARK BOWDEN, *The Open University, United Kingdom* Plasma breakdown phenomena in low-pressure argon gas were investigated by making time-resolved images of the plasma light emission, using an intensified charge coupled device (ICCD) camera. The breakdown arrangement consisted of 2 electrodes mounted inside a vacuum chamber creating a 3.3 mm discharge gap. A flow of argon gas was directed through the system, while a needle valve maintained the pressure at 465 Pa (3.5 torr). The electrodes were cylindrically symmetric and had a parabolic cross section. A repetitive, quasi-dc breakdown was created by applying voltage pulses with an amplitude of about 350 V, a duration of 100 μs and a repetition rate between 10 and 2000 Hz. Our measurements show a general breakdown behavior consistent with the Townsend breakdown theory. Additionally, we observed the appearance of a light flash near the anode at a time when the applied voltage was below the static breakdown voltage. This phenomenon could not be explained by Townsend theory and was investigated further by varying the rise time, repetition rate, polarity and shape of the applied voltage pulses. It was concluded that this feature was the result of charges close to the discharge volume, left over from the previous discharge cycle. These charges created weak electron avalanches at low applied voltages, before the main breakdown phase started.

SW 54 Characterization of Anode Boundary Layer of a High Intensity Arc with Cross Flow* GUANG YANG, JOACHIM HEBERLEIN, EMIL PFENDER, *Department of Mechanical Engineering, University of Minnesota* Anode boundary layers of high intensity arcs are characterized by large gradients in temperature, electrical potential and velocity. They determine anode life time and processing efficiency in many industrial applications. It has been shown that when a strong cold cross flow is applied to a high intensity arc, a new anode arc attachment mode can be formed, with a larger anode boundary layer area and thus smaller thermal load to the anode. In this study, we have used Langmuir probe and laser Thomson scattering diagnostics to measure the electron temperature and electron density in the anode boundary layer for this attachment mode for an atmospheric pressure argon arc. The arc is operated with working gas flow rates from 2 slpm to 18 slpm, and with currents from 50A to 100A. Argon and nitrogen are used as cross flow gases, and they have been shown to have quite different effects on the anode attachment. Our results indicate a strong effect of the attachment mode on the electron temperature and steeper electron density gradients than predicted by models.

*The research was supported through NSF grant No. CTS-0225962.

SW 55 Optical Emission Spectroscopy of an Atmospheric Arc RUSSELL RHOTON, MARY BRAKE, *Eastern Michigan University, Ypsilanti, MI 48197* An arc plasma was generated in atmospheric air between two carbon electrodes powered by a high voltage transformer controlled by a variable input source. A voltage of up to 12,000 V and current of 30 mA was delivered to an arc about 1.5 cm long. The diameter of the arc is estimated to be 0.1 cm, giving a current density of 4 A/cm^2. Optical emissions spectroscopy from 250 nm to 800 nm revealed a variety species ranging from molecular species like OH and N_2^+ to atomic lines of oxygen and nitrogen. When the arc is first ignited, molecular lines dominate while atomic lines begin to grow in intensity the longer the arc runs and as the gas heats up. Thermal equilibrium calculations between nitrogen atoms and molecules suggest that the plasma gas temperature is no more than 4500 K. The electron density is estimated to be about 10^{12} #/cm^3 based upon the relationship between current density and electron density in Ref. [1]. The spectral evolution of the discharge as a function of time will be discussed with respect to heating mechanisms. [1] Lan Yu et al., J. Appl. Phys., 91(5) 2678, 2002.

SW 56 An Experimental Study of Cold Helium Arc-Jet Flowing along Diverging Magnetic Field HIROSHI AKATSUKA, TOSHIAKI KANUMA, HARUAKI MATSUURA, MITSUO MATSUZAKI, *Tokyo Tech.* We experimentally examined plasma parameters of a supersonic cold helium arc jet accelerated along diverging magnetic field from a uniform magnetic channel, particularly relationship between plasma potential and ion Mach number. The atmospheric pressure arc plasma is generated and ejected into a rarefied gas wind tunnel with a uniform longitudinal magnetic field of 0.16 T. The strength of the magnetic field decreases to 0.01 T at 20 cm down from the end of the coils. The longitudinal velocity of the plasma jet was measured by Mach

probes. At the maximum gradient of the magnetic field, the peak of the Mach number 3.1 of the flow velocity was observed. We found lowering of the plasma potential at the exit of the nozzle from 2.5 to 0.4 V. The radial measurement shows that the lowest plasma potential was situated along the centerline of the plasma jet. It is well explained that he acceleration was caused by the change in the plasma potential rather than fluid dynamic effect. It is also found that the MHD effect like Hall acceleration ($j_\theta B_r$) or pumping force ($j_\theta B_z$) is insignificant. In addition, the swirl acceleration due to the conservation of the magnetic moment $\mu_m = mv_\perp^2/(2B)$ is also less significant than the electrostatic acceleration.

SW 57 ELECTRONEGATIVE PLASMAS

SW 58 Modelling electronegative plasmas separated by an internal sheath NICOLAS PLIHON, CORMAC S. CORR, PASCAL CHABERT, JEAN-LUC RAIMBAULT, *Laboratoire de Physique et Technologie des Plasmas, Ecole Polytechnique, Palaiseau* ALLAN J. LICHTENBERG, *Department of Electrical Engineering and Computer Science, University of California, Berkeley* It has experimentally been shown that in an ICP with an expanding chamber, adding a small concentration of SF_6 to argon can lead to the formation of a stationary double layer [1] separating two plasmas: a high density electropositive plasma in the source, and a low density, high electronegativity plasma downstream. This double layer periodically forms and propagates when increasing the the electronegativity [2]. We present calculation of the discharge equilibrium in the stationary double layer case based on a 1D description of the discharge. The source plasma appears to be only sligthly affected by the downstream plasma. The particles densities downstream are set by the incoming flux of positive ions from the source and attachment ocurring in the downstream volume. Our calculations show fairly good agreement to our experimental data. [1] Plihon et al. 2005 App. Phys. Lett **86** 091501 [2] Plihon et al. 2005 J. Appl. Phys. to be published.

SW 59 Hairpin probes: time-resolution and electronegative plasma NICHOLAS BRAITHWAITE, EVA VASEKOVA, JAFAR AL-KUZEE, MARK BOWDEN, *The Open University* A hairpin probe is an open, quarter-wave transmission line. When immersed in a plasma its resonant frequency measures local electron density directly and immediately through the plasma's dielectric response. At low electron density the sheath around the hairpin wires can be relatively large so it is necessary to allow for this. The use of a hairpin in photodetachment studies is explored: issues of time, electronegativity and spatial sensitivity are addressed. Temporal response is expected be limited by the time to establish resonance and the time for the sheath to equilibrate. The resonance is typically $\sim$ GHz so the former limit is $\sim$ 10 ns. The latter limit applies when the sheath is wide. Experimentally, in pulsed RF plasmas (eg He), a fully-floating hairpin is seen to have $\sim$ 100 ns resolution in the after-glow. In electronegative plasmas the effect of negative ions on the sheath structure is important. Test show that the hairpin functions with adequate sensitivity in the highly electronegative environment of SF_6; it is even possible to track the effects of fluorine-based etching of the hairpin wire (W). The spatial sensitivity of the hairpin peaks close to the open end. A dielectric rod has been used to mimic a photodetachment trail indicating that photodetachment signals will be a only a few % of full volume detachment.

SW 60 Negative Ions in Rare Gas/Oxygen Discharges* M. KATSCH, A. WAGNER, *Universitaet Duisburg-Essen* The temporal behavior of negative oxygen ions in argon-, krypton- and neon/oxygen mixtures is investigated in a pulsed inductively excited GEC reactor. The negative ion densities are measured by laser photodetachment of negative ions in combination with a Langmuir probe. In the early afterglow an unexpected high density of negative oxygen ions is found in mixtures with a high content of rare gas. These findings are in contrast to the predictions of our global model. It is, therefore, necessary to invoke an additional production channel for the negative ions, in order to explain the observed high negative ion density. It is likely that additional negative ions are generated by dissociative attachment of highly excited oxygen molecules. It is also possible that Rydberg states of the oxygen molecules are excited via collisions with metastable rare gas atoms. These excited Rydberg molecules may also lead to a generation of negative oxygen ions. Comparative measurements show that it is unlikely that Rydberg states are responsible for the enhanced generation of negative ions.

*Supported by the ''DFG'' (SFB 591).

SW 61 Negative ion formation and motion in a mixture of CCl_4 and Ar F.B. YOUSIF, *Facultad de Ciencias-Universidad Autónoma del Estado de Morelos* H. MARTÍNEZ, *Centro de Ciencias Físicas, Universidad Nacional Autónoma de México* A.B. MONDRAGÓN, *Facultad de Ciencias-Universidad Autónoma del Estado de Morelos* FACULTAD DE CIENCIAS, UAEM TEAM, CENTRO DE CIENCIAS FÍSICAS, UNAM TEAM This work deals with the measurement of the mobility of negative ions in the mixtures of CCl_4 with Ar with the CCl_4 ratio up to 33.3%. The Pulsed Townsend Technique was employed to produce an integrated ionic avalanches over a range of the density-reduced electric field E/N for which ionization is either negligible or absent, and attachment processes are dominant, leading to the formation of mostly CCl_4^-. The E/N range of measurement was 1 to 50 Td ($1Td = 10^{-17}Vcm^2$) and gas pressure of $80Torr$. Our measurements strongly suggest that attachment is the dominant process and only negative ions are formed. The characteristics of the measured transients, indicating that there is only one drifting ionic species. That, and the low E/N values used, led to the assumption that the majority ion species under investigation is CCl_4^-. This method proved to be highly sensitive for detecting negative ion signals even for small amounts of CCl_4 in the mixture. The relevance of electron attachment processes in these mixtures are desirable and it is our hope that the present data are of use for gas discharge simulation and complexion chemistry of CCl_4/Ar mixtures.

SW 62 Global Model of Electronegative Discharges for Neutral Radical Control SUNGJIN KIM, M.A. LIEBERMAN, A.J. LICHTENBERG, *University of California, Berkeley* J.T. GUDMUNDSSON, *University of Iceland, Reykjavik, Iceland* Control and reduction of the ratio of neutral radical flux to ion flux at the wafer surface is required for the next generation plasma etching processes in the microelectronics industry. To explore these pro-

cesses, the electronegative plasmas driven by steady power and by time-modulated power, with oxygen as the feedstock gas, have been investigated utilizing volume-averaged (global) models of a cylindrical plasma discharge. The variations of the time-average flux ratio of oxygen neutrals to O_2^+ ions depending on the chamber geometry and power modulation conditions were examined using a simple model with uniform spatial profiles and a new model with non-uniform spatial profiles, and the results from the models were compared. In both models, at a fixed duty-ratio, the flux ratio of neutrals to ions is found to have a minimum value as the pulse period is varied, with the minimum value decreasing as the duty-ratio decreases. The flux ratio is reduced in the chamber geometry with lower aspect ratio, and the pulse period that yields minimum value also decreases. In future work, we will compare the simulation results with measured experimental results.

SW 63 IONIZATION OF ATOMS AND MOLECULES

SW 64 An Electron Momentum Spectroscopy, Density Functional and Greens Function Theories study of the Outer Valence Electronic Structure of Bicyclo[2.2.1]heptane-2,5-dione MICHAEL BRUNGER, DARRYL JONES, *School of Chemistry, Physics and Earth Sciences, Flinders University* STEFAN KNIPPENBERG, JEAN-PIERRE FRANCOIS, MICHAEL DELEUZE, *Department SBG, Limburgs Universitair Centrum* SAUMITRA SAHA, FENG WANG, *Centre for Molecular Simulation and School of Information Technology, Swinburne University of Technology* ROLF GLEITER, JOHANNES BUEBER, *Organic Chemistry Institute, University of Heidelberg* DAVE WINKLER, *CSIRO Molecular Science* We report our preliminary results for an electron momentum spectroscopy (EMS) study of the outer valence electronic region of bicyclo[2.2.1]heptane-2,5-dione. The measured binding energy spectra are presented for the azimuthal angles 0°, 10° and 0°+10° and are compared to new He(Iα) photoelectron spectroscopy results. These data are then compared with results from theoretical computations, using Greens Function theories. Derived momentum distributions are compared against those obtained by calculations which employ the plane-wave impulse approximation. These calculations use basis sets obtained from Density Functional Theory calculations at the triple zeta valence polarization level with a collection of different exchange correlation functionals.

SW 65 Electron Impact Ionization of Silicontetrachloride ($SiCl_4$)* RALF BASNER, *INP Greifswald* MICHAEL GUTKIN, JENNY MAHONEY, VLADIMIR TARNOVSKY, *Stevens Institute of Technology* HANS DEUTSCH, *Institut fur Physik, Greifswald* KURT BECKER, *Stevens Institute of Technology* We measured absolute partial cross sections for the formation of various singly charged and doubly charged positive ions produced by electron impact on silicon tetrachloride ($SiCl_4$) using two different experimental techniques, a time-of-flight mass spectrometer (TOF-MS) and a fast-neutral-beam apparatus. The energy range covered was from the threshold to 900 eV in the TOF-MS and to 200 eV in the neutral beam apparatus. The results obtained by the two different experimental techniques were found to agree very well (better than their combined margin of error). The $SiCl_3^+$ fragment ion has the largest partial ionization cross section with a maximum value of slightly above 6 x 10^{-20} m^2 at about 100 eV. The cross sections for the formation of $SiCl_4^+$, $SiCl^+$, and Cl^+ have maximum values around 4 x 10^{-20} m^2. Some of the cross section curves exhibit an unusual energy dependence with a pronounced low-energy maximum at an energy around 30 eV followed by a broad second maximum at around 100 eV. The maximum cross section values for the formation of the doubly charged ions, with the exception of $SiCl_3^{++}$, are 0.05 x 10^{-20} m^2 or less.

*Work supported in part by the US Department of Energy.

SW 66 Formation of positive ions of quadricyclane* C.Q. JIAO, *Innovative Scientific Solutions, Inc., Dayton, OH* C.A. DEJOSEPH, JR., R.H. LEE, A. GARSCADDEN, *Air Force Research Laboratory, Wright-Patterson AFB, OH* Quadricyclane (QC) is one of the strained hydrocarbons that have potential as high-energy density materials used as aerospace fuel or as additives to kerosene rocket fuel. We have studied the formation of positive ions of QC by electron impact and by charge-transfer reactions, using Fourier-transform mass spectrum (FTMS) techniques. The electron ionization cross sections in the energy range of 10-200 eV have been measured. The total cross section reaches a maximum of 2.3x10^{-15} cm^2 at 60 eV. Parent ion $C_7H_8^+$ and 21 fragment ions including $C_5H_6^+$ and $C_5H_5^+$ that dominate the dissociation channels at low energies ($<$ 25 eV) are observed. Ar^+ charge-transfer reaction with QC produces $C_5H_5^+$ and $C_7H_7^+$ as the major ionic species. Some selected hydrocarbon ions, i.e., $C_3H_3^+$, $C_5H_3^+$, $C_5H_5^+$ and $C_5H_6^+$, which are formed from QC by electron ionization, are found to react with QC forming $C_7H_7^+$ and $C_7H_8^+$ as the major product ions, while the latter two ions are unreactive with QC. The relative rates of the hydrocarbon ion reactions, compared to the Ar^+ charge-transfer reaction, are rather low; while the rate for $C_3H_3^+$ is less than 20 percent of the Ar^+ reaction rate, the rates for $C_5H_3^+$, $C_5H_5^+$ and $C_5H_6^+$ are less than 3 percent.

*This work supported by the Air Force Office of Scientific Research.

SW 67 Approximating the Green's Function in Evaluating Second-Order Amplitudes ZHANGJIN CHEN, DON MADISON, *Laboratory for Atomic and Molecular Research, University of Missouri-Rolla, Rolla, MO 65401* KLAUS BARTSCHAT, *Department of Physics and Astronomy, Drake University, Des Moines, Iowa 50311, USA* It is well established that second-order effects are often important for electron impact ionization processes. Due the complexity of evaluating second order amplitudes, approximations are typically made in their evaluation. One of the approximations that have been used is accounting only for the imaginary part of the Green's function, so that the second-order amplitude reduces to a sum of products of two first-order terms. To check the validity of this approximation, we performed second-order distorted-wave calculations, in which the first-order amplitudes were evaluated by a convergent *R*-matrix with pseudostates (close-coupling) model to describe the initial bound state and the ejected-electron–residual-ion interaction. The results obtained without making any approximations are compared with those obtained by simplifying the Green's function for electron impact ionization of helium to $He^+(1s)$ and $He^+(2s,2p)$. The approximation is found to be reasonably good for direct ionization to $He^+(1s)$ at incident energies greater than about 600 eV. The accuracy decreases with decreasing incident electron energy.

SW 68 Electron-impact Fully Differential Cross Sections of Helium for Simultaneous Excitation- Ionization M. FOSTER, D.H. MADISON, J.L. PEACHER, A.L. HARRIS, *University of Missouri - Rolla* LABORATORY FOR ATOMIC, MOLECULAR AND OPTICAL RESEARCH TEAM We have examined fully differential cross sections for electron- impact ionization of helium with simultaneous excitation of the atomic electron to either the 2s or 2p state. This process has attracted considerable attention due to the fact that second order effects are known to be very important and there have been several studies within the framework of the second Born approach which treats the projectile-atom interaction to second order. We will report results for a complete quantum mechanical four-body model known as the 6DW (six-distorted-wave) model. The 6DW model takes all two particle Coulomb interactions (six in total) into account exactly which means that all two-particle interactions are taken into account to all orders of perturbation theory. One of the advantages of this approach is that the importance of each two-particle subsystem can be independently studied. 6DW results will be compared with experimental data and other theoretical approaches.

SW 69 Experimental and Theoretical study of the Fully Differential Cross Section both in and out of the Scattering Plane for Electron-Impact Ionization of Magnesium M. FOSTER, D.H. MADISON, J.L. PEACHER, A. WALTERS, *University of Missouri - Rolla* R. VANBOEYEN, M. COPLAN, *University of Maryland, Department of Physics* LABORATORY FOR ATOMIC, MOLECULAR AND OPTICAL RESEARCH COLLABORATION, UNIVERSITY OF MARYLAND, DEPARTMENT OF PHYSICS COLLABORATION Most of the experimental and theoretical studies of electron- impact ionization of atoms, normally referred to as (e,2e), have concentrated on the scattering plane defined by the initial and final momentum vectors of the projectile. The assumption has been that all the important physical effects will be observable in the scattering plane. However, very recently it has been shown that, for C^{6+}-helium ionization, experiment and theory are in nice agreement in the scattering plane and in very bad agreement out of the scattering plane. This lack of agreement between experiment and theory has been explained in terms of higher order scattering effects between the projectile and ion which would never be seen in the scattering plane. In this paper we will examine electron-impact ionization of magnesium to see if similar higher order effects might be present here as well.

SW 70 Proton Impact Transfer-Ionization of Helium D.H. MADISON, M. FOSTER, J.L. PEACHER, *University of Missouri - Rolla* M. SCHOEFFLER, R. DOERNER, *Institut fur Kernphysik, Universitat Frankfurt* For the first time experimentally all the final state particles in the process of transfer ionization are measured in triple coincidence. Transfer-ionization is the process in which one electron is transferred to a fast proton and the other electron is ionized into the continuum. In this paper, we will present fully differential transfer-ionization cross section (FDTICS) for 630 keV $p + He \rightarrow H^0 + He^{2+} + e^-$. In order to fully understand the electronic correlation in atoms such as helium, we will present a complete quantum mechanical four-body model known as the 6DW (six-distorted-wave) model. The 6DW model takes all two particle Coulomb interactions (six in total) into account on equal footing. The 6DW approach also allows for the probing of high level electronic correlation effects in atoms such as helium. The atomic correlation effects can be studied in great detail through various types of (e, 2e) and ion impact collisions. The first of the impact collisions that will be examined is referred to as transfer-ionization. Preliminary results will be reported for both transfer-ionization of helium.

SW 71 Ionization of silicon, germanium, tin, and lead by electron impact PHILIP STONE, YONG-KI KIM, *NIST, Gaithersburg, MD* We continue our investigation of electron impact ionization of neutral atoms that are important in modeling of low temperature plasmas and gases. Cross sections for ionization have been calculated for ionization from ground levels and low-lying metastable levels of Si, Ge, Sn and Pb. We use the binary-encounter-Bethe approximation (BEB) for direct ionization and scaled plane-wave-Born approximation for dipole- and spin-allowed transitions to autoionizing levels.[1,2] Multiconfiguration Dirac-Fock wavefunctions have been used for the atomic structure. The calculated values are in agreement with the few experimental results available for comparison. It is clear that autoionization is important in these elements and must be included accurately. These results complement earlier calculations of H, He, Li, B, C, N, O, Al, Ga, and In. The results for these atoms, along with ionization cross sections for many molecules are being made available on a NIST web site.[3] Work supported in part by the U.S. DOE Office of Fusion Sciences. [1] Kim Y-K and Desclaux JP, Phys. Rev. A 2002; **66**; 012708. [2] Kim Y-K and Stone PM, Phys. Rev. A 2001; **64**; 052707. [3] http://physics.nist.gov/ionxsechttp://physics.nist.gov/ionxsec (2005).

SW 72 Ionization of neutral W and W^+ ion by electron impact* DUCH-HEE KWON, YONG-JOO RHEE, *KAERI, Daejeon, Korea* YONG-KI KIM, *NIST, Gaithersbur, MD* Ionization cross sections for the neutral W and W^+ ion by electron impact are being calculated using binary-encounter- Bethe (BEB) model for the direct ionization and scaled Born cross sections for excitation-autoionization as was done successfully for the ionization of C, N, and O.[1] Two sets of experimental data for W^+ are available in the literature, while there are no experimental data for the neutral W. Both sets of the experimental data indicate the presence of metastable W^+ ions in their target beams, but the magnitude and shape are comparable to our preliminary results for W^+ ion in the ground level. Theoretical results that include cross sections for both direct ionization and excitation-autoionization of W and W^+ will be reported at the conference.

*Work supported in part by the Office of Fusion Sciences, US-DOE and by the Fusion Plasma Users Support Program of the Korea Basic Science Institute.

[1]Y.-K. Kim and J. P. Desclaux, Phys. Rev. A **66**, 012708 (2002).

SESSION UH1: ETCHING MECHANISMS
Thursday morning, 20 October 2005
Pine, Doubletree Hotel at 8:00
Eric Hudson, LAM Research, presiding

8:00
UH1 1 Profile simulation of high-aspect-ratio contact etching including charging effect SEOKHYUN LIM, YONGJIN KIM, YERO LEE, TAIKYUNG KIM, GYUNG-JIN MIN, CHANG-JIN KANG, HANKU CHO, JOO-TAE MOON, *Samsung Electronics Co., Ltd.* As the design rule of semiconductor devices shrinks, high- aspect-ratio contact (HARC) etching of dielectrics becomes one of the most critical processes. Etch loading, bowing and pattern deformation at the bottom are serious problems in the HARC etching process, while the mechanism of the phenomena has not been fully understood yet. HARC etching requires high ion energy flux, resulting in severe charge build-up on the surface, which is an important factor that should be considered to understand the mechanism. In the present work, we perform particle simulation of ion and electron under the electric field generated by the charges accumulated on the dielectric surface and investigate the effects of various parameters of ion energy, ion angle, electron energy and pattern geometry on the charge build- up and ion energy flux distribution along the dielectric surface in detail. The charging effect on the profile evolution and the mechanism of various phenomena during the HARC etching process is also investigated.

8:15
UH1 2 A self-consistent modeling of feature profile evolution under competition between etching and deposition TAKASHI SHIMADA, TAKASHI YAGISAWA, TOSHIAKI MAKABE, *Keio University* KEIO UNIVERSITY TEAM Radical deposition is one of the important issues for SiO_2 etching as the radicals contribute to the protection of side wall as well as the acceleration of etching by the formation of a mixing layer on the bottom. We investigate the relationship among local wall charging, etching and deposition in a SiO_2 trench etching, by considering the transport of electrons, positive ions, and neutral radicals in the two-dimensional sheath structure in a two frequency-capacitively coupled plasma in CF_4/Ar. Emphasis is given on the influence of both charging and neutral radical accumulation inside the SiO_2 trench during plasma etching. Feature profiles of the SiO_2 trench are estimated by the Level Set method under conditions with/without charging and neutral deposition. In particular, the effect of the bias amplitude on the profile evolution is discussed under the competition between etching and deposition.

8:30
UH1 3 Development of Nano-Contact Etch Process Using New Gas Chemistry. JONG-WOO SUN, CHUL-HO SHIN, GYUNG-JIN MIN, CHANG-JIN KANG, HANKU CHO, JOO-TAE MOON, *Samsung Electronics Co., Ltd.* As device feature size shrinks to sub-0.1μm, oxide contact etching has become difficult to satisfy the process requirements. Especially, the aspect ratio of device has become higher and the mask thickness thinner. These trends require the ability to etch with high selectivity against mask and better profile control. In this paper, development of oxide contact etch process using new gas chemistry(CxFyHz) is investigated. It has already been proposed that the reactive gas mixture contain polymer and etchant gases. However, with current gas species, we have some limitations to meet process specification for next generation device. Compared to other common polymer former gases, it is found that our new additive gas has significant effect to increase selectivity against mask and to control feature profile. From the experiments, the selectivity of oxide over mask is enhanced up to 30% and it provides some potential possibility for profile control compared to other gases. These effects have also been analyzed by QMS (Quadrupole Mass Spectrometer).

8:45
UH1 4 Etching of high-k and metal gate materials in high-density chlorine-containing plasmas KOUICHI ONO, KEISUKE NAKAMURA, KAZUSHI OSARI, TOMOHIKO KITAGAWA, KAZUO TAKAHASHI, *Department of Aeronautics and Astronautics, Kyoto University, Japan* KYOTO UNIVERSITY TEAM Plasma etching of high dielectric constant (k) films and metal electrodes is indispensable for the fabrication of high-k gate stacks. This paper presents the etching characteristics of high-k materials of HfO_2 and metals of Pt and TaN using high-density chlorine-containing plasmas, along with the plasma and surface diagnostics concerned. Attention was focused on etch chemistries and plasma conditions to achieve a high etch selectivity of $>>1$ for HfO_2 over the underlying Si and SiO_2; regarding Pt and TaN, the emphasis was placed on the etch anisotropy and selectivity of metal electrodes over the underlying HfO_2 and overlying SiO_2. The etching of HfO_2 was performed in BCl_3 without rf biasing, giving an etch rate of about 5 nm/min with a high selectivity of >10 over Si and SiO_2. At lower pressures, the deposition of BCl_x was found to occur on all the surfaces of interest; however, on HfO_2 surfaces, the deposition followed the etching during a few tens of seconds. The etching of Pt and TaN was performed with high and low rf biasing, respectively, giving a Pt etch rate of about several tens nm/min and a TaN etch rate of about 200 nm/min, with a high selectivity of >8 over HfO_2 and SiO_2 in Ar/O_2 for Pt and in Ar/Cl_2 for TaN. The etched profiles were outwardly tapered for Pt, while the TaN profiles were found to be almost anisotropic.

9:00
UH1 5 SiO_2 and Si_3N_4 Etch Mechanisms in NF_3/C_2H_4 Plasma* PUTHAJAT MACHIMA, NOAH HERSHKOWITZ, *Department of Engineering Physics, University of Wisconsin-Madison* Low-pressure inductive plasma was used to study SiO_2 and Si_3N_4 etching with the NF_3/C_2H_4 chemistry. NF_3 and C_2H_4 were used so that fluorine and carbon could be supplied from feed gases other than global warming fluorocarbons. Etch rates of SiO_2 over a wide range of conditions are less than 0.8 times the Si_3N_4 etch rates. Ex-situ XPS was used to determine the characteristics of a very thin steady-state film, to establish etch mechanisms. XPS results show that CH_xF, CF_2, and CF_3 were produced but in small concentrations compared to CH_x and CN. Mass spectrometry and optical emission gave consistent results. C1s spectra from etched oxide samples show a large percentage of H_xC-CH_x structures. Si_3N_4 appears to react easily with H_xC-CH_x structures, yielding CN-bearing products and SiC. Etch rate and selectivity results of NF_3-based discharges fed with C_2H_2, C_4H_{10}, and CH_3F are similar to the NF_3/C_2H_4 plasma. Comparisons of normalized F1s spectra of nitride and oxide etched under the same conditions show that relative concentrations of CF_2 and CF_3 on SiO_2 are much lower than the concentrations on Si_3N_4. It appears that

SiO_2 preferentially reacts with only CF_2 and CF_3 but not with $H_xC\text{-}CH_x$ or CH_xF. Differences in the abilities of SiO_2 and Si_3N_4 to react with $H_xC\text{-}CH_x$ contributed to higher etch rates of Si_3N_4. Effects of bias frequency are presented.

*Work Supported by US EPA Grant No. RD-83145901-0.

9:15

UH1 6 Performance Tunable High-Frequency Inductively Coupled Plasma Technology in Application to Polysilicon Etcher and High Density Plasma CVD* JONG W. SHON, *Ju Sung Engineering Ltd.* GICHUNG KWON, *JuSung Engineering Ltd.* HONG Y. CHANG, *KAIST* JUSUNG ENGINEERING TEAM, KAIST TEAM High frequency ICP plasma technology is uniquely suited for 45nm technology node and below for its ability to produce plasma with low electron temperature and controllable ion energy. In this presentation we will discuss principles of this technology and its application to Poly etcher and HDP CVD. The low impedance resonance antenna can accomplish impedance matching in 13.56 MHz or 27.12 MHz source frequency. High density plasma is generated by the high current coils. Also, plasma uniformity can be controlled by the current in each antenna turns. The low capacitive voltage applied to antenna can minimize capacitive damage and reduce particles from ceramic plate. High frequency ICP source can generate plasma with low electron temperature compared to lower frequency ICP sources using 400 KHz or 2 MHz), which can minimize plasma damage on the wafer. The plasma density from this source is $1 \times 10^{11} \sim 1 \times 10^{12}$ $cm^{-3}$and the electron temperature is less than 2.5 eV in 27.12 MHz and 4 eV in 13.56 MHz. We obtained the plasma uniformity less than 5%. For the applications, patterned WSi gate, poly-Si gate, and W-Bit line wafers were etched using a parallel resonance antenna. STI (Shallow Trench Isolation), ILD (Inter Layer Dielectric), and IMD (Inter Metal Dielectric) wafers were processed in a dome-typed antenna source for HDP CVD. The process characteristics of HDP CVD has proven in 0.13 micrometer technology with AR (aspect ratio) 5:1 and expected to provide next generation gap fill solution. The process characteristics of dry etcher have obtained minimal micro-loading effect less than +-5%, high selectivity W to Hard Mask (SiN) more than 1.5:1, wide range CD bias control within 20 nm, and vertical profile more than 89 degree.

*Performance Tunable High-Frequency Inductively Coupled Plasma Technology in Application to Polysilicon Etcher and High Density Plasma CVD.

SESSION UH2: GLOWS II
Thursday morning, 20 October 2005
Cedar, Doubletree Hotel at 8:00
Y. Sakai, Hokkaido University, presiding

8:00

UH2 1 Analysis of the spatiotemporal behaviour of a He-Xe column plasma by self-consistent modelling DETLEF LOFFHAGEN, FLORIAN SIGENEGER, *INP Greifswald, F.-L.-Jahn-Str. 19, 17489 Greifswald, Germany* The positive column plasma of a glow discharge constitutes a typical representative of a non-equilibrium plasma. Large effort has been spent in recent years to get a deeper understanding of its inherent temporal and spatial dynamics. This presentation reports on a new self-consistent method for the analysis of the space- and time-dependent behaviour occurring in a cylindrical, axially homogeneous column plasma of low-pressure glows. The model consists of hydrodynamic equations for all charged and neutral particles in the plasma, Poisson's equation describing the behaviour of the radial space charge field, the balance equation of the discharge current for the determination of the axial electric field and the time-dependent, radially inhomogeneous Boltzmann equation providing transport and rate coefficients of the electrons. First results obtained for the spatiotemporal evolution of a He-Xe mixture plasma containing 2% of xenon in a discharge tube with a radius of 9 mm at a gas pressure of 2.5 Torr and given time-dependence of the discharge current are discussed. Starting from a homogeneous and field-free initial situation the transition to steady state at a discharge current of 60 mA is considered showing large structural changes in space and time for the electric field and the particle and flux densities of the different plasma components.

8:15

UH2 2 Self pulsing microdischarge in argon ANTOINE ROUSSEAU, XAVIER AUBERT, LPTP-ECOLE POLYTECHNIQUE CNRS PALAISEAU FRANCE TEAM Microdischarge is generated in the hole made in a conductor-dielectric-conductor sandwich in pure argon [1]. At low discharge current, the plasma is confined inside the micro-hole and the voltage increases with the current (abnormal regime). At higher current the plasma is expended in the backside cathode region and the voltage is insensitive to the discharge current (normal regime). Between these two stable operating mode, for intermediate current value self-pulsing current oscillations are observed [2]. It is shown that the self-pulsing frequency is a linear function of the averaged current and depends only on the pxD product, for a wide range of hole diameter D and gas pressure p. Time resolved optical emission spectroscopy measurements performed in the cathode backside indicate that such oscillations are caused by short plasma expansions (2-5 μs) towards the cathode backside and correspond to a transient change between the abnormal and normal regime. The related pulse duration does not depend on the averaged current. Authors thank L.C. Pitchford, J.P. Boeuf and V. Puech for discussions. [1] K. H. Schoenbach, R. Verhappen, T. Tessnow, F. E. Peterkin, W. W. Byszewski, Appl. Phys. Lett. **68** (1996) 13. [2] D.D. Hsu and D. B. Graves J. Phys. D: Appl. Phys. 36 (2003) 2898.

8:30

UH2 3 Spatiotemporal development of low-pressure low-current discharges in argon DRAGANA MARIĆ, ZORAN PETROVIĆ, *Institute of Physics, POB 68, 11080 Zemun, Belgrade, Serbia and Montenegro* We present analysis of time and space resolved development of low-pressure, low-current discharges in argon. We detect light emission by an intensified charge coupled device (ICCD) camera and support those recordings by voltage-current measurements. The goal was to extend the knowledge of kinetics of formation and maintenance of different modes of discharge – low current diffuse Townsend discharge, constricted normal glow and abnormal glow discharge. We have performed measurements at pd = 150 Pa · cm and 45 Pa · cm. Special care was taken in recording of the spatiotemporal development of discharge oscillations and constrictions. The develop-

ment of glow and abnormal glow discharges was recorded in 2 dimensions, revealing radial dependence of the discharge and showing radial development of constrictions. During oscillations at low currents there are both axial and radial oscillations of the ionized gas.

8:45

UH2 4 Kinetics of electrons in BF_3 O. ŠAŠIĆ, Z. LJ. PETROVIĆ, Z. RASPOPOVIĆ, *Institute of Physics, POB 68, 11080 Zemun, Belgrade, Serbia and Montenegro* L. GODET, S. RADOVANOV, *Varian Semiconductor Equipment Associates, Gloucester, MA01930, USA* We have used the available data for electron scattering cross sections for electrons in BF_3 to calculate the transport coefficients for electrons. Monte Carlo simulation was used to perform calculations for a broad range of E/N for DC and RF fields. Even though the drift velocity does not show the negative differential conductivity (NDC), the shape of the cross sections is such that it supports the NDC so the drift velocity has a broad plateau from 20 Td to 80 Td. The diffusion is very anisotropic with D_T/D_L ratio of up to 4. One may expect the kinetic phenomena that were observed for other gases with Ramsauer Townsend minimum and large vibrational cross sections to take place. These calculations will be taken as the basis for interpretation or modelling of electron kinetics in pulsed plasma sources of ions for implantation during the glow and afterglow periods.

9:00

UH2 5 Radial distribution of plasma parameters in a BF_3 discharge LUDOVIC GODET, SVETLANA RADOVANOV, RAJESH DORAI, *Varian Semiconductor Equipment Associates* GILLES CARTRY, CHRISTOPHE CARDINAUD, *Nantes University, France* VARIAN SEMICONDUCTOR EQUIPMENT ASSOCIATES TEAM, NANTES UNIVERSITY, FRANCE COLLABORATION The radial distributions of discharge parameters in a pulsed DC plasma doping system have been studied using measurements of time-resolved electron density, relative ion density, plasma potential and electron temperature in BF_3 and Ar plasmas during active discharges. The effects of the electric field on the radial distribution of the plasma parameters are investigated. These measurements could be taken as the basis for interpreting on-wafer uniformity. Negative plasma potentials are observed when using a hollow cathode to create plasma while implanting at ultra low energies. The kinetics of plasma generation during the pulse-on phase has been discussed.

9:15

UH2 6 Time resolved energy distribution of ions from a cathode sheath in a plasma doping system in BF_3 LUDOVIC GODET, SVETLANA RADOVANOV, *V* ZIWEI FANG, JAMES BUFF, *Varian Semiconductor Equipment Associates* GILLES CARTRY, CHRISTOPHE CARDINAUD, *Nantes University, France* VARIAN SEMICONDUCTOR EQUIPMENT ASSOCIATES TEAM, NANTES UNIVERSITY, FRANCE COLLABORATION The time resolved energy distribution of ions present in a BF_3 glow discharge was sampled from the cathode sheath in a plasma doping system (PLAD). Plasma is generated by applying negative voltage pulses to a wafer in the presence of low pressure gas. An energy analyzer was placed behind the biased wafer and configured to measure the energy of ions striking the wafer during the pulse-on and pulse-off periods. The electrostatic optics and axial potential distribution in the energy analyzer were optimized to provide the best ion transmission efficiency. For very low energy implantation, a hollow cathode is used to create and maintain the plasma. The hollow cathode modifies the electric field in such a manner that the effective anode to cathode gap is reduced which in turn increases the plasma density and reduces the sheath thickness. The effects of the hollow cathode and the anode gap on the ion energy distribution are presented. The electron energy distribution function, measured with a Langmuir probe, and plasma sheath parameters are discussed.

SESSION VH1: PLASMA DIAGNOSTICS II
Thursday morning, 20 October 2005
Pine, Doubletree Hotel at 10:00
Nick Braithwaite, Open University, UK, presiding

10:00

VH1 1 Diagnostics of Oxygen Atoms in Surface Wave Plasma with Vacuum Ultraviolet Laser Absorption Spectroscopy KEIGO TAKEDA, YOSHIKI KUBOTA, *Graduate School of Eng., Nagoya Univ.* ANNA SERDYUCHENKO, *Institute for Experimental Physics V, Ruhr-Univ. Bochum* SEIGO TAKASHIMA, MASARU HORI, *Graduate School of Eng., Nagoya Univ.* Oxygen plasmas have been frequently used for oxidation process of materials, chamber cleaning, etc. In the case of the fabrication of ultra-thin dielectric films such as a gate oxide film, the surface wave excited oxygen plasmas diluted by rare gases was especially focused on realizing a higher oxidation rate and lower leakage current than the conventional plasma oxidation process. However, the detailed knowledge of mechanism of the plasma oxidation process is not obtained due to few powerful measurement techniques of oxygen atoms which are most important in plasma oxidation process. Therefore, in this study, we have carried out the measurement of the absolute oxygen atom density in the Kr dilution surface wave excited oxygen plasma using tunable vacuum ultraviolet laser absorption spectroscopy with the resonance lines of ground state and that of excited state. The densities were evaluated as a function of Kr dilution ratio. The excited oxygen atom density increased with the increase of Kr dilution ratio and had a peak at the high dilution ratio of 97 %. The behaviors of ground state oxygen atoms in the surface wave excited oxygen and Kr mixture plasma were also evaluated.

10:15

VH1 2 Detection of $N_2(A^3\Sigma_u^+)$ metastable in DBD discharge by OODR-LIF spectroscopy* SANTOLO DE BENEDICTIS, PAOLO FRANCESCO AMBRICO, GIORGIO DILECCE, *Institute of Inorganic Methodologies and Plasmas, CNR, Bari, Italy* MILAN SIMEK, *Institute of Plasma Physics, Laboratory of Pulse Plasma Systems, Prague, Czech Republic* The $N_2(A^3\Sigma_u^+)$ metastable has been detected for first time in dielectric barrier discharge at atmospheric pressure in N_2 and N_2-O_2 gas mixtures by Optical-Optical Double Resonance –Laser Induced Fluorescence spectroscopy (OODR-LIF). The DBD discharge occurs over a thin ceramic plate on which one metallic electrode comb structured is deposited. The second electrode is a full deposit on the back of the plate external to the chamber. The $N_2(A)$ OODR-LIF detection takes place by one laser photon tuned on the (3,0) band of N_2(FPS) and a second one on the (2,3) band of N_2(SPS) as described in previous papers[1]. The fluorescence signal of (2,1) band of SPS is measured. The measurement is time resolved in the radiofre-

quency cycle (11KHz) of applied voltage and space resolved in the discharge gap. $N_2(A)$ metastable LIF signal varies in the voltage cycle as well as with the distance (1 - 5 mm) above the surface of comb electrode. It is significantly quenched as a few percentage of O_2 is added to N_2. [1] G. Dilecce, P.F. Ambrico, S. De Benedictis, PSST (on line July 2005)

*M. Simek was supported by CNR STM 2005 programme.

10:30

VH1 3 Development of ultracompact absolute density measurement system for atomic radicals and simultaneous measurement technique of H, N, O radicals employing the system SEIGO TAKASHIMA, *Dept. of Electrical Engineering and Computer Science, Nagoya Univ.* HIROYUKI KANO, *NU Eco-Engineering* MASARU HORI, *Dept. of Electrical Engineering and Computer Science, Nagoya Univ.* Atomic radicals such as hydrogen (H), Nitrogen (N), and oxygen (O) play important roles in reactive process plasmas. In previous study, we have developed a measurement system of absolute densities of H, N, O atoms in process plasmas employing the vacuum ultraviolet absorption spectroscopy (VUVAS) with an atmospheric pressure microdischarge hollow cathode lamp (MHCL). Using this system, the measurements of absolute densities have been carried out and hereby the behaviors of these atomic radicals in various process plasmas have been clarified. However, in this system, when the measurements were carried out in the high density plasmas, the pipes of about 30 mm in diameter had to be introduced into the plasma in order to prevent the saturation of the absorption intensity. Moreover, three atomic radicals were not able to be measured simultaneously. In this study, we have developed the ultracompact measurement system of mm size and simultaneous measurement technique of H, N, O atoms.

10:45

VH1 4 Multipurpose temperature gradient probe: operation and applications PAVLO RUTKEVYCH, *PSAC/NIE/NTU, Singapore* KOSTYA OSTRIKOV,* *School of Physics, The University of Sydney, Sydney NSW 2006, Australia* JIDONG LONG, SHUYAN XU, *PSAC/NIE/NTU, Singapore* Development and applications of a versatile temperature gradient probe (TGP) for advanced in situ plasma diagnostics are reported. The probe is made of three stainless steel-shielded thermocouples. Hardware and software compensations provide stable and reproducible temperature readings even in high-power RF discharges. In addition to TG measurements, the metallic shields are used as cylindrical Langmuir probes (LPs), and provide valuable information about ion and electron densities and ion temperature by using the Laframboise model of ion collection. Independent estimation of plasma potential and thermo-emission current is made through direct temperature readings. This high-efficiency and low-cost hybrid TG/LP in situ diagnostics has been used to map the species distribution in Ar+H2+CH4 inductively coupled plasmas used for plasma enhanced chemical vapour deposition of ordered carbon microemitter arrays. In particular, the TGP diagnostics confirms that the quality of microemitter structures can be managed by thermophoretically manipulating plasma-grown nanoparticles in the near-substrate areas.

*Also with: PSAC/NIE/NTU, Singapore.

11:00

VH1 5 Monitoring Ion Energy at a Wafer Surface During Plasma Etching MARK SOBOLEWSKI, *NIST* A better understanding and control of plasma etching could be obtained if the energy distributions of ions striking the wafer surface were known. Unfortunately, directly measuring ion energies at a wafer surface during etching is difficult or impossible. Ion energies can be indirectly monitored, however, by measuring the rf voltage and current applied to a plasma reactor and analyzing these measurements with sheath models. This approach has previously been validated[1] and used to monitor ion energy drift[2] at a bare metallic electrode. When a wafer is present, however, it contributes an electrical impedance which may cause errors in the monitoring technique. In this study experiments were performed to characterize the wafer impedance and its effect on the monitoring technique, for oxidized and bare Si wafers being etched by Ar/CF_4 plasmas in an inductively coupled plasma reactor. Wafer impedance was found to be significant at low bias frequencies but negligible at high bias frequencies (10 MHz). At 10 MHz, the technique was able to accurately monitor ion energy during a normal etch process and during simulated equipment faults.

[1]M. A. Sobolewski, J. Appl. Phys. **95**, 4593 (2004).
[2]M. A. Sobolewski, J. Appl. Phys. **97**, 033301 (2005).

A
Abdallah, J. FM 69
Abramzon, N. **SW 42**, SW 43
Adamovich, Igor **BM1 4**, DM1 5, PW1 3
Adams, S.F. **FM 60**
Akaike, Takumi EM1 4, SW 34, **SW 35**
Akashi, Haruaki **DM1 4**
Akatsuka, Hiroshi FM 7, **SW 19**, **SW 56**
Al-Kuzee, Jafar SW 22, SW 59
Alexandrovich, Benjamen QW2 8
Ali, M. Asgar QW1 4
Allan, Michael **FM 44**, **FM 45**, **FM 46**, **LT1 1**
Ambrico, Paolo Francesco VH1 2
Anderson, Graydon LT2 3
Arakoni, Ramesh PW1 2
Aramaki, M. FM 55, MT2 1
Aranda Gonzalvo, Yolanda **SW 20**
Arefiev, Alexey GT2 2
Asahi, Daisuke CM2 3
Atkinson, Gerard FM 43
Atzmon, Michael FM 10
Aubert, Xavier **SW 28**, UH2 2
Awakowicz, Peter FM 28, PW2 5

B
Baalrud, S. PW2 2
Babaeva, Natalia **PW1 2**
Babkina, Tatiana **DM2 5**
Bao, Ainan BM1 4
Barnat, E. **PW2 3**, RW1 3
Baronavski, Andrew FM 62
Bartschat, Klaus FM 40, **QW1 1**, SW 67
Basner, Ralf **SW 65**
Becerra, Gabriel DM1 3, LT2 3
Becker, Kurt BM2 4, FM 14, FM 56, MT2 2, SW 65
Behnke, J.F. **SW 27**
Belkind, Abraham **BM2 4**, FM 14, FM 56, MT2 2
Benck, Eric **SW 12**
Bent, S. MT1 4
Biazaran, Reza SW 26
Blackburn, Joel SW 2
Bletzinger, Peter FM 56, MT2 2
Boeuf, J.P. SW 49
Booth, Jean-Paul EM1 1, EM2 4, SW 37
Bowden, M.D. SW 18, SW 21, SW 52, SW 53, SW 59
Braithwaite, Nicholas **SW 22**, **SW 59**
Brake, Mary SW 55
Bray, J. SW 42
Breizman, Boris GT2 2
Brelles-Marino, G. SW 42
Brennscheidt, Martin QW2 3
Brok, W.J.M. **PW1 5**, **SW 48**, **SW 52**
Broks, B.H.P. SW 48
Brooke, George **SW 50**
Brunger, Michael **SW 64**
Buckman, Stephen FM 43, LT1 4, QW1 6
Bueber, Johannes SW 64
Buff, James UH2 6

C
Cappelli, Mark BM1 3, DM1 7, FM 27
Cardinaud, Christophe UH2 5, UH2 6
Carman, Robert **DM1 2**
Carter, Mark **FM 12**
Cartry, Gilles UH2 5, UH2 6
Castillo, F. SW 25
Cha, SungHo FM 9
Chabert, Pascal **EM1 5**, MT2 6, RW1 4, SW 58
Chakrabarty, Chandan Kumar **SW 40**
Chandrashekar, Anand **CM2 6**
Chang, Hong-Young FM 13, FM 37, SW 9, UH1 6
Chen, Francis F. **EM2 1**
Chen, Guangye **GT2 2**
Chen, Zhangjin **SW 67**
Cheng, QiJin FM 21
Childers, J.G. **GT1 1**
Cho, HanKu UH1 1, UH1 3
Choe, Ikjin **EM2 2**
Choi, S.M. **FM 18**
Chung, Chinwook EM2 2, EM2 5, FM 9, PW2 4, QW2 4
Coates, Don LT2 3
Coburn, J.W. QW2 6
Colgan, James **GT1 2**
Coplan, M. SW 69
Corr, Cormac EM1 1, EM2 4, **SW 37**, SW 58
Crintea, Dragos QW2 3
Csanak, G. FM 69
Curley, Garrett **EM1 1**, EM2 4, SW 37
Czarnetzki, Uwe DM2 5, EM2 3, QW2 3, QW2 5, RW1 2

D
Dabringhausen, Lars FM 28, PW2 5
Dalton, T.J. MT1 4
Dateo, Christopher RW2 4
De Benedictis, Santolo **VH1 2**
Deconinck, Thomas **LT2 6**
DeJoseph Jr., C.A. **FM 47**, FM 60, SW 66
Deleuze, Michael SW 64
Demidov, V.I. FM 47
Deutsch, Hans SW 65
Dilecce, Giorgio VH1 2
Dimopoulou, Christina **QW1 2**
Dine, Sebastien EM1 1, **EM2 4**
Ding, Ruhang **FM 4**
Djordjevic, Antonije SW 3
Do, Hyungrok DM1 7
Dodd, E. FM 69
Doerner, R. SW 70
Doggett, Brendan FM 26
Doherty, Declan FM 16
Donnelly, Vincent M. **DM2 4**
Dorai, Rajesh UH2 5
Doyle, J. MT1 4
Drake, Dereth Janette **SW 26**

E
Eden, J. Gary **LT2 1**
Ellingboe, Albert R. FM 5, MT2 4, QW2 7, SW 5, SW 10, SW 13, SW 38
Eriksson, Mark FM 4

F
Faenov, Y. FM 69
Falconer, Ian DM1 2
Fang, Ziwei UH2 6
Faulkner, Ronan FM 16
Fernsler, R.F. EM1 2, MT1 5
Ferreri, Vincent DM1 3, LT2 3
Foster, M. **QW1 3**, **SW 68**, **SW 69**, SW 70
Francois, Jean-Pierre SW 64
Franklin, Raoul **FM 25**
Fridman, Alexander **RW2 1**
Fruchtman, Amnon **MT2 6**
Fujimaki, Akira BM2 3
Fukuda, Y. FM 69
Fuller, N.C.M. MT1 4

G
Gahan, David **SW 5**
Gaman, Cezar-Mihai **SW 10**
Ganguly, Biswa FM 38, FM 52, FM 56, MT2 2, MT2 3, SW 17
Gans, Timo DM2 5, **EM2 3**, QW2 3, QW2 5, **RW1 2**
Gao, Junfang **GT1 3**
Gao, Junsi **BM2 3**
Garscadden, A. SW 66
Gascon, Nicolas BM1 3
Gatilova, Lina **FM 34**
Gibson, Ray **PW1 4**
Gilgenbach, Ron FM 10
Gleiter, Rolf SW 64
Godet, L. UH2 4, **UH2 5**, **UH2 6**
Godyak, Valery QW2 4, **QW2 8**, SW 2
Goeckner, Matthew DM2 2, DM2 3
Gorchakov, Sergey **FM 20**
Goshe, Matthew PW1 3
Graham, W.G. DM1 1, FM 19, MT2 5, RW2 3
Graves, D.B. QW2 6
Greene, Chris H. CM1 5
Grill, Verena **RW2 2**
Guaitella, Olivier FM 34, **FM 57**, LT2 2, **SW 45**
Gudmundsson, J.T. **FM 48**, SW 6, SW 62
Guha, Joydeep DM2 4
Guillard, Chantal LT2 2, SW 45
Guillon, Jean EM1 1, EM2 4
Gutkin, Michael SW 65

H
Haas, Fred SW 22
Hagelaar, G. SW 49
Hamaguchi, Satoshi FM 30
Hamaoka, Fukutaro **SW 8**
Han, Jeunghoon **MT1 2**

Hanai, Takamasa FM 51
Harris, A.L. SW 68
Hatton, Peter SW 20
Hattori, Yosuke FM 51
Haxton, Daniel **CM1 4**
Hayashi, Kenji **SW 34**, SW 35
Hayden, Chanel **MT2 4**
Heberlein, Joachim CM2 5, LT2 4, MT1 1, SW 54
Hebner, Greg **RW1 3**, SW 17
Herd, M.T. FM 65
Hershkowitz, N. FM 29, **PW2 2**, SW 15, SW 16, UH1 5
Hicks, Adam DM1 5
Hlina, Michal SW 46
Hoffman, Daniel FM 12, **RW1 6**, SW 2
Holland, J. BM2 1, RW1 3
Hopkins, Michael B. FM 16, SW 5
Hori, Masaru FM 66, SW 36, VH1 1, VH1 3
Horner, Daniel A. **GT1 4**
Hotta, Eiki SW 44
Houfek, K. **CM1 6**
Hrabovsky, Milan **SW 46**
Hsu, C.C. **QW2 6**
Huewel, Lutz **MT2 5**
Huft, Jens FM 43
Hughes, G. FM 5
Huo, Winifred **RW2 4**
Hur, Ji Hyun **FM 31**

I

Ibanescu, Bogdan FM 46
Inoue, Masumi BM2 3
Ionikh, Yury FM 34
Iordanov, Petar FM 16
Ishimaru, Mikio SW 35
Islyaikin, A. **FM 5**, MT2 4
Itatani, Ryohei SW 47
Ito, Haruhiko **FM 66**
Ito, Masafumi SW 36
Ito, Tsuyohito **BM1 3**, **FM 27**
Itoh, Haruo FM 59
Iwata, Satoshi BM2 3

J

Jang, Dongchan FM 10
Jang, SungHo **EM2 5**
Jelisavcic, Milica LT1 4
Jiang, Tao **SW 21**
Jiao, C.Q. **SW 66**
Jindal, Ashish **DM2 2**
Joaquin, J.C. SW 42
Jolly, Jacques EM2 4
Jones, Adric FM 43
Jones, Darryl SW 64
Jones, Michael FM 10
Jonkers, Jeroen **PW1 1**
Jordan, Nicholas M. **FM 10**
Joseph, Eric DM2 3
Joyce, G. EM1 2
Jun, Sanghyun **FM 13**

K

K. Goto, Takeshi EM1 4
Kadetov, Victor EM2 3
Kakizaka, Satoru **FM 7**
Kang, Chang-Jin UH1 1, UH1 3
Kang, Daebong MT1 2
Kano, Hiroyuki FM 66, VH1 3
Kanuma, Toshiaki SW 56
Karkari, S.K. **SW 13**
Katsch, M. **SW 60**
Kawamura, E. **SW 7**
Kedzierski, Wladek FM 41
Kersten, H. SW 27
Keum, Gyung Soo FM 31
Keville, Bernard **FM 16**
Khakhaev, Anatoly SW 32
Khudik, V.N. **SW 29**, SW 30
Kim, Gon Jun **FM 6**
Kim, K.N. FM 18
Kim, Sung Jin FM 6, **MT1 3**
Kim, Sungjin FM 48, **SW 6**, **SW 62**
Kim, SungSik SW 9
Kim, Taikyung UH1 1
Kim, Wookyung **DM1 7**
Kim, Yong-Ki **QW1 4**, SW 71, SW 72
Kim, Yongho DM1 3, **LT2 3**
Kim, Yongjin UH1 1
Kimura, Takashi **FM 17**, **FM 51**
Kitagawa, Tomohiko UH1 4
Kitajima, Takeshi EM1 4, SW 34, SW 35
Klein, Levente FM 4
Knippenberg, Stefan SW 64
Ko, Eunsuk **SW 15**
Kobayashi, J. MT2 1
Kokoouline, Viatcheslav CM1 5
Kondo, Keiichi FM 64
Kono, A. **FM 55**, **MT2 1**
Konrad, Milos SW 46
Kopecky, Vladimir SW 46
Kortshagen, Uwe **CM2 1**, CM2 2, CM2 5, FM 53
Kothnur, Prashanth **GT2 1**
Krastev, V. FM 5
Kravchenko, Aleksandr **SW 32**
Kroesen, G.M.W. PW1 5, SW 18, SW 21, SW 53
Kubota, Yoshiki VH1 1
Kuroiwa, Shunji BM2 2
Kurunczi, Peter DM2 4
Kushner, Mark J. **BM2 5**, PW1 2
Kwon, Duch-Hee **SW 72**
Kwon, GiChung FM 9, UH1 6

L

Ladouceur, Harold FM 62
Lagmich, Y. **SW 49**
Lampe, M. **EM1 2**, MT1 5
Langenscheidt, Oliver **FM 28**, **PW2 5**
Larson, Aasa CM1 5
Lau, Y.Y. FM 10
Lawler, J.E. **FM 65**
Lee, Dong-Seok FM 37
Lee, Dongsoo **SW 16**
Lee, Gil Sik CM2 6
Lee, Hae June MT1 3
Lee, J.K. FM 18
Lee, Jae Koo FM 6, MT1 3, QW2 1, **RW1 5**
Lee, Jeong Soo CM2 6
Lee, Minhyong EM2 5, PW2 4
Lee, PyungWoo PW2 4
Lee, R. MT2 1
Lee, R.H. SW 66
Lee, S.H. FM 18
Lee, Sang-Won FM 37
Lee, Sung Hee **QW2 1**
Lee, WonKi **QW2 4**
Lee, Yero UH1 1
Leiweke, Robert **FM 52**, FM 56
Lempert, Walter BM1 4, **DM1 5**, PW1 3
Leonhardt, D. EM1 2, **FM 2**, MT1 5
Levchenko, Igor **FM 72**
Levif, Pierre **RW1 4**
Lichtenberg, A.J. SW 6, SW 58, SW 62
Lichtenberg, Stefan FM 28, PW2 5
Lieberman, M.A. FM 48, **HT 1**, RW1 4, SW 6, SW 7, SW 62
Lieder, H. SW 27
Lill, T. BM2 1, RW1 3
Lim, Seokhyun **UH1 1**
Lin, Wei-Jen SW 43
Lindsay, Jon LT2 4
Loffhagen, Detlef SW 24, **UH2 1**
Long, JiDong FM 21, VH1 4
Longmier, B. PW2 2
Lopez, Jose BM2 4, **FM 14**, **FM 56**, **MT2 2**
Lou, Guofeng BM1 4
Luizova, Lidia SW 32
Lukomski, Michal FM 41
Lunney, James G. FM 26

M

Macheret, Sergey **GT2 4**
Machima, Puthajat **UH1 5**
Madison, D.H. GT1 3, QW1 3, SW 67, SW 68, SW 69, **SW 70**
Madzawa-Nussinov, Tsitsi **DM1 3**, LT2 3
Mahadevan, Shankar LT2 6
Mahoney, Jenny SW 65
Makabe, Toshiaki BM2 2, EM1 4, QW2 2, SW 8, SW 34, SW 35, UH1 2
Makrinich, Gennady MT2 6
Malovic, Gordana FM 49, SW 3
Mangolini, Lorenzo **CM2 2**
Maric, Dragana **UH2 3**
Marke, Swen SW 39
Marro, F.G. **FM 19**
Martin, Elijah LT2 3
Martinez, H. **SW 25**, SW 61
Matsuura, Haruaki FM 7, SW 56
Matsuzaki, Mitsuo SW 56
May, Olivier FM 46
McConkey, William **FM 41**
McCurdy, C.W. CM1 4, CM1 6, GT1 4
McEachran, Robert FM 42
McLaren, Jami **MT1 1**
Mentel, Juergen FM 28, PW2 5

Mikhaylov, Ivan CM1 5
Milde, Falk SW 39
Mildren, Richard DM1 2
Miller, P. RW1 3
Miller, Thomas M. **EM1 3**
Milosavljevic, Vladimir **SW 38**
Min, Gyung-Jin UH1 1, UH1 3
Mitchell, Brian **CM1 2**
Monahan, Derek **FM 35**, **FM 36**, MT2 4
Mondragon, A.B. SW 25, SW 61
Moon, Joo-Tae UH1 1, UH1 3
Morgan, Tom MT2 5
Mungal, Godfrey DM1 7
Murakami, Yukio **FM 64**

N
Nafarizal, Nayan BM2 3
Nagorny, V.P. SW 30
Nakamura, Keisuke UH1 4
Neale, Ian D. SW 20
Nersisyan, Gagik **DM1 1**, RW2 3
Ngassam, V. CM1 3
Nierode, M.A. QW2 6
Nikitovic, Zeljka **FM 49**
Nishihara, Munetake BM1 4, DM1 5
Norberg, Seth DM1 5
Noto, Masahisa FM 17
Nozaki, Tomohiro **CM2 3**, **CM2 5**

O
O'Connell, Deborah EM2 3, **QW2 3**, **QW2 5**
Oh, Jae Joon FM 31
Oh, SeJin **FM 9**, **PW2 4**
Ohmori, Takeshi **EM1 4**, SW 34, SW 35
Ohnishi, Kuma CM2 5
Ohta, Takayuki SW 36
Okazaki, Ken CM2 3, CM2 5
Oksuz, L. **QW2 7**
Ono, Kouichi **BM1 1**, **UH1 4**
Orel, Ann E. **CM1 1**, CM1 3, LT1 5
Osari, Kazushi UH1 4
Ostrikov, Ken **FM 71**, FM 72
Ostrikov, Kostya FM 21, **FM 61**, VH1 4
Otsuki, T. MT2 1
Oulevey, Patric FM 46
Overzet, Lawrence CM2 6, DM2 2, DM2 3

P
Pamarthy, Sharma BM2 1
Panagopoulos, Theodoros BM2 1
Park, Jaeyoung DM1 3, LT2 3
Paterson, A. **BM2 1**, RW1 3
Peacher, J.L. GT1 3, QW1 3, SW 68, SW 69, SW 70
Pekarek, Stanislav FM 54
Perriens, Niels SW 53
Peters, John **LT2 4**
Petrova, Tzvetelina **FM 62**
Petrovic, Z. Lj. FM 49, LT2 7, QW1 6, SW 3, UH2 3, UH2 4
Pfender, Emil SW 54
Phelps, A.V. **FM 33**
Pitchford, L.C. SW 49
Plihon, Nicolas **SW 58**
Popovic, Svetozar FM 3, SW 26
Puac, Nevena **SW 3**

R
Radjenovic, Branislav FM 6
Radovanov, S. UH2 4, UH2 5, UH2 6
Raimbault, Jean-Luc RW1 4, SW 58
Raja, Laxminarayan FM 58, GT2 1, GT2 2, LT2 6
Raskovic, Marija **FM 3**
Raspopovic, Z. UH2 4
Rax, Jean-Marcel MT2 6, RW1 4
Reddish, TImothy FM 41
Redwitz, Marco PW2 5
Rees, Alan SW 20
Reid, I. FM 5
Remy, J. SW 48
Ren, YuPing **FM 21**
Rescigno, T.N. CM1 4, CM1 6, GT1 4, LT1 5
Rhee, Yong-Joo SW 72
Rhoton, Russell **SW 55**
Rich, J. William BM1 4, DM1 5, PW1 3
Riemann, Karl-Ulrich **FM 24**, **PW2 1**
Ristivojevic, Zoran **LT2 7**
Robledo, A. SW 25
Roepcke, Jurgen FM 34, SW 45
Rosenblum, Stephen SW 2
Rosocha, Louis DM1 3, LT2 3
Rothwell, M. MT1 4
Rousseau, Antoine FM 34, FM 57, LT2 2, SW 28, SW 45, **UH2 2**
Royal, J. **CM1 3**
Rutkevych, Pavlo **CM2 4**, FM 21, **VH1 4**
Ryan, Philip FM 12

S
Saha, Saumitra SW 64
Sakai, Yosuke **FM 8**
Sakai, Yusuke SW 44
Sakamoto, Takeshi FM 7
Samara, Vladimir FM 49
Sant, Sanket **DM2 3**
Santra, Robin CM1 5
Sasaki, Kenji CM2 3
Sasaki, Koichi BM2 3
Sato, Toshikazu **QW2 2**
Savsic, O. **UH2 4**
Scanlan, Declan BM2 1
Scarborough, K. DM2 6
Scheibner, H. SW 27
Schoeffler, M. SW 70
Schulz, M. QW1 3
Schulze, Julian RW1 2
Seeley, Megan DM1 6, SW 33
Seo, Sang-Hun **FM 37**
Serdyuchenko, Anna VH1 1
Severn, Greg **FM 29**
Severn, Gregory SW 15
Seymour, Dave L. SW 20
Shanmugamurthy, Shanmugamurthy BM2 4
Shannon, Steven **SW 2**
Sheerin, Peter **FM 26**
Sherrill, Manolo **FM 69**
Shibata, Tomoyuki FM 55
Shimada, Masashi **FM 22**
Shimada, Takashi **UH1 2**
Shin, Chul-Ho UH1 3
Shin, Jai Kwang FM 31
Shin, Jichul **FM 58**
Shon, Jong W. **UH1 6**
Shvydky, A. SW 29, **SW 30**
Siefert, Nicholas **FM 38**, **MT2 3**, **SW 17**
Sigeneger, Florian FM 20, **SW 24**, UH2 1
Simek, Milan **FM 54**, VH1 2
Slinker, S.P. EM1 2
Snorrason, Narfi T. FM 48
Sobolewski, Mark **VH1 5**
Solovev, Aleksei SW 32
Stalder, Kenneth DM1 6, **RW2 3**, SW 33
Stancu, Gabi SW 45
Starikovskaia, Svetlana **GT2 3**
Stauffer, Allan **FM 42**
Steffens, Kristen SW 12
Stone, Philip **SW 71**
Suda, Yoshiyuki FM 8
Sugai, Hideo BM2 3
Sugawara, Hirotake FM 8
Sullivan, James **FM 43**, LT1 4
Sun, Jong-Woo **UH1 3**
Surko, C.M. QW1 5
Sutton, Sean FM 41
Suvakov, M. **QW1 6**
Suzuki, Susumu **FM 59**

T
Tai, T.L. MT1 4
Takahashi, Kazuo UH1 4
Takashima, Seigo FM 66, VH1 1, **VH1 3**
Takeda, Keigo **SW 36**, **VH1 1**
Tanaka, Hiroshi **LT1 2**
Tarnovsky, Vladimir SW 65
Tazawa, Shota FM 8
Theodosiou, C.E. SW 29, SW 30
Thevenet, Frederic **LT2 2**, SW 45
Thimsen, Elijah CM2 2
Ting, Yuk-Hong FM 30
Todorow, Valentin BM2 1
Tonzani, Stefano **CM1 5**
Toyoda, Hirotaka BM2 3
Trevisan, Cynthia **LT1 5**
Tseng, Shawn **SW 43**
Turner, M.M. FM 26, FM 29, FM 35, FM 36, **FM 68**, MT2 4, **RW1 1**, RW1 2, **SW 4**
Tuszewski, M. **DM2 6**
Tynan, George R. FM 22

U
Uhrlandt, Dirk FM 20
Utkin, Yurii **PW1 3**

V
van de Sanden, Richard **DM2 1**
van der Mullen, J.J.A.M. PW1 5, SW 48, SW 52
Van Doren, Jane M. EM1 3
van Helden, Jean-Pierre DM1 1
VanBoeyen, R. SW 69
Vasekova, Eva SW 59
Vidmar, Robert **DM1 6**, **SW 33**
Viggiano, A.A. EM1 3
Vizcaino, Violaine FM 43, **LT1 4**
Vuskovic, Leposava FM 3, SW 26

W
Wagenaars, E. **SW 18**, SW 21, SW 52, **SW 53**
Wagner, A. SW 60
Wallendorf, Till **SW 39**
Walters, A. SW 69
Walton, S.G. EM1 2, FM 2, MT1 5
Wang, Feng SW 64
Wang, Jiankun **SW 47**
Wang, Lumin FM 10
Wang, Xu SW 15
Watanabe, Masato **SW 44**
Welzel, Stefan FM 34
Wendt, Amy FM 4, **FM 30**
Williams, Shuntel FM 30
Williams, Skip **BM1 2**
Williamson, J.M. FM 56, FM 60, MT2 2
Winkler, Dave SW 64
Won, Jae Hyung FM 31
Worsley, M.A. MT1 4
Wu, Alan **SW 11**

X
Xu, ShuYan FM 21, FM 71, VH1 4

Y
Yagisawa, Takashi **BM2 2**, SW 8, UH1 2
Yang, Guang **SW 54**
Yang, Jang Gyoo SW 2
Yasuda, Tohru SW 47
Yeom, G.Y. FM 18
Yoo, Jinhyuk MT1 2
You, Shin-Jae FM 37, **SW 9**
Young, J.A. **QW1 5**
Yousif, F.B. SW 25, **SW 61**

Z
Zajfman, Daniel **LT1 3**
Zajickova, Lenka MT1 1
Zatsarinny, Oleg **FM 40**
Zhang, Peng **FM 53**
Zhou, Baosuo DM2 3
Zhou, Ning **LT2 5**
Zhu, Sha FM 10
Zhu, WeiDong FM 14, MT2 2
Ziock, Hans LT2 3
Zivanov, Svetlana FM 46

NOTES

Double Tree Hotel, San Jose

Space Allocation

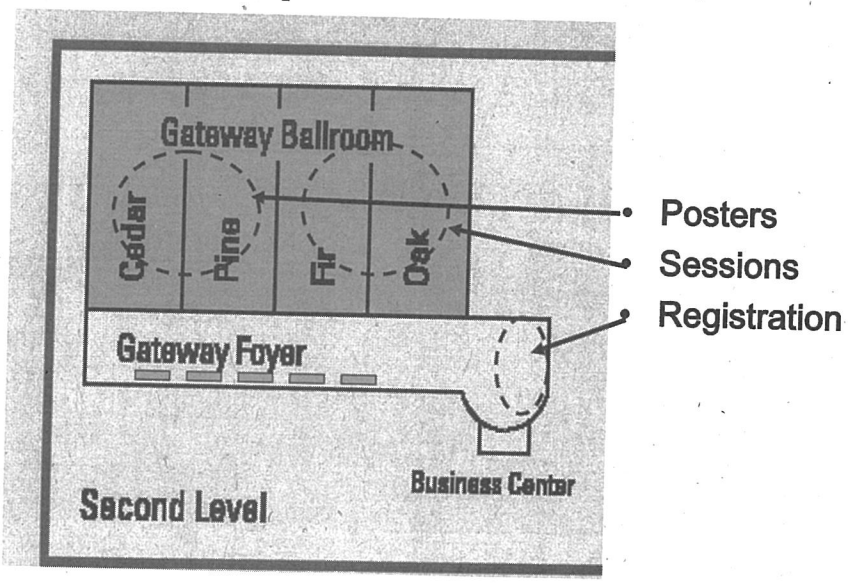

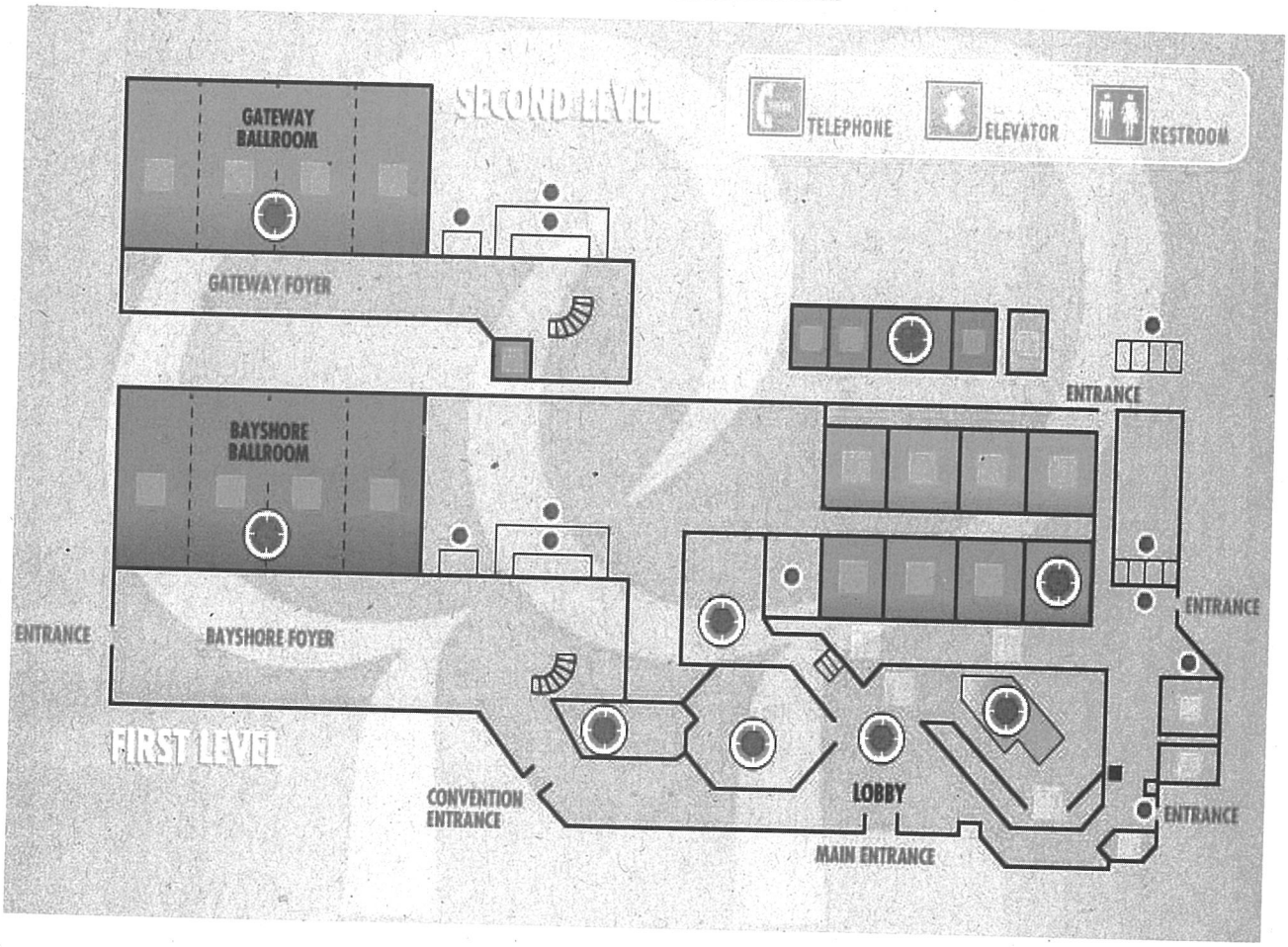

On the Cover: Top view of optical light scattering from three plasma crystals comprised of different numbers of 8.3 μm diameter, melamine formaldehyde particles suspended in a 1.8 W, 110 mTorr argon plasma. The length scale is shown in each image. Horizontal confinement is provided by a parabolic depression in the lower electrode. The radial variation in nearest neighbor spacing is visible for the larger crystals. Work performed at Sandia National Laboratories.

Epitome of the 58th Annual Gaseous Electronics Conference of the American Physical Society

18:00 SUNDAY EVENING
16 OCTOBER 2005

AS **Opening Reception**
Pine/Cedar, Doubletree Hotel

8:00 MONDAY MORNING
17 OCTOBER 2005

BM1 **Plasma Propulsion and Combustion I**
Ono, Williams
Pine, Doubletree Hotel

BM2 **Magnetically-enhanced Plasmas**
Kushner
Cedar, Doubletree Hotel

10:00 MONDAY MORNING
17 OCTOBER 2005

CM1 **Dissociation, Recombination, and Attachment**
Orel, Mitchell
Pine, Doubletree Hotel

CM2 **Nanoparticles and Nanotubes**
Kortshagen
Cedar, Doubletree Hotel

13:30 MONDAY AFTERNOON
17 OCTOBER 2005

DM1 **High Pressure Plasma I**
Akashi
Pine, Doubletree Hotel

DM2 **Plasma Chemistry and Plasma-Surface Interactions**
van de Sanden
Cedar, Doubletree Hotel

16:00 MONDAY AFTERNOON
17 OCTOBER 2005

EM1 **Electronegative Plasmas**
Chabert
Pine, Doubletree Hotel

EM2 **Plasma Diagnostics I**
Chen
Cedar, Doubletree Hotel

19:15 MONDAY EVENING
17 OCTOBER 2005

FM **Poster Session I**
Fir/Oak, Doubletree Hotel

8:00 TUESDAY MORNING
18 OCTOBER 2005

GT1 **Ionization of Atoms and Molecules**
Childers, Colgan
Pine, Doubletree Hotel

GT2 **Plasma Propulsion and Combustion II**
Starikovskaia, Macheret
Cedar, Doubletree Hotel

10:00 TUESDAY MORNING
18 OCTOBER 2005

HT **GEC Foundation Talk**
Lieberman
Pine/Cedar, Doubletree Hotel

11:15 TUESDAY MORNING
18 OCTOBER 2005

JT **Business Meeting**
Doubletree Hotel

12:00 TUESDAY NOON
18 OCTOBER 2005

KT **General Committee Meeting**
Boardroom, Doubletree Hotel

13:30 TUESDAY AFTERNOON
18 OCTOBER 2005

LT1 **Electron-Molecule Collisions**
Allan, Tanaka, Zajfman
Pine, Doubletree Hotel

LT2 **High Pressure Plasmas II**
Eden
Cedar, Doubletree Hotel

16:00 TUESDAY AFTERNOON
18 OCTOBER 2005

MT1 **Material Processing**
Pine, Doubletree Hotel

MT2 **Glows I**
Cedar, Doubletree Hotel

18:00 TUESDAY EVENING
18 OCTOBER 2005

NT **Reception and Banquet**
Pine/Cedar, Doubletree Hotel

8:00 WEDNESDAY MORNING
19 OCTOBER 2005

PW1 **Lighting and Lasers**
Jonkers
Pine, Doubletree Hotel

PW2 **Plasma Sheaths**
Barnat
Cedar, Doubletree Hotel

10:00 WEDNESDAY MORNING
19 OCTOBER 2005

QW1 **Electron and Positron Collisions**
Bartschat, Dimopoulou
Pine, Doubletree Hotel

QW2 **Inductively Coupled Plasmas**
Cedar, Doubletree Hotel

13:30 WEDNESDAY AFTERNOON
19 OCTOBER 2005

RW1 **Capacitively Coupled Plasmas**
Lee, Hoffman
Pine, Doubletree Hotel

RW2 **Biological Applications of Plasmas**
Fridman, Grill
Cedar, Doubletree Hotel

16:00 WEDNESDAY AFTERNOON
19 OCTOBER 2005

SW **Poster Session II**
Fir/Oak, Doubletree Hotel

8:00 THURSDAY MORNING
20 OCTOBER 2005

UH1 **Etching Mechanisms**
Pine, Doubletree Hotel

UH2 **Glows II**
Cedar, Doubletree Hotel

10:00 THURSDAY MORNING
20 OCTOBER 2005

VH1 **Plasma Diagnostics II**
Pine, Doubletree Hotel

0003-0503(200510)50:7;1-U